

UNESCO-IHE
**Transient Groundwater Flow, Analytical
Solutions**

Prof. T. N. Olsthoorn, PhD, MSc

December 2018

Contents

1	Introduction	9
1.1	Objectives of the course	9
1.2	Note with respect to the exercises	10
2	Introduction to transient phenomena in groundwater	12
3	Irreversible transient phenomena	14
3.1	Consolidation	14
3.2	Liquefaction	15
3.3	Intrusion of salt water	17
3.4	Questions	19
4	Reversible groundwater storage	20
4.1	Phreatic storage (water table storage, specific yield, S_y)	20
4.1.1	Phreatic responses	26
4.1.2	Questions	27
4.2	Elastic Storage	30
4.2.1	Introduction	30
4.2.2	Loading efficiency	30
4.2.3	Barometer efficiency	31
4.2.4	How much are the loading efficiency barometer efficiency expressed in the properties of the water and the porous medium ?	34
4.2.5	Specific (elastic) storage coefficient	36
4.2.6	Application (not for exam)	37
4.2.7	Questions	38
4.3	Earth tides (not for exam)	41
5	One-dimensional transient groundwater flow	43
5.1	Scope	43
5.2	Governing equations	43
5.3	Sinusoidal fluctuations	45
5.3.1	Tidal fluctuations in groundwater	45
5.3.2	Fluctuations of temperature in the subsurface	48
5.3.3	Questions	49
5.4	Non-fluctuating interaction with surface water	51
5.4.1	Basins of half-infinite lateral extent	51
5.4.2	Questions	54
5.4.3	Higher-order solutions (not for exam)	56

5.4.4	Questions	58
5.4.5	Superposition in time, half-infinite aquifer	58
5.5	Groundwater basins as land strips of limited width between straight head boundaries	59
5.5.1	Introduction	59
5.5.2	Water level at the left hand side suddenly rises by a height a , the level at the right-hand side remains at zero	60
5.5.3	Shifting the zero point of the x -axis	61
5.5.4	Arbitrary non-symmetrical case	61
5.5.5	Symmetrical case, $A = B$	63
5.5.6	Questions	65
5.6	Symmetrical drainage from a land strip bounded by straight head boundaries (characteristic time of flow basins)	65
5.6.1	Analytical solution	65
5.6.2	Long-term drainage behavior, characteristic drainage time	67
5.6.3	Questions	69
6	Transient flow to wells	70
6.1	Introduction	70
6.2	Wells and well functions overview	70
6.3	Theis: transient well in an infinite aquifer with constant transmissivity and storativity	74
6.3.1	Implementation of the Theis well function in Excel	77
6.3.2	Type-curve for the Theis well function	78
6.3.3	Theis classic pumping-test analysis	80
6.3.4	Standard behavior obtained from simplified Theis well function	81
6.3.5	Derived behavior using the logarithmic approximation of $W(u)$	82
6.3.6	Drawdown at a fixed time at different r	85
6.3.7	Radius of influence	87
6.3.8	Relation with the solution for the steady-state situation	88
6.3.9	Exercises	89
6.3.10	Flow at distance r from the well	93
6.3.11	Pumping test Oude Korendijk	94
6.3.12	Superposition in time	98
6.3.13	Superposition in space	99
6.3.14	Questions	101
6.4	Partial penetration of well screens	103
6.4.1	Huisman's method	103
6.4.2	Hantush's solution for partial penetrating screens	105
6.4.3	Example	107
6.4.4	Questions	107
6.5	Hantush: transient flow due to a well in a semi-confined (leaky) aquifer	109
6.5.1	Hantush's partial differential equation and solution	109
6.5.2	Implement Hantush's well function in Excel	111

6.5.3	Hantush type curves and comparison with Theis	112
6.5.4	Questions	115
6.5.5	Assignment: pumping test Dalem (Kruseman & De Ridder, 1994) with new data	116
6.6	Delayed yield (delayed water-table response)	117
6.6.1	Introduction	117
6.6.2	Water-table aquifer	119
6.6.3	Generalization to semi-confined aquifers	121
6.6.4	The two Theis bounding curves	122
6.6.5	Influence of partial penetration of the well screen	124
6.6.6	Questions	124
6.7	Large-diameter wells (not for the exam)	128
7	Convolution	131
7.1	What convolution is and how it works	131
7.2	Examples in Excel	136
7.2.1	Arbitrarily fluctuating river stage	136
7.2.2	Impulse response, block response, and step response comparison	139
7.2.3	Arbitrarily fluctuating extraction of multiple Theis wells	140
7.3	Questions	141
8	Laplace solutions (illustration, not for exam)	143
8.1	Sudden head rise at the boundary of a one-dimensional semi-infinite aquifer	143
8.2	Laplace solution for the Theis well function	144

Nomenclature

General

x, y, z [L] Coordinates. z is upward positive relative to top of model, sea level, ground surface, top of aquifer or any other suitable fixed datum elevation.

r [L] Distance from the well or center of model in the case of axial symmetric flow. Also used for the radius of a capillary.

R [L] Radius of influence, outer radius of circular aquifer or island.

$t, \Delta t$ [T] Time.

A [L²] Surface area

V [L³] Volume.

Hydraulic and mechanical properties

μ [FT/L²] Water viscosity, e.g. [Ns/m²] = [Pa s]

κ [L²], k [L/T] Permeability (independent of fluid) and hydraulic conductivity. $k = \rho_w g \frac{\kappa}{\mu}$. Note that κ and k are vectors, i.e. they are direction dependent.

c [T] Vertical hydraulic resistance of aquitards or a low-conductive layer, $c = d/k_v$ with d [L] the thickness of this layer and k_v [L/T] its vertical hydraulic conductivity.

S [-] Elastic storage coefficient [L³/L²/L]

S_s [L⁻¹] Specific elastic storage coefficient [L³/L³/L]

S_y [-] Specific yield [L³/L²/L]. Specific yield is storage from draining pores.

α, β [L²/F] compressibility of water and bulk porous matrix respectively. $\beta = 1/E$ where E is the compression modulus.

E_w, E_m [F/L²] Compression modulus of water and porous medium respectively. $E = 1/\beta$, where β is the compressibility.

$\rho_w, \rho_s, \rho_b, \rho$ [M/L³] Density of water, solids, bulk porous medium respectively

Heat properties and flow

c, c_w, c_s [E/M/K] Bulk heat capacity, heat capacity of water and solids. $c = \epsilon c_w + (1 - \epsilon) c_s$

$\lambda, \lambda_w, \lambda_s$ [E/T/L/K] Bulk, water and solids heat conductance, $\lambda = \epsilon \lambda_w + (1 - \epsilon) \lambda_s$

ϵ [-] Porosity of the porous medium

\mathbb{D} [L²/T] For heat flow $\mathbb{D} = \frac{\lambda}{\rho c}$, i.e. heat conductivity over bulk volumetric heat capacity of water plus medium, $\lambda = \epsilon \lambda_w + (1 - \epsilon) \lambda_s$ and $\rho c = \epsilon \rho_w c_w + (1 - \epsilon) \rho_s c_s$. For diffusivity in the context of groundwater flow see under **Aquifer system**.

\mathbb{R} [-] Retardation, i.e. the factor by which transport of mass or heat is delayed relative to that of the pore water. It is the amount of mass or heat in the water over the total amount of mass or heat in the water plus sorbed to/in the grains. Hence for heat $\mathbb{R} = \rho_w c_w \epsilon / (\rho_w c_w \epsilon + \rho_s c_s (1 - \epsilon))$ with indices w and s referring to water and grains respectively.

Aquifer system

q, q_x, q_y, q_z [L/T] Specific discharge, which generally is direction-specific (a vector)

Q [L³/T], [L²/T] Discharge. It can mean the total discharge over the thickness of the aquifer in a cross section [L²/T] or the extraction or injection of a well, in which case its dimension is L³/T.

N, \bar{N} [L/T] Net recharge and the time or space average net recharge respectively

h [L] Phreatic head, in the case of a water table aquifer, the head relative to the bottom of this aquifer, i.e. the wetted aquifer thickness

ϕ [L] Head in semi-confined and confined aquifers, relative to some predefined datum, i.e. sea level.

s [L] Drawdown, or head relative to initial situation (lower case s)

$p, \sigma_w, \sigma_s, \sigma_e$ [F/L²] Pressure, water pressure, total or soil pressure and effective pressure. σ_t also used for total pressure.

H [L] Thickness of aquifer. Often used only for water table aquifer, sometimes for any aquifer.

D [L] Total thickness of aquifer

kD [L²/T] Transmissivity of an aquifer. kH may be used in an water-table aquifer.

T [T] Characteristic time of a dynamic groundwater system.

$\mathbb{D} [\text{L}^2/\text{T}]$ Diffusivity. For flow $\mathbb{D} = \frac{kD}{S}$ for thermal flow $\mathbb{D} = \frac{\lambda}{\rho c}$, see under Heat

$\lambda [\text{L}]$ Characteristic length or spreading length of a semi-confined aquifer system, i.e. $\lambda = \sqrt{kDc}$ with $kD [\text{L}^2/\text{T}]$ the aquifer's transmissivity and $c [\text{T}]$ the aquitard's vertical resistance.

$R, R_0 [\text{L}]$ Fixed radial distance to the center of axial symmetric flow system at which the head is fixed or zero.

$LE [-]$ Loading efficiency, $LE = \frac{\beta_m}{\epsilon\beta_w + \beta_m}$. Note that $LE + BE = 1$

$BE [-]$ Barometric efficiency. $BE = \frac{\epsilon\beta_w}{\epsilon\beta_w + \beta_m}$. Note that $LE + BE = 1$

Groundwater waves

$A [\text{L}], B \text{ L}$ Wave amplitude.

$L [\text{L}]$ Width of the groundwater system.

a Damping factor of groundwater head wave moving through the aquifer, caused by a kind of tide. $a = \sqrt{\frac{\omega}{2\mathbb{D}}}$

$\omega [\text{T}^{-1}]$ or rather radians per time. The angle velocity of the wave. Full wave time $T = 2\pi/\omega$

$T [\text{T}]$ Cycle time, time of a full wave. $T = 2\pi/\omega$

Physics, math and mechanics

$g [\text{F/M}], [\text{L/T}^2]$ Gravity, acceleration in the Earth's gravity field or the force with which the earth's gravity field pulls at a unit mass at ground surface in the direction of the earth's center.

$\gamma [\text{F/L}]$ Surface tension, cohesion in capillary systems.

$IR(\tau), BR(\tau, \Delta\tau), SR(\tau)$ Respectively: Impulse response, Block response, Step response of a system. $\Delta\tau$ step size, τ lapsed time since event started. See chapter on convolution.

$\text{erfc}(u)$ Complementary Bessel function, i.e. $\text{erfc}(u) = \frac{2}{\sqrt{\pi}} \int_u^\infty e^{-\zeta^2} d\zeta$, and, therefore, $\frac{d\text{erfc}(u)}{du} = -\frac{2}{\sqrt{\pi}} e^{-u^2}$

$\mathbf{W}(u)$ Theis' well function, for transient flow to a well in a confined aquifer, i.e. $\mathbf{W}(u) = \text{iexp}(u) = \int_u^\infty \frac{e^{-\zeta}}{\zeta} d\zeta$, iexp is the exponential integral.

$W(u, \frac{r}{\lambda})$ Hantush's well function for semi-confined transient flow to a well, $W(u, \frac{r}{\lambda}) = \int_u^\infty \frac{1}{\zeta} \exp\left(-\zeta - \frac{1}{4\zeta} \left(\frac{r}{\lambda}\right)^2\right) d\zeta$

$u [-]$ In 1D (cross sections as argument of the erfc-function), $u = \sqrt{\frac{x^2 S}{4kDt}}$. In axial symmetric situations, as argument of the Theis and Hantush solutions, $u = \frac{r^2 S}{4kDt}$

$I_o(z)$, $I_1(z)$, $K_o(z)$, $K_1(z)$ dimensionless modified Bessel function using in axial-symmetric semi-confined steady-state solutions. They depend on the scaled distance $z = r/\lambda$, with $\lambda = \sqrt{kDc}$

1 Introduction

This syllabus has been prepared as part of the IHE masters program in Hydrology and Water Resources, at IHE Delft. The part given by the author, i.e. transient analytical solutions, consists of a total of 20 lecture hours divided over five days, half of which are oral lectures and half are practical exercises in which the students learn to solve their own problems by implementing the given groundwater solutions in python.

1.1 Objectives of the course

- The students will become familiar with the basic 1D and axially symmetric transient groundwater solutions that can readily be applied in practical situations when a computer models is not readily available, where a fast idea of the effect of groundwater impacts is required, where a model is to be verified and so on.
- Students will learn how to deal with and apply superposition, which is perhaps the most important tool to handle more complex systems with analytically.
- Students will obtain insight in the transient behavior of groundwater systems, with their characteristics such as halftime and the relations between parameters and the way parameters workout in the effect on the system.
- Students will learn to simplify analytical solution to extract behavior characteristics that are easy to understand and apply for under specified conditions.
- Closed analytical solution for transient groundwater flow are only available for linear system, i.e. systems with a constant transmissivity and storativity. Students will learn how to deal in an approximate way with situations where transmissivity varies due to extractions or injection.
- Students will gain insight in the behavior of real-world groundwater systems and learn how to read their reaction.
- Students will also learn what physics cause a given behavior of groundwater systems. Storage characteristics and barometric and tidal reactions will be dealt with.
- Students will learn and exercise how to implement transient analytical solutions in python and visualize their results.
- Students will learn how to analyze basic pumping tests to obtain parameter values for a groundwater system.

- Depending on the group, students will learn how to handle complicated time varying systems by means of convolution.
- Students will carry out an assignment in which the various aspects learned are applied.

1.2 Note with respect to the exercises

Today there are two skills that students should acquire: python and QGIS

With python there is no limit to what you may compute (and visualize) on your laptop and almost not limit to the amount of data you can handle and process, or the complexity you can handle. And it is free.

With QGIS there is no limit to spatial data you can handle and analyze and process. And it is free.

With these two tools you are equipped for the future as an engineer and scientist. Both are free, which is a unique feature of our time. Never before was so much computing power in your hands. And nobody can ever take it from you, because it's free, it's on your own laptop. Therefore it's only up to you to learn these two skills. There is an immense amount of resources and information on the internet about both, so you should never be without an answer to your questions. There are also numerous tutorials, both written and on video on the internet, and, of course, there is a large number of books. Python and QGIS, around only a little over 1.5 decades, have already changed the world for scientists and are doing more so every day. So if you don't want to be left behind, pick it up. My advice to your, dear students, is to start using both for all your projects from now on.

The exercises will be done in IPython (now called Jupyter) notebooks, which are a terrific means to communicate your work with others, including your teacher. These notebooks, that were originally developed for python only, have since been extended to over 47 other computer languages. That's why the name was changed to Jupyter notebooks, but that's actually quite the same from the user perspective. These notebooks allow you to combine, text, formulas and code, in which all is neatly formatted. Computations are done within the notebook, so when the notebook is correct the work is correct. And because the text can be nicely formatted within the notebook, the notebooks is also great for sharing as a living document of, if you like, as a pdf document.

- To convince yourselves read what Nature (world's most famous scientific journal) said about it in 2014:

<https://www.nature.com/news/interactive-notebooks-sharing-the-code-1.16261>

- Want some examples and tutorials see:

<https://github.com/Carreau/ipython-wiki/blob/master/A-gallery-of-interesting-IPython-Notebooks.md>

<https://github.com/ipython/ipython/wiki/A-gallery-of-interesting-IPython-Notebooks>

- Just do a few of the examples. You'll see that you can reach out over the entire internet, and could even embed life webcam from home (or form your data loggers, of course) in your own notebook.
- For exploratory computing, which is what you'll be doing most of the time, see:

http://nbviewer.jupyter.org/github/mbakker7/exploratory_computing_with_python/blob/master/notebooks/

- Jupyter notebook implies: 1) Rich web client. 2) Text and Math 3) Code 4) Results
5) Share and reproduce

See https://www.dataone.org/sites/default/files/sites/all/documents/perez2017webinar_sm.pdf

https://www.dataone.org/sites/default/files/sites/all/documents/perez2017webinar_sm.pdf

Theo Olsthoorn, Dec. 2017

2 Introduction to transient phenomena in groundwater

Transient phenomena can only occur if there is some form of storage for water under pressure. Without storage, at least theoretically, all changes of water pressures would spread out with infinite speed across the entire medium. The studied system would then always be in steady state. Clearly, this is never the case in physical reality. Every groundwater system has ways to store and release water under changes of pressure. The specific change of water volume in the porous medium per unit change of pressure (or head) determines the transient behavior of the groundwater system.

Under confined groundwater flow conditions, part of the storage comes from compressibility of the porous medium and part from the compressibility of the water. Under conditions of a free water table, i.e. under unconfined flow conditions, meaning when a free water table is present, also called phreatic groundwater, most storage comes from filling and emptying pores above the water table and only a minor part from elastic storage. The elastic storage is about two orders of magnitude smaller than the phreatic storage. Because of this, elastic storage is mostly neglected for aquifer systems with a free water table.

Groundwater systems can be very slow and very fast. Whether a groundwater system is slow or fast depends on factors that we will study later in section [5.6.2 on page 67](#). An example of a very slow groundwater system, one that takes tens of thousands of years to reach equilibrium, is presented in figure [2.1 on the next page](#), which shows the ongoing decay of the groundwater mound in the Kalahari Desert since the last wet episode, which happened some 12500 years ago (De Vries, 2000). The line along which the cross section was made is shown in figure [2.2 on the following page](#) together with the elevation profile.

Dynamics of groundwater may also be divided into **reversible** and **irreversible** behavior. In this syllabus, we will deal with reversible systems only. Forms of irreversible storage may nevertheless be important under specific circumstances, or may even be quite common. Therefore, we will start with an illustration of some forms of irreversible transient behavior of water-filled porous media.

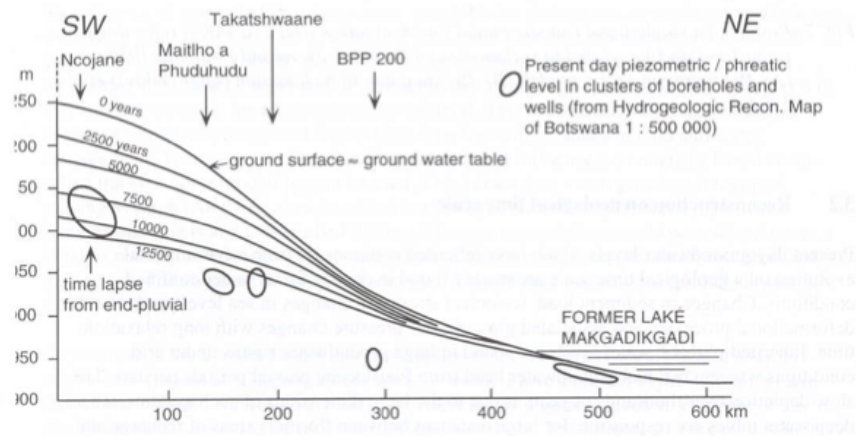


Figure 2.1: Gradual decay of the water table in the Kalahari Desert (De Vries, 1984)

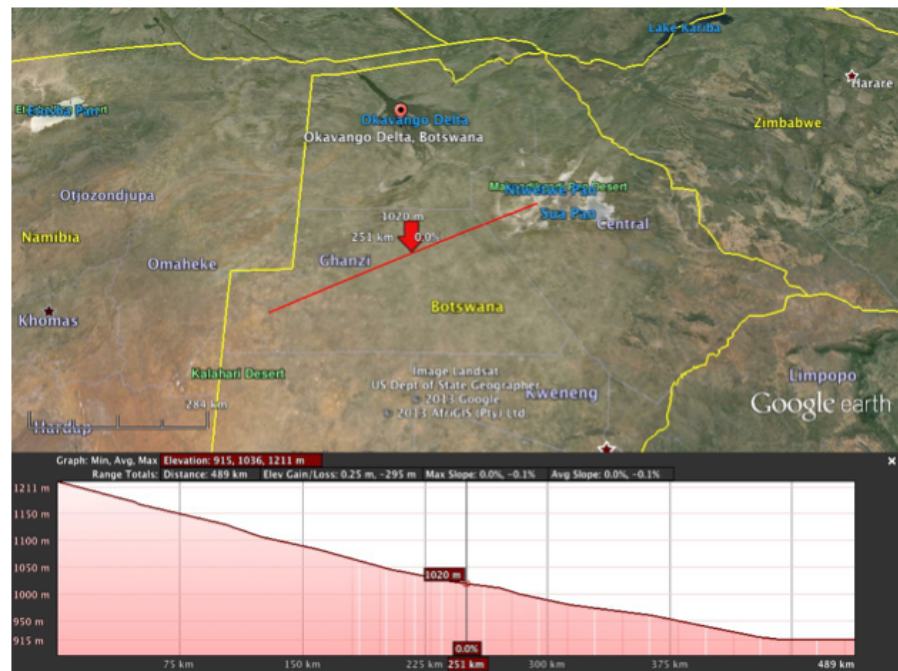


Figure 2.2: Approximately 500 km long cross section studied by De Vries (1984), the water table of which is shown in figure 2.1

3 Irreversible transient phenomena

3.1 Consolidation

One possible form of volume change is due to reordering of ground particles, which may happen due to an increase of the effective pressure (= grain pressure), and is characterized by the squeezing out of water to an irreversible decline of pore space. This phenomenon is called consolidation and leads to land subsidence. The effective stress, σ_e , is the pressure transmitted between the grains. Consolidation is especially well known for clay. In clay, under increased effective stress, that micrometer-scale clay plates get reordered and the pore space thus becomes irreversibly smaller.

As long as grain stresses on vertical planes are horizontal, as is the case in undisturbed horizontal sediments, the total vertical stress, σ_z , (in following chapters we will often use the symbol p instead of σ_e , but they are the same), working on a horizontal plane in the subsoil always equals the total weight above this plane. This weight includes possible loads on ground surface. The total vertical stress σ_z itself is the sum of the water pressure, σ_w , and the effective vertical stress σ_e

$$\sigma_z = \sigma_w + \sigma_e$$

If we increase the vertical stress, for instance by loading the surface with a layer of sand, or by filling a surface reservoir, or due to rainwater infiltrating during the winter season, both stresses will change

$$\Delta\sigma_z = \Delta\sigma_w + \Delta\sigma_e$$

If the water pressure changes, while the total weight remains constant, as is the case when we lower the head in a confined aquifer (reflect on why this must be so?), then the water pressure and the effective stress are directly related

$$\begin{aligned} 0 &= \Delta\sigma_w + \Delta\sigma_e \\ \Delta\sigma_w &= -\Delta\sigma_e \end{aligned}$$

Therefore, if we lower the head, i.e. the water pressure, the effective stress increases and the water pressure decreases. This works the other way around in case the head were increased instead of lowered.

It follows, that the lowering of the water pressure puts the grains of the porous medium under higher stress, which may, therefore, lead to (irreversible) subsidence in vulnerable soils.

An increased effective stress causes a reduction of the volume of the porous medium and, therefore, also of its pore space. To compensate for this reduced space, water will be squeezed out. The speed at which this happens depends on the conductivity of the compressed layer as well as its thickness, as with thicker layers it takes more time for the compressed water to reach the top or bottom of the layer, from which the water could escape.

Large-scale groundwater extractions have, therefore, led to large subsidences affecting large areas in Mexico, USA and the UK (figure 3.1 on the next page).

Subsidence can be relatively fast (happening within weeks) or slow (taking place over centuries) on local to regional scales.

Subsidence also occurs as a result of drainage of wetlands and peat areas. Peat means organic soil, which can decay. This lowering of the shallow water table also increases the effective stress as we saw above. This subsidence is especially evident in a low country like the Netherlands, where drainage of wetlands by ditches has taken place for about a thousand years.

With regard to organic soils, called peat, it is not only the increase of the effective stress caused by drainage that causes the subsidence. It is also the entry of oxygen that can enter peaty soils when they are drained. This oxygen causes oxidation (“burning”) of the peat, giving an extra boost to the subsidence. Subsidence caused by oxidation may continue until it all peat has disappeared!

The peaty areas in the west and north of the country have thus subsided several meters (figure 3.2 on page 17). This is why about half the country lies nowadays below sea level.

In case the original soil layers consisted of alternations of peat and clay, as they often do, the shallow subsoil will consist more and more of pure clay at the top where all peat was burnt away by oxidation, with the original mixture still present below the water table. This clay layer at the top is the collection of all the clay that was present in the original profile, which may have been several meters thick.

3.2 Liquefaction

Another irreversible phenomenon involving reordering of grains, is known as liquefaction, which can happen very fast and spectacularly. Liquefaction is associated with pressure waves, or shocks. Fine sand may have been at rest for thousands of years, even with its pore space being greater than according to the most dense packing of the grains. In the case of a shock, for instance due to an earthquake, the sudden change of water pressure may be so great as to cause the effective stress to be zero for a fraction of a second, during which the grains lose their mutual friction. The ground then loses its internal friction and momentarily turns into a quick sand, in fact it suddenly becomes a “liquid” in which grains float as freely moving particles. The matrix will resettle at a smaller overall volume. During this resettling, the pore water no longer fits between the grains in their denser packing. As soon as the surplus water has escaped the soil resettles and



Figure 3.1: Over 3 m subsidence in the UK

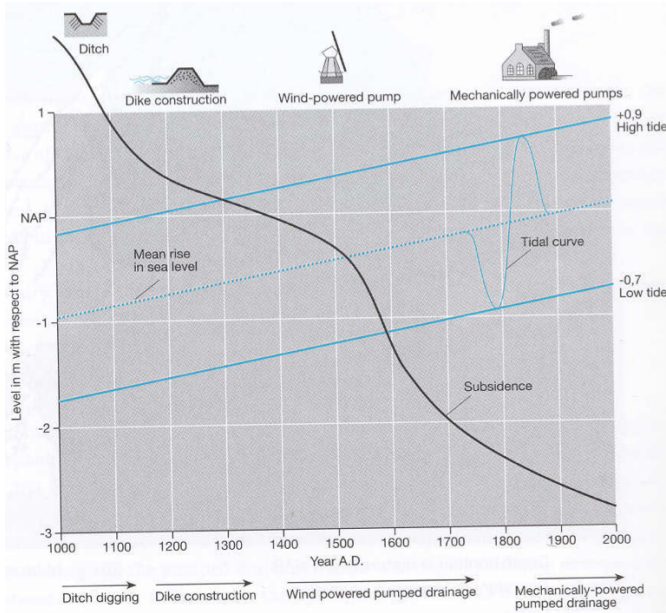


Figure 3.2: Rising sea level since the year 1000 with tide fluctuation curve and subsidence (descending curve) all relative to mean sea level (about NAP). Also shown are water management technologies available over time (From Dufour (1998))

everything sunk into the heavy liquid is stuck forever (see figure 3.3 on the next page
<http://www.ce.washington.edu/~liquefaction>)

3.3 Intrusion of salt water

In many regions, especially deltaic regions, fresh groundwater floats on saline water, which is heavier (denser) than fresh water. (The difference between fresh and ocean water is about 2.5%). The fresh groundwater in the Netherlands is largely floating on salt water as is shown in the cross section in Figure 6. It will generally take several hundred years to a thousand years for a fresh water lens is built up from natural precipitation. The equilibrium may easily be disturbed by extraction of fresh water, but also by construction of harbors, canals and polders. This will cause upconing of salt water from below and lateral intrusion of salt water into aquifers along the coast. Given the time it takes to restore such systems under natural conditions, mining of these systems may be considered irreversible under many practical situations as there are no real means (or sufficient fresh water) to restore the systems within the time horizon of a generation. Good groundwater management is, therefore, essential, but hard to realize in situations of water scarcity.



Figure 3.3: Liquefaction in the USA (<http://www.ce.washington.edu/~liquefaction>)

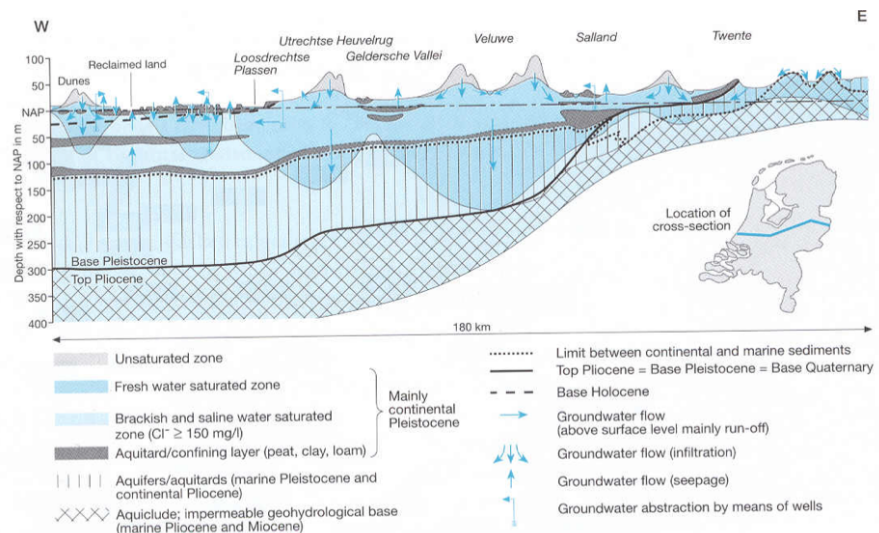


Figure 3.4: Dynamically floating fresh water on salt water in the cross section through the Netherlands. The interface may take hundreds of years to reach its equilibrium. It will be continuously adapt to changing circumstances such as climate and sea level rise, as well as to artificial changes in the water cycle (from Dufour (1998), Dufour (2000))

3.4 Questions

1. Mention some processes due to which the subsurface may lose water that are irreversible.
2. Explain how these processes work, i.e. what the mechanism is behind them and the conditions under which they occur.
3. Why would one call extraction of fresh water from a freshwater body floating on salt water irreversible?

4 Reversible groundwater storage

In the remainder of this syllabus, we will restrict ourselves to reversible groundwater storage phenomena, i.e. phenomena in which the porous medium is not changed.

In groundwater flow systems, three separate forms of storage may be distinguished:

1. Phreatic storage, which occurs in unconfined aquifers, i.e. aquifers with a free water table. It is due to filling and emptying of pores at the top of the saturated zone.
2. Elastic storage, which is due to combined compressibility of the water, the grains and the porous matrix (soil skeleton). This storage releases or stores water wherever the pressure changes.
3. Sometimes, the interface between fresh water and another fluid (be it saline water, oil or gas) can provide a third type of storage. This works by displacement of the interface, generally between the fresh water and the saline water. When displacing an interface, the total volume of water in the subsurface remains essentially the same, however, the amount of usable fresh water may increase (or decrease) at the cost of saline water, and therefore, one may consider this storage of fresh water.

4.1 Phreatic storage (water table storage, specific yield, S_y)

Phreatic storage is due to the filling and emptying of pores above the saturated zone, i.e. above the water table. Because it is related to changes of the water table, it is limited to phreatic (unconfined) aquifers.

The storage coefficient for an unconfined aquifer is called specific yield and is denoted by the symbol S_y . It is dimensionless, as follows from its definition

$$S_y = \frac{\partial V_w}{\partial h} \quad (4.1)$$

where ∂V_w is the change of volume of water from a column of aquifer per unit of surface area and ∂h is the change of the water table elevation.

S_y , therefore, is the amount of water released from storage per square meter of aquifer per m drawdown of the water table.

Hydrogeologists, and groundwater engineers alike, often treat specific yield as a constant. In reality, the draining and filling of pores is more complex and this should be kept in mind in order to judge differences of S_y values under different circumstances even with the same aquifer material. This will be explained further down.

There is no such thing as a sharp boundary between the saturated and the unsaturated porous medium above and below the water table. In fact, the water content is continuous across the water table.

The water table is, by definition, the elevation where the pressure equals atmospheric pressure.

Because we relate all pressures relative to atmospheric, we may say the water table is the elevation where the water pressure is zero (relative to the pressure of the atmosphere).

The simplest model for the zone above the water table is a vertical straw or radius r standing with its open end in water. Due to adhesion between the water and the straw, the water level will be sucked upward in the straw against gravity, thereby reaching an equilibrium height h as shown in figure 4.1.

The soil itself may be considered to consist of a dense network of connected tortuous pores of small but widely varying diameter that may be fully or partially filled with water. Due to adhesive forces pores may even be fully filled above the water table.

In pores above the water table the pressure is negative (i.e. below atmospheric).

If grains can be wetted (attract water), as is generally the case with water, water will be sucked against gravity, into the pores above the water table over a certain height. This height mainly depends on the diameter of the pores.

One can immediately compute the equilibrium of the water in the pore. We have gravity pulling down the water column reaching above the water table, and we have the cohesion force. Hence,

$$\pi r^2 \rho g h = 2\pi r \gamma \cos(\alpha)$$

where ρ [kg/m³] is the density of water, g [N/kg] is gravity, τ [N/m²] is the cohesion stress, and α the angle between the cohesion force and the vertical. Hence

$$h = \frac{2\gamma}{\rho g r} \cos(\alpha)$$

which shows that the suction height h is proportional with $1/r$, the inverse radius of the straw.

In practical situations α is small so that $\tau \cos \alpha \approx \tau$. as τ is in the direction of the surface of the water level in the straw, we may say that

$$\tau \approx \gamma$$

with τ the surface tension of the water surface, which equals $\tau = 75 \times 10^{-3}$ N/m, see any physical handbook. Therefore, we can compute the suction head h immediately given a pore radius.

$$h \approx \frac{2\tau}{\rho g r}$$

Numerically,

$$\begin{aligned} h &\approx \frac{150 \times 10^{-3}}{10^4} \frac{1}{r} \\ &\approx \frac{1.5 \times 10^{-5}}{r} [\text{m}] \end{aligned}$$

If we express h and r in mm, (using h^* and r^* to indicate mm), we get

$$h^* = \frac{15}{r^*}$$

This implies that water in a pore of 1 mm radius may be sucked up over about 15 mm and water in a pore of radius 0.1 mm over 15 cm and water in a pore of 0.01 mm radius over 1.5 m. In reality it may be 50% smaller because of the angle α that was ignored here.

A porous medium has pores of varying diameter, which may coarsely be imagined as in figure 4.2 on the following page. This implies that the line of filled pores will not be sharp. Therefore, the saturation above the water table will gradually decline as shown in the right-hand figure.

The diameter of the widest pores will determine the height over which the porous medium is fully saturated above the water table, i.e. the thickness of the so-called capillary fringe. In gravel, the capillary fringe will be almost zero, but it may be several decimeters or even meters thick in fine-grained materials such as fine sand, loess, loam and clay. In sands, the capillary zone is usually 15-30 cm thick, depending on the grain size. The thickness of the capillary zone is sometimes visible as a wet zone in the banks of surface water. Note that all water above the water table is under negative pressure.

When the water table is lowered, for instance in a column of sand, and we measure the amount of water drained over time, we see that drainage is not immediate (Figure 4.3). After a couple of days, the drainage rate becomes negligibly small. We may thus call the amount drained during a couple of days the specific yield. It is immediately obvious that specific yield is not a unique physical parameter. The more time we take the higher it becomes. It implies that the duration of the test determines the value to some extent. It also implies that a specific yield, when determined from a pumping test of a couple of days duration, is likely to be smaller than that determined from the seasonal fluctuation of the groundwater.

While the amount drained from the subsurface due to lowering of the water table is called specific yield, the amount retained in the soil is specific retention. Together they add up to the porosity (figure 4.4). Specific retention is closely related to so-called field capacity, i.e. the amount of water the soil can hold against gravity. It is the amount of water retained in an originally saturated soil sample after a few days of free drainage at a suction head of about 200 cm.

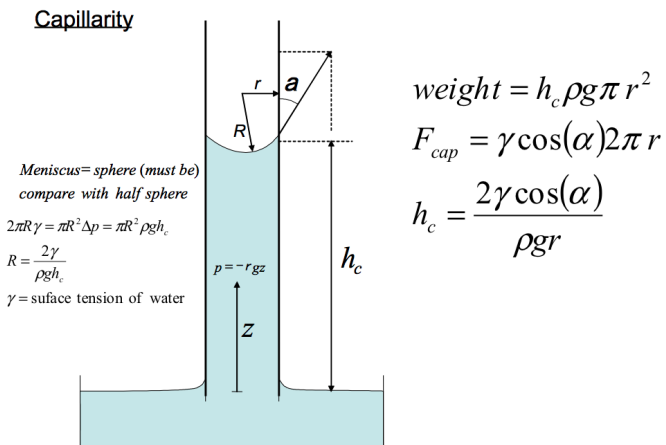


Figure 4.1: Straw of radius r representing a pore connected to the water table

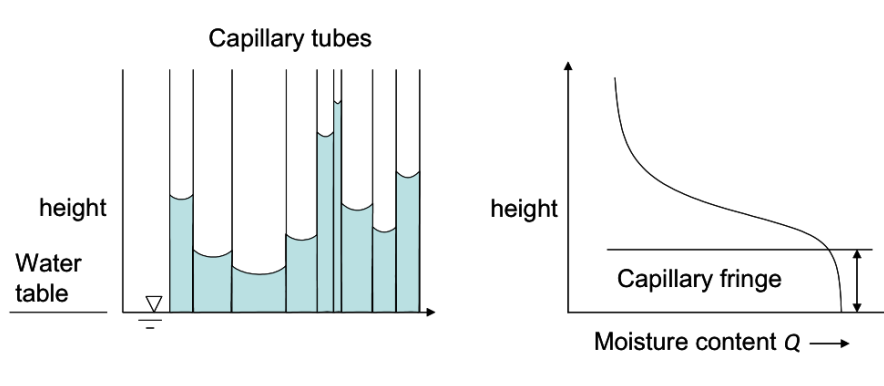


Figure 4.2: A porous medium imagined as a large set of pores of varying diameter

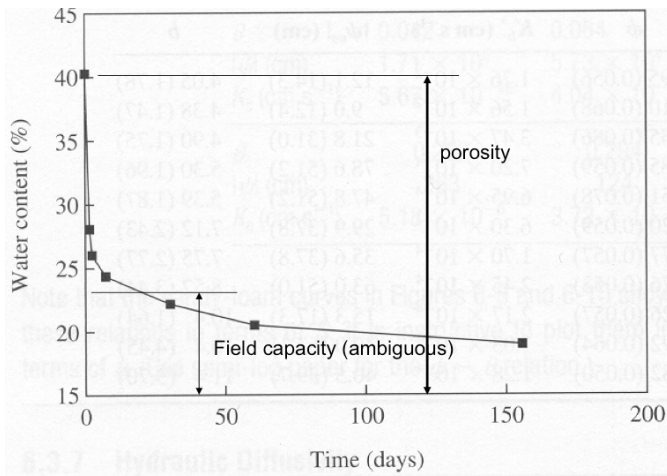


Figure 4.3: Drainage of water from column after lowering the water table

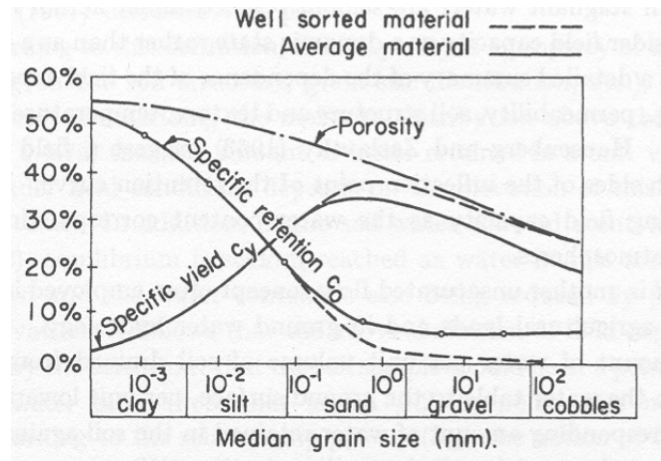


Figure 4.4: Relation between grain size, porosity, specific yield and specific retention (Bear, 1972)

Porosity of porous materials varies, but that of sands tends to be around 35%. Fine sands tend to have somewhat higher values, while coarse sands tend to have somewhat lower porosities. This is related to the ease of compaction at the original time of sedimentation. Smaller grains have a higher surface area and are, therefore, more difficult to compact. In natural gravels, the pore space is often filled by finer grains. This reduces the porosity further as well as the specific yield. Figure 10 shows that for very fine sands the specific yield declines despite the higher porosity. This is mainly due to the higher specific retention (also known as field capacity) of finer grained materials (figure 4.5) as well as the lower hydraulic conductivity, which hinders rapid drainage and therefore, reduces specific yield.

The behavior of water in the unsaturated zone is determined largely by the soil's moisture retention curve of which a number is sketched in 4.5 (For the moisture retention curves of the Dutch soils see Wösten et al. (1994)).

These curves relate the moisture content to suction head, i.e. the negative head in the pores. Figure 4.5 gives the general shape of these curves for typical soil materials. Therefore, in the case of perfect equilibrium between suction and gravity, the moisture characteristic curves represent the moisture content in the soil above the water table. The moisture content at 200 cm suction is generally taken as the field capacity. For sandy soils, the moisture content at this suction head is a good measure of the amount of water the soil can hold against gravity under free drainage conditions.

This implies that the moisture content depends on the distance to the water table (i.e. the suction). Hence, the ground surface above a shallow water table tends to be wetter than above a deep water table under the same circumstances. This must influence the specific yield as illustrated in figure 4.6.

When the water table is lowered, the entire moisture retention curve is lowered as is

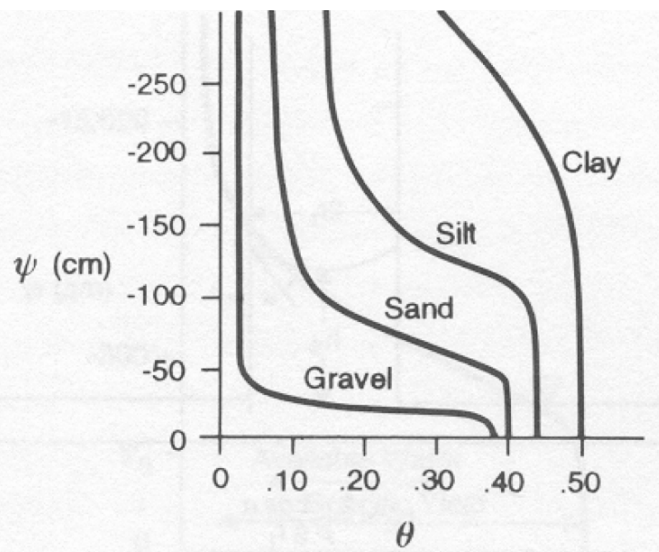


Figure 4.5: Moisture content versus pressure head Ψ , moisture retention curves (Bear, 1972).

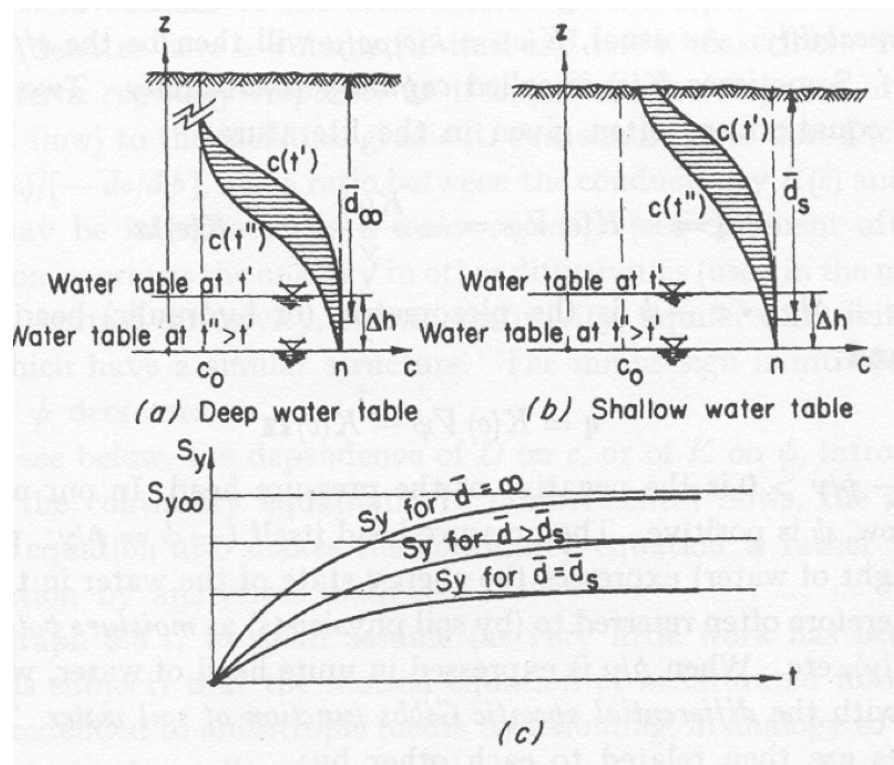


Figure 4.6: Influence of depth and time on specific yield (Bear, 1972)

shown in figure 4.6 (a). The specific yield equals the water from the hatched area. It demonstrates that the entire unsaturated profile is involved in the specific yield. As already mentioned and shown in figure 4.6-c, specific yield increases with available drainage time.

If the water table is shallow (or the material is fine), a major part of the moisture retention curve will be cut off at ground surface as is shown in figure 4.6-b. Lowering of the water table will thus miss part of the hatched area of 4.6-a. Therefore, the specific yield is smaller the shallower the water table. This is also shown in figure 4.6-c.

We should thus not be surprised to find that the same fine dune sand may have a specific yield of 22% inside a large dune area, where the water table is usually several meters below ground surface, and only 8% in an adjacent flower bulb field with the same sand, but with a water table of only 60 cm below ground surface.

Soil characteristics may vary between wide limits. Generally, the coarser the soil, the thinner the capillary fringe (see Figure 11). A complication is that the moisture characteristic curves differ during wetting and drying. This phenomenon is called hysteresis, but this is beyond this course.

Groundwater hydrologists dealing with saturated groundwater usually just use a single constant value for the specific yield in their formulas and models. The specific yield can be estimated from the soil in question, from moisture characteristic curves, in the laboratory, from field measurements, from pumping tests or groundwater model calibration.

Even though this approach may seem doubtful or just wrong in the eyes of some, using a constant but appropriately chosen specific yield works remarkably well in practice. It is more a matter of realizing oneself when a constant specific yield of a certain value it is not applicable. The above outline is meant as a help in deciding on this and to conscious about what is behind this simple value.

Some models, like MODFLOW, have an option to vary specific yield automatically with water table depth.

4.1.1 Phreatic responses

By sensitive continuous measurements of the phreatic head, daily variations in evapotranspiration can be often determined. While in the past the groundwater head could be gauged continuously on paper only, modern head loggers may register the head at short regular intervals and store large amounts of data internally for later use. With such instruments, accurate data become widely available and allow more detailed views on phenomena to be studied and analyzed. Such measurements are already known from Todd (1959), Todd and Mays (2005). Figure 4.7 shows the daily fluctuation of the water table due to daily evapotranspiration measured more than fifty years ago. However, we find such fluctuations in all frequent registrations of the water table under summer circumstances.

If the specific yield is known, evapotranspiration rates can sometimes be determined, or at least the upward flux from the water table. This can be demonstrated on the hand

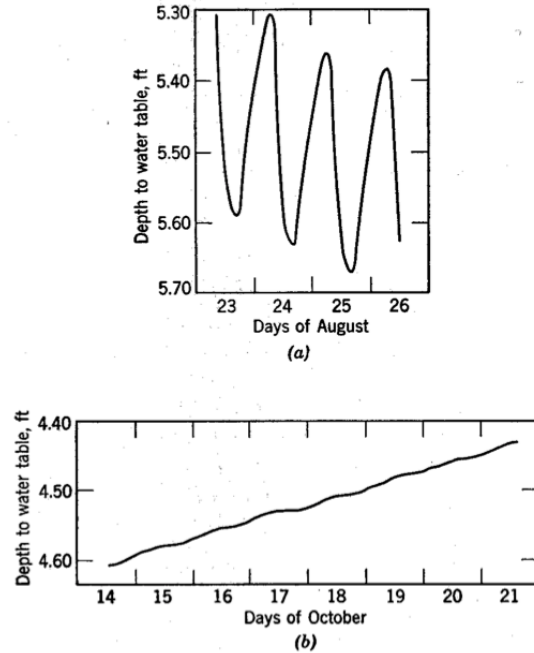


Figure 4.7: Measured water-table fluctuations due to evapotranspiration variations Todd and Mays (2005)

of these old measurements.

The groundwater balance at this point may be expressed as

$$\bar{N} + N(t) = S_y \frac{\partial \phi}{\partial t}$$

Where \bar{N} is the long-term trend of the net water-table recharge (positive or negative, i.e. precipitation minus evapotranspiration from the water table). $N(t)$ is the short-term variation (during the day). So if one plots the derivative of the water table in a point versus time, it may be split into a more or less constant (long-term) trend and a the remainder due to short-term (daily) variation. If this short-term variation can be attributed to evapotranspiration from the water table, as is obviously the case in the figure, one may determine it by taking the surface area between the measured head curve and its long-term trend, multiplied by the specific yield (hatched surface in figure 4.8).

4.1.2 Questions

1. What is the dimension of specific yield? What is the dimension of the elastic storage coefficient. What is the dimension of the specific storage coefficient?
2. How do specific retention, specific yield and porosity relate with each other?
3. How does porosity relate to grain size in general, and what is the reason?

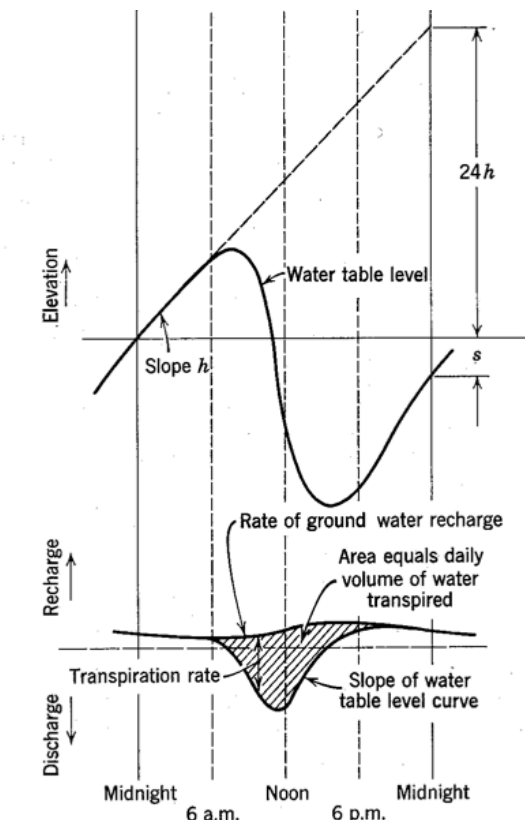


Figure 4.8: Determining the evapotranspiration from water-table variations and a given specific yield Todd and Mays (2005).

4. Given another term for specific retention, one that is generally used in agriculture.
5. How does specific retention relate to grain size?
6. If the water table is lowered, which water is released around or above the water table?
7. What is the definition of the unsaturated zone?
8. Is it likely that the water from a pouring rain easily infiltrates through worm and rabbit holes? If so explain why. If not also explain why?
9. What is a probable value for specific yield in a sand with porosity of 35%? And why?
10. How does capillary zone relate to air-entry pressure?
11. What is actually measured with the air-entry pressure?
12. How does the specific yield relate to the depth of the water table?
13. Using the model of a straw, how does capillary rise relate to the straw radius and the water surface tension?
14. Given a grain diameter of 0.2 mm, a radius that is 1/7th of this radius, and a water surface tension $\gamma = 75 \times 10^{-3}$ N/m, what would be the capillarity rise if the angle of the water surface and the straw is assumed zero?

4.2 Elastic Storage

4.2.1 Introduction

Till now, we only considered storage at the water table and gave very simple, but practical examples largely ignoring spatial dimensions. Spatial dimensions will be dealt with later. In this section, we handle the physics of elastic storage and will give some interesting everyday examples that are sometimes easily overlooked.

Elastic storage is the only storage occurring in confined (and semi-confined) aquifers, i.e. in aquifers without a water table, aquifer that are completely filled with water from floor to ceiling. In such aquifers we have no lowering of the water table whatsoever, unless the head is lowered to beneath the ceiling of the aquifer, a case further ignored here.

Therefore, in confined aquifers storage can only result from compression of the water and depression of the aquifer. The compressibility of the water and the grains themselves is quite obvious, but often the less obvious storage is the most important part. This is the deformation of the soil skeleton, the bulk matrix or the (bulk) porous medium as it is called.

4.2.2 Loading efficiency

To analyze the physics of elastic storage, we start with noting that the total load at any depth is carried by the total (vertical pressure) σ_z or $p \text{ N/m}^2$. This total pressure must equal the sum of the vertical grain pressure (the so-called effective stress, σ_e) and the water pressure σ_w

$$p = \sigma_e + \sigma_w$$

This is indicated in figure 4.9. The brown beams and the springs are imaginary. They replace the volume V_0 (1 m^3 say) that has been cut out of the aquifer. The two imaginary springs have the same properties as the water and the porous medium respectively. Let us see what happens when the pressure is increased by Δp .

In that case, the volume (or height) V_0 is reduced by ΔV and the springs pressures are increased by $\Delta\sigma_w$ and $\Delta\sigma_e$ respectively. The springs have different stiffness, so $\Delta\sigma_w \neq \Delta\sigma_e$. However, each string will always carry a fixed proportion of the total stress. Therefore, we may write

$$\Delta\sigma_w = LE \Delta p$$

where LE is this fixed proportion and is called the **loading efficiency**. The LE must obviously lie between 0 and 1 and is fixed for any particular porous medium. So if we put a weight, like a layer of sand, on ground surface, p in figure 4.9 will increase by Δp , a change that is equal to the weight of the layer of sand per m^2 placed on ground surface. We may then say $\Delta\sigma_w = LE \Delta p$, where the loading efficiency LE is a fixed number between 0 and 1, specific to a aquifer in question. If we have a piezometer in the aquifer, we'll that water level (hence, the head) has risen by placing the sand on top by

$$\Delta\phi = \frac{LE}{\rho g} \Delta p$$

Now assume that Δp is not due to a layer of sand placed on ground surface, but due to a change of the barometer pressure as in figure 4.11. Then the same reasoning applies, because the subsoil cannot know whether the pressure changes due to a layer of sand or the barometer.

A nice and famous early example of loading efficiency is the impact of a train stopping at a station and leaving again some time later (figure 4.10). The weight of the locomotive compresses the aquifer a bit, thus reducing its pore space. This in turn compresses the groundwater, which cannot readily escape. Hence, its pressure rises and it starts to flow sideways, so that the pressure gradually decreases towards its original trend. When the train leaves, the opposite occurs. The removal of the load reduces the effective stress, which causes the aquifer to bounce back, providing more pore space to the water, which depressurizes and increases somewhat in volume. This reduced water pressure causes surrounding groundwater to flow towards to fill up the gap because of which the pressure gradually normalizes.

Q: Think of another way for the water to escape from a semi-confined aquifer.

4.2.3 Barometer efficiency

Figure 4.11 left shows the situation where the pressure increase is caused by a load (of sand) on ground surface; the right hand picture show how the same pressure increase is caused by an increase of the barometer pressure. The question is, how does the barometer pressure change alter the head (water level) in the piezometer?

As said above, for the pressure in the aquifer there is no difference between the two pictures. However, there is a difference in the piezometer. When placing a layer of sand on ground surface, the pressure on the water surface in the piezometer does not change. However, when the barometer pressure changes, the pressure on the water surface in the piezometer does change. That change is, of course, exactly equal to the change of the barometer pressure. To see how the head changes due to a change of the barometer pressure let us just write out the water pressure at the bottom of the piezometer.

It is clear that this pressure changes by the change at ground surface, hence by the barometer pressure $\Delta a = \Delta p$.

Now assume that the head in the piezometer changes by an amount $\Delta\phi$. Change of the water pressure at the bottom of the piezometer is

$$\Delta\sigma_w = \rho g \Delta\phi + \Delta a$$

But we know the change of the water pressure. It equals

$$\Delta\sigma_w = LE \Delta a$$

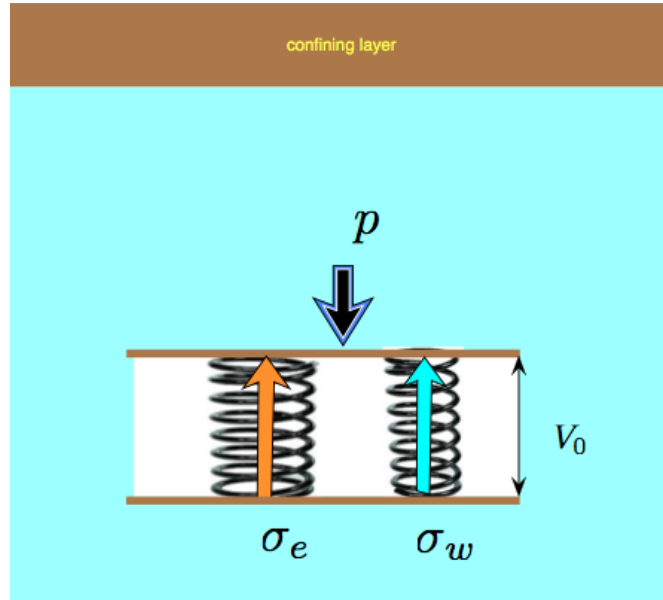


Figure 4.9: The weight of the ground plus water is supported by two pressures, the water pressure σ_w and the effective pressure σ_e

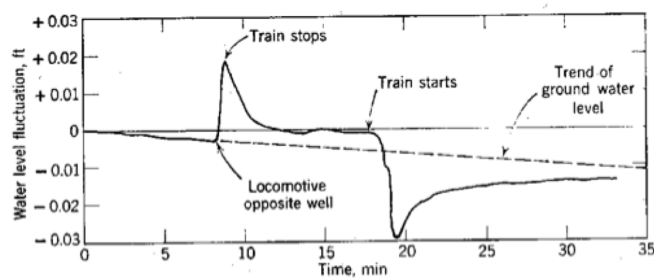


Figure 4.10: Water level fluctuation in a confined aquifer produced by a train stopping near an observation well [Todd (1959), Todd and Mays (2005)]

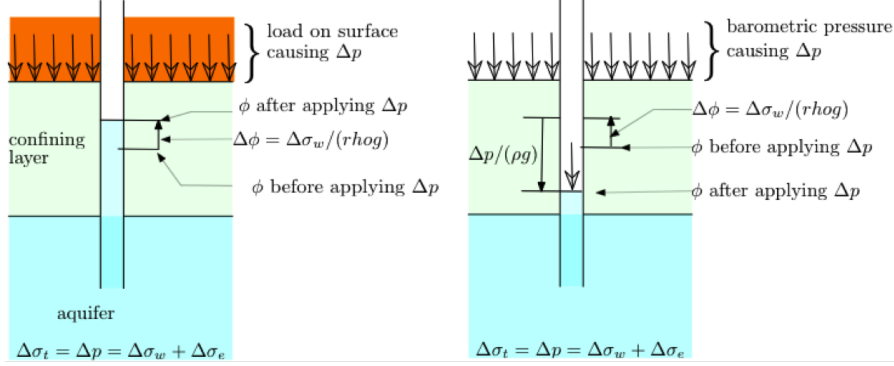


Figure 4.11: Effect on head in confined aquifer by a load Δp on surface versus an increase of the barometric pressure.

Hence

$$\rho g \Delta \phi + \Delta a = LE \Delta a$$

and so

$$\begin{aligned} \rho g \Delta \phi &= -(1 - LE) \Delta a \\ &= -BE \Delta a \end{aligned}$$

Where $1 - LE$ is called the barometer efficiency, BE . Just like the loading efficiency, the barometer efficiency varies between 0 and 1.

The minus sign indicates that the head in the piezometer declines when the barometer goes up. This should be obvious as the the water pressure increases by $LE \Delta a$ which is a fraction of the barometer pressure, which would cause the water level in the piezometer to rise, but at the same time the full barometer pressure pushes on the water table in the piezometer, which causes the water level to decline accordingly. Together, the net effect is a decline of the head in the piezometer by $BE \Delta a$, a fraction of the barometer pressure change.

From the equivalence of previous equation couple it follows that

$$BE + LE = 1$$

A famous example of the barometer efficiency was given by [Todd (1959), Todd and Mays (2005)], figure 4.12. This example is used here because its is famous as one of the first published. However, barometer effects are always seen in piezometers in confined aquifers. The barometer efficiency generally varies between 20% and 80%.

The barometer influence causes a noisy behavior of head time series form confined and semi-confined aquifers, because, even if the groundwater was in perfect rest, barometer fluctuations do affect both the head measured in piezometers as the pressure measured in pressure gauges. Only if heads are measured a short time intervals of hours

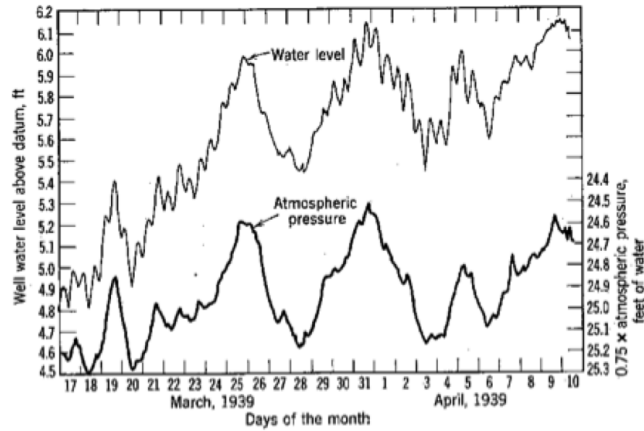


Figure 4.12: Example of a high degree (75%) of barometric efficiency [Todd (1959), Todd and Mays (2005)]. It shows the response of the head in a well penetrating a confined aquifer together with the barometric pressure. Note that the axes on the right is reversed to show the similarity of the two curves (head down when barometer pressure goes up and vice versa).

rather than weeks, the noisy behavior of the head in confined aquifers actually shows its clear one-to-one relation with the course of the barometer pressure. Therefore, such a noisy time series behavior actually shows that a piezometer is in a (semi)-confined aquifer. Unless we have very thick unsaturated zones with substantial resistance against air flow, we will not see much if any barometer fluctuation in water table aquifers ([Rasmussen and Crawford (1997)]).

4.2.4 How much are the loading efficiency barometer efficiency expressed in the properties of the water and the porous medium ?

If the total pressure p is increased by Δp , the the porous medium is compressed together with the water that it contains. Clearly, the increase of the water pressure will also compress the individual grains. However, sand grains are about 50 times harder, or stiffer, than they are far less compressible than water. Therefore, the effect of the grains being compressed themselves can be safely neglected.

On the other hand, the porous medium itself is far less stiff than the grains. It is compressed due to some deformation of the grains at the expense of the porosity. In fact as it turns out, the compressibility of the porous medium is of the same order of magnitude as that of the water, so they must both be taken into account.

Hence the volume V_0 is compressed by ΔV when the pressure p is increased by Δp .

Assume the aquifer to be of infinite lateral extent, so that the only possible compression is downward. This implies that $\Delta V = \Delta H$, which is the change of the thickness of the considered part of the layer that we replaced by the springs in figure 4.9. Hence, both

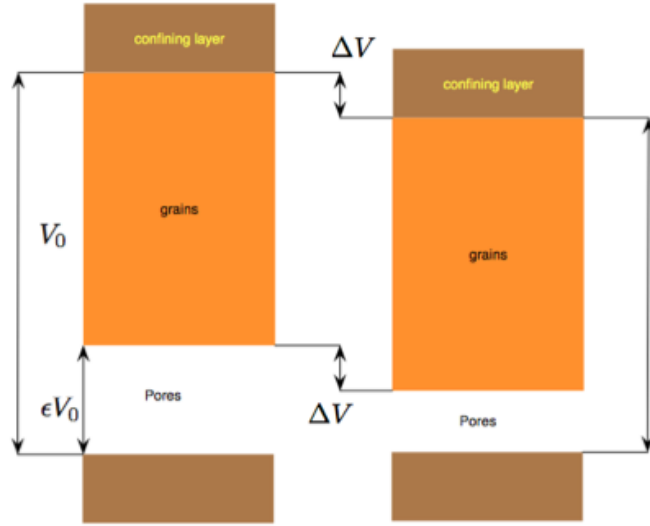


Figure 4.13: Compression of the porous medium, while the volume of the grains remains unchanged because their compressibility is negligible compared to that of both the water and the porous medium.

springs underlie the same compression ΔH .

Let the water have a compressibility α meaning that a m^3 of water would be compressed by the fraction α for each increase of the water pressure by 1 N/m^2 . Similarly, let the porous medium have a compressibility of β , meaning that one m^3 of the porous medium would be compressed by the factor β for each N/m^2 increase of effective σ_e . These compressibilities, therefore, have dimension $m^3/m^3/(N/m^2) = m^2/N$.

Now consider that the soil was put under an extra total pressure of Δp causing it to be compressed by the fraction $\Delta H/H_0 = \Delta V/V_0$. Then the effective pressure increases due to this compression ΔH by

$$\Delta\sigma_e = -\frac{\Delta V/V_0}{\beta}$$

Because the grains are considered incompressible, it follows that the change of pore volume equals the change of the total volume. Therefore, for the water we have a relative volume change (= compression) of ΔV per ϵV_0 . Therefore, the water pressure increase is

$$\begin{aligned}\Delta\sigma_w &= \frac{\Delta V / (\epsilon V_0)}{\alpha} \\ &= \frac{\Delta V/V_0}{\epsilon\alpha}\end{aligned}$$

Because we have now related both $\Delta\sigma_w$ and $\Delta\sigma_w$ to the relative volume change $\Delta V/V_0$,

we also know the ratio between the change of the effective pressure and the water pressure

$$\frac{\Delta\sigma_e}{\Delta\sigma_w} = \frac{\epsilon\alpha}{\beta}$$

and so

$$\Delta\sigma_e = \frac{\epsilon\alpha}{\beta}\Delta\sigma_w$$

With this, we can eliminate $\Delta\sigma_e$ from the pressure equation:

$$\Delta p = \Delta\sigma_w + \Delta\sigma_e$$

to obtain

$$\Delta p = \left(1 + \frac{\epsilon\alpha}{\beta}\right)\Delta\sigma_w$$

And because $\Delta\sigma_w/\Delta p = LE$ we have

$$LE = \frac{\beta}{\beta + \epsilon\alpha}$$

And because $BE = 1 - LE$ we also have

$$BE = \frac{\epsilon\alpha}{\beta + \epsilon\alpha}$$

4.2.5 Specific (elastic) storage coefficient

The specific storage coefficient is

$$S_s = -\frac{\partial V/V_0}{\partial \phi} \quad (4.2)$$

it is the volume of water released from the porous medium per m of lowering of the head ϕ (a negative $\Delta\phi$ yields a positive amount of water). It is also immediately clear that the dimension of S_s is $(m^3/m^3)/m = m^{-1}$, the volume of water released per m^3 of the porous medium per m of head decline.

Now consider the situation in which we lower the water pressure, for instance because by extracting water from the aquifer. Lowering of the water pressure in no way change the total pressure. Therefore, $\Delta p = 0$, which yields

$$0 = \Delta\sigma_w + \Delta\sigma_e \quad (4.3)$$

The amount of water squeezed out of the porous medium changes, however. A lowering of head causes an increase of the effective pressure (grain pressure), and hence is associated with a compression of the porous medium. Therefore, an increase of the effective pressure ($\Delta\sigma_e > 0$, reduces the pore volume by ΔV due to which the same volume of water is squeeze form the porous medium

$$\Delta V_{pm} = +V_0\beta\Delta\sigma_e$$

Where pm means "porous medium".

An increase of the water, would cause a compression of the water within the pores ϵV_0 , by

$$\Delta V_w = -\alpha (\epsilon V_0) \Delta\sigma_w$$

The total amount of water released equals the volume squeezed out due to the reduction of the pore space plus the volume that is generated by expansion of the water due to the reduction of the water pressure:

$$\Delta V = -\alpha (\epsilon V_0) \Delta\sigma_w + V_0\beta\Delta\sigma_e$$

and because $\Delta\sigma_e = -\Delta\sigma_w$ in this case (see equation 4.3) we have

$$\frac{\Delta V}{V_0} = -(\alpha\epsilon + \beta) \Delta\sigma_w$$

and so

$$\frac{\Delta V/V_0}{\Delta\sigma_w} = -(\epsilon\alpha + \beta)$$

using $\Delta\sigma_w = \rho g \Delta\phi$ yields

$$S_s = -\frac{\Delta V/V_0}{\Delta\phi} \quad (4.4)$$

$$= \rho g (\epsilon\alpha + \beta) \quad (4.5)$$

which, considering that we reduce the Δ to the infinitesimally small ∂ completes the proof (see equation 4.2).

4.2.6 Application (not for exam)

The compressibility of water is

$$\alpha = -\frac{1}{V_{w,0}} \frac{\partial V_w}{\partial \sigma_w} [L^2/F]^2$$

$\alpha \approx 4.4 \times 10^{10} \text{ m}^2/\text{N}$. Clearly, $\partial W_w/V_{w,0}$ is the relative change of the water volume. There is some dependency on dissolved components, water containing dissolved gas, may be up to three times more compressible than water without dissolved gas under normal pore pressure (Lyons, William C. (2010): Working Guide to Reservoir Engineering; Elsevier).

The compressibility of the porous medium is

$$\beta = -\frac{1}{V_{T,0}} \frac{\partial V_T}{\partial \sigma_e}$$

where $\partial V_T/V_{T,0}$ is the relative change of the volume of the porous medium. V_T is, the total volume of the considered soil (including its pores). σ_e is the effective stress (=pressure), i.e. that part of the total stress, p , that is not carried by the water pressure σ_w . The total pressure equals the weight of the overburden, i.e. that of the overlying formations including the water that it contains. Hence $\sigma_e = p - \sigma_w$.

The soil compressibility α is the gradient of a stress-strain curve (relative volume change versus applied effective stress) of a dry soil sample put under increased stress in the laboratory, such that side-ward movement is prevented, exactly as it is the case in the actual soil under uniform vertical stress. Unlike water, the compressibility of soil is not necessarily a constant. If the soil is put under higher stress than it ever supported, then it consolidates, meaning that the change of volume is largely irreversible. But under lower than historic stresses, a compressibility can be determined, and truly elastic behavior assumed. It is clear that this compressibility depends on porosity.

[Van der Gun (1980)] presented the following relation between the compressibility of aquifers and depth based on laboratory measurements from laboratory carried out by Van der Knaap (1959)

$$\beta = \epsilon (3 \times 10^{-11} + 6.6 \times 10^{-11} z^{-0.7}) \quad (4.6)$$

where z is the depth below ground surface and ϵ is porosity. Then applying 4.4

$$S_s = \rho g (\epsilon \alpha + \beta)$$

With the relation of [Van der Gun (1980)] we obtain the graphs shown in 4.14. As can be concluded from the graph, values in the order of 10^{-5} Pa^{-1} are often found in practice, where we generally have porosities of around 35% in fluviatile and eolian sandy aquifers.

Question: Is it feasible that compressibility of the porous medium is proportional to porosity?

4.2.7 Questions

1. Explain what loading efficiency is.

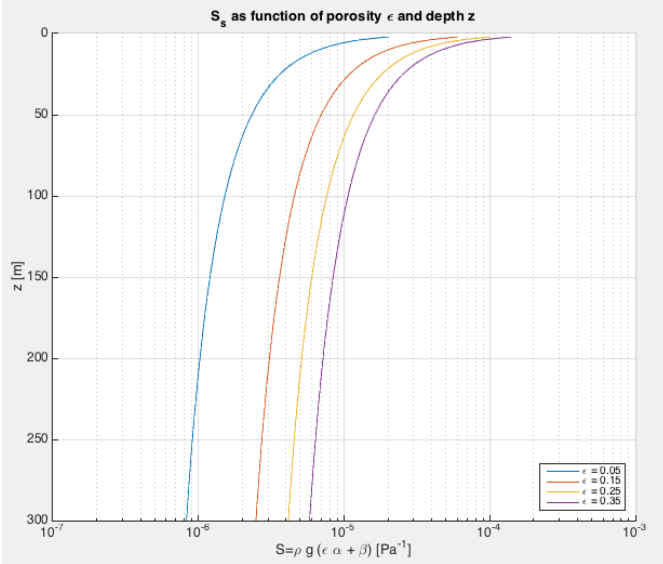


Figure 4.14: Computed specific storage coefficient $Ss = \rho g (\epsilon\alpha + \beta)$ [m^{-1}] as a function of depth below ground surface using the relation by [Van der Gun (1980)])

2. What factors contribute to the elastic storage coefficient and what factor may be neglected?
3. If a load Δp is placed on top of a confined aquifer and the water pressure in the aquifer is increased to $\Delta\sigma_w = LE \Delta p$, then how much does the head in a piezometer in that aquifer change?
4. The same question for the situation where Δp is caused by an increase of the barometer.
5. Assume we have a pressure gauge (pressure transducer or pressure sensor) in a piezometer in the confined aquifer that measures the absolute pressure (air pressure + water pressure). On day 1, the barometer rises by Δp and later with zero rise of the barometer, a load Δp is placed on ground surface. What is the difference if any in the registration by the pressure gauge in the piezometer, and what is the difference in head?
6. The measurements of pressure gauges confined and semi-confined aquifers are corrected for barometer pressure changes by subtracting the barometer pressure from the pressure measurement. Does this mean that the fluctuations of the barometer pressure are eliminated by this correction? If so explain why. If not also explain why.
7. What is actually the result of this correction of the registered pressures? What actually do we get by this correction?

8. How can we compute the specific yield from the measured barometric efficiency?

Note:

$$BE = 1 - \frac{\beta}{\epsilon\alpha + \beta}$$

$$Sy = \rho g(\epsilon\alpha + \beta)$$

Think of what we can easily estimate and what we know, respectively what we don't know? Assume that porosity ϵ can be reasonably well estimated.

9. Consider a confined aquifer and the following two situations. First there is a loading on ground surface with value Δp . The head is measured both in a piezometer and in a pressure gauge (which measures the absolute water pressure in the aquifer). What is the difference between the two measurements?
10. In the same location, consider an increase of the barometer pressure that is of the same magnitude as the surface loading Δp before, so $\Delta a = \Delta p$. What is the difference in the head measured with a piezometer and that measured with a pressure gauge?
11. What is the difference between the heads measured with the piezometer in the two cases?
12. What is the difference between the pressures measured with the pressure gauges in the two cases?
13. How much is the barometer effect in an unconfined aquifer.
14. If an infinitely extended surface load would remain constant. How will the head or pressure in a piezometer in a semi-confined aquifer behave?
15. What could we do with such behavior?
16. With two pressure transducers, one measuring the barometer pressure and the other the water pressure in some piezometer in a confined aquifer how can we compute the barometer efficiency? What parameter we still miss to obtain true numerical values?
17. How does the head in a water-table aquifer react to barometer fluctuations?
18. How large may the variation of the head due to barometer fluctuations become given a range of atmospheric pressure from variation between 970 to 1040 mbar (=cm head)?
19. What values do you expect for total elastic storage coefficients of aquifers in practice?

20. How could we measure the elastic storage coefficient in a confined aquifer below the sea bottom?
21. Does the value of the specific yield that we may derive from barometer efficiency, water storativity and porosity refer to the value of the measuring point or to the thickness of the entire aquifer?
22. How useful is it to measure local porosity at the screen position of the piezometer to compute the storage coefficient of the aquifer?

4.3 Earth tides (not for exam)

Even far from the ocean and even after correcting for varying barometer pressures ground-water head in confined aquifers may show a response that closely resembles tides. This fluctuation matches the passage of sun and moon, exactly like sea tides, ([[Todd \(1959\)](#), [Todd and Mays \(2005\)](#), [Bloemen et al. \(1989\)](#)]), Figure 4.15.

Like normal tides, earth tides are an indirect consequence such gravity variations. It can be shown that they are caused as an indirect effect of the deformation of the earth's mantle on which the stiff crust floats. A bulge is formed by the mantle by the attraction of sun and moon. The earth crust itself is so thin compared to the earth mantle that it behaves like a thin hard sheet floating on the mantle and is stretched by the mantle as it bulges out under tidal attraction. During stretching porosity increases and the head lowers. When the stretching is released, the opposite occurs as is shown in equation 4.15.

This variation may be estimated with up to 50% accuracy from solid earth-tide theory [[Shieh et al. \(1987\)](#)]. The dilatation (stretching) is more or less fixed due to the relation with the mantle, but different, for any point on earth. According to [[Bredehoeft \(1967\)](#)] it is about

$$\Delta\phi \approx \frac{10^{-8}}{S_s}$$

on moderated latitudes it is about. Using this number, one may relate the expected magnitude of the water level fluctuations directly to the specific storage coefficient. With S_s in the order of $10^{-6}/m$ for sandstones and $10^{-7}/m$ for granites, a fluctuation amplitude of 1 to 10 cm may be expected.

A thorough analysis of earth tides is beyond the scope of this course. There is a wealth of literature on the subject a good quantitative paper is [[Kamp and Gale \(1983\)](#)].

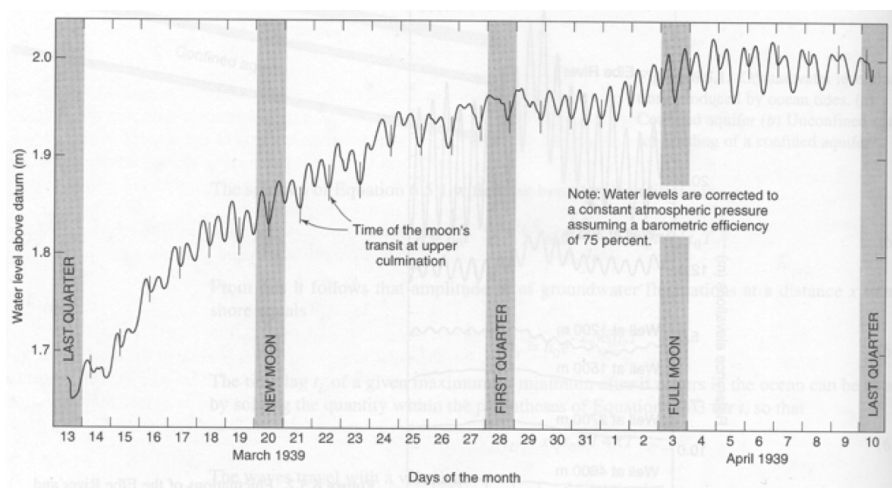


Figure 4.15: Water level fluctuations in a confined aquifer produced by earth tides (from [Todd (1959), Todd and Mays (2005)])

5 One-dimensional transient groundwater flow

5.1 Scope

In this course, we will deal with transient groundwater flow in one-dimensional and radial situations (wells) for which analytic solutions are available. Analytic solutions are important because they allow insight in the behavior of the groundwater system, whereas numerical solutions do not; they only produce numbers. Analytic solutions are also important because they allow checking numerical models and checking numerical models is always necessary, not just because of possible errors in the model, but also because of possible errors in the input of the model. Analytical solutions also allow analysis of numerical models, which helps to understand their outcome. Finally, analytical solutions are powerful because they allow a rapid result with minimal input. They become even more powerful if combined with superposition and convolution.

5.2 Governing equations

We will always start our discussion with the governing differential equation at hand. Once we have it, we need to solve it. To be able to do that we need boundary conditions specifying fixed heads or fixed discharges along certain parts of the model boundaries. In the case of transient solutions we also need initial conditions specifying the head everywhere in the considered domain at time zero. Initial and boundary conditions are as important as the differential equation itself.

One-dimensional flow means a cross section with no flow components perpendicular to it.

We will treat analytical solutions for one layer only. Analytical solutions for more than one layer exist and have been extended to arbitrary numbers of layers in the 1980s by Kick Hemker and Kees Maas, see for instance Maas (1986) and Hemker and Maas (1987). These solutions require matrix computations, which were cumbersome at the time, but which may nowadays be readily computed in programs like Matlab and Maple. An implementation of the so-called eigen values and eigen vectors would be necessary to compute such solutions in a spreadsheet. This is possible, but beyond this course. Therefore, we limit ourselves to single-layer cases.

Let us first derive the partial differential equation, starting with continuity. Considering an small section of the cross section, of length Δx , the water balance over a short time Δt may, continuity can be expressed as follows:

$$\left[Q_x - \left(Q_x + \frac{\partial Q_x}{\partial x} \Delta x \right) \right] \Delta t + N \Delta x \Delta t = S \Delta x (\phi_{t+\Delta t} - \phi_t)$$

with Q [L^2/T] the discharge in the aquifer integrated over its full height, N [L/T] recharge and S [–] the storage coefficient. Taking the limit for $\Delta x \rightarrow dx$ and $\Delta t \rightarrow dt$ yields the continuity equation

$$-\frac{\partial Q}{\partial x} + N = S \frac{\partial \phi}{\partial t} \quad (5.1)$$

Now inserting Darcy's law, with $Q = -kD \frac{\partial \phi}{\partial x}$ yields the governing partial differential equation

$$-\frac{\partial}{\partial x} \left(-kD \frac{\partial \phi}{\partial x} \right) + N = S \frac{\partial \phi}{\partial t} \quad (5.2)$$

and with kD is constant

$$\frac{\partial^2 \phi}{\partial x^2} + \frac{N}{kD} = \frac{S}{kD} \frac{\partial \phi}{\partial t} \quad (5.3)$$

We will predominantly ignore recharge, so $N = 0$. Ignoring recharge is seldom a problem because we can solve most problems using superposition. Further notice that we may write $s(x, t) = \phi(x, t) - \phi_0$ where $s(x, t)$ is the head change relative to the initial situation ϕ_0 , which may even depend on x .

So that for 1D groundwater dynamics we will mostly work with solutions of the following partial differential equation where $s = s(x, t)$ is called the head change or often also the drawdown, especially when dealing with groundwater extraction and wells

$$\frac{\partial s}{\partial t} = \frac{kD}{S} \frac{\partial^2 s}{\partial x^2} \quad (5.4)$$

Equation 5.4 is known as the diffusion equation. It appears in many scientific fields like with diffusion, dispersion, heat conduction, sorption, consolidation and so on. Many researchers have derived solutions for it for specific boundary conditions. The coefficient S/kD is called the diffusivity, often written as a thick D, like \mathbb{D} , which always has dimension $[L^2/T]$ whatever the scientific branch is. The diffusivity is the ratio of the ease of the flow (transmissivity) and the storage:

$$\mathbb{D} = \frac{kD}{S}$$

In the case of a phreatic (unconfined, water table) aquifer, the aquifer thickness is no longer constant. However, there are no transient solutions that take a time varying aquifer thickness into account. Linearization is then unavoidable, meaning that one has to choose a proper average aquifer thickness and be aware that the head change should remain small with respect to the saturated aquifer thickness.

5.3 Sinusoidal fluctuations

This section deals exclusively with sinusoidal fluctuations in groundwater caused by a sinusoidal fluctuating head at the boundary at $x = 0$. We deal with tidal fluctuations in groundwater first and then show temperature as another application of the same basic partial differential equation.

5.3.1 Tidal fluctuations in groundwater

A number of transient problems can be analyzed by assuming regular sinusoidal fluctuations of some boundary conditions. Generally the result will also behave like a sine in the same frequency. If we have the solution of a general harmonic fluctuation, we may solve many problems by superposition of any combination of frequencies that we need to adjust the fluctuations at the boundary to our liking. This way, hourly, daily, weekly and seasonal fluctuations may be readily combined. Examples of applications are tides in groundwater, penetration of temperature fluctuations, consolidation etc.

Figure 5.1 shows a half space (confined aquifer) in direct connection with a surface water body with a fluctuating water level, causing fluctuations in the adjacent aquifer that are delayed and damped relative to the forced fluctuation at $x = 0$.

The differential equation for this system was already derived (see equation 5.4). It may be solved for a sinusoidal fluctuation of the water level at $x = 0$. For this we assume the head change relative to the mean head is

$$s(x, t) = A e^{-ax} \sin(\omega t - bx) \quad (5.5)$$

where A is the amplitude of the tide at $x = 0$, and ω is the angular velocity of the tide. Its dimension is [radians/T] = [T⁻¹]. A full tide time T relates to ω as

$$\omega T = 2\pi \quad (5.6)$$

Notice that we can always change the phase of the tide by adding an arbitrary angle ν to the argument of the sine. ν is then the angle at $t = nT$, where n is an arbitrary integer. For an aquifer with constant kD and S this solution is indeed valid for

$$a = b, \quad a = \sqrt{\frac{\omega}{2D}} = \sqrt{\frac{\omega S}{2 kD}} \quad (5.7)$$

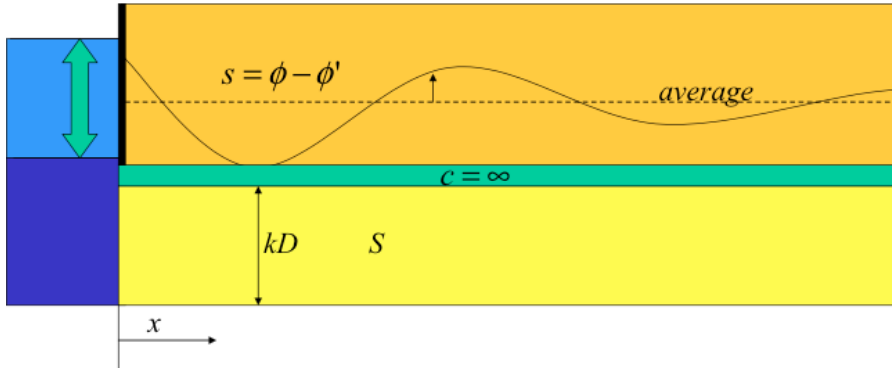


Figure 5.1: Sinusoidal water level fluctuation in surface water causing tide in the groundwater system

Semi-confined case (not for exam)

Notice that in the semi-confined case, where linear tide-induced leakage occurs between the aquifer and the overlying layer with constant head, $a <> b$. In that was worked out in the PhD Thesis of Bosch (1951). The results are

$$\begin{aligned} a &= \frac{1}{\lambda} \sqrt{\frac{1}{2} + \frac{1}{2} \sqrt{1 - (\omega Sc)^2}} \\ b &= \frac{1}{\lambda} \sqrt{-\frac{1}{2} + \frac{1}{2} \sqrt{1 + (\omega Sc)^2}} \\ \lambda &= \sqrt{kDc} \end{aligned}$$

Below the proof is given for the solution

Proof that the solution in equation 5.8 is correct. We have to proof that equation 5.5 fulfills equation 5.4. The constant is dropped, as it does not affect the proof. Taking the needed derivatives

$$\begin{aligned}\frac{1}{A} \frac{\partial s}{\partial x} &= -a e^{-ax} \sin(\omega t - bx) - b e^{-ax} \cos(\omega t - bx) \\ \frac{1}{A} \frac{\partial^2 s}{\partial x^2} &= a^2 e^{-ax} \sin(\omega t - bx) + ab e^{-ax} \cos(\omega t - bx) + \\ &\quad + ab e^{-ax} \cos(\omega t - bx) - b^2 e^{-ax} \sin(\omega t - bx) \\ \frac{1}{A} \frac{\partial s}{\partial t} &= \omega e^{-ax} \cos(\omega t - bx)\end{aligned}$$

by collecting the sines and the cosines separately, we get

$$a^2 - b^2 = 0 \rightarrow a = b$$

and so,

$$\frac{kD}{S} ab = \omega \rightarrow a = \sqrt{\frac{\omega}{2} \frac{S}{kD}}$$

Which completes the proof.

The solution, therefore, is, because the arbitrary constant β_0 does not affect the proof of correctness.

$$s(x, t) = A e^{-ax} \sin(\omega t - ax + \beta_0) \quad (5.8)$$

with β_0 a constant, namely the phase at $x = 0$ and $t = 0$.

The discharge is obtained by using Darcy

$$\begin{aligned}Q(x, t) &= -kD \frac{\partial s}{\partial x} \\ &= a kD A [e^{-ax} \sin(\omega t - ax + \beta_0) + e^{-ax} \cos(\omega t - ax + \beta_0)] \quad (5.9)\end{aligned}$$

What is the velocity of the wave, or what is the delay of the wave at any distance x from the sea or river? To find the answer we move along with the wave such that the phase is constant, e.d. equal to c . Hence

$$\omega t - ax + \beta_0 = c$$

Then determine the velocity by computing dx/dt . So

$$\omega - a \frac{dx}{dt} + 0 = 0$$

leading to

$$v = \frac{dx}{dt} = \frac{\omega}{a} \quad (5.10)$$

The delay of the wave at any x relative to the wave at $x = 0$ is then

$$t = \frac{x}{v}$$

How much is the wavelength in the ground? One answer is that $\omega\Delta t = 2\pi$ so that $\Delta t = 2\pi/\omega$ and so $\Delta x = v\Delta t = v2\pi/\omega = 2\pi/a$.

The other approach is taking the argument of the sinus and demanding that

$$\omega t - a(x + \Delta x) + \beta_0 - [\omega t - ax + \beta_0] = 2\pi$$

hence

$$\begin{aligned} a\Delta x &= 2\pi \\ \Delta x &= 2\pi/a \end{aligned}$$

which is the same answer.

Instead of ω , we may use the cycle time as given above in equation 5.6, $\omega = 2\pi/T$ and so $a = \sqrt{\frac{\pi S}{T kD}}$

So we see that the head is indeed a damped sine. The damping is stronger for higher frequencies and larger storage coefficients and for lower conductivities.

5.3.2 Fluctuations of temperature in the subsurface

For heat conduction the same diffusion equation applies if we replace head change by temperature. The only thing that changes is the Diffusivity. The ease of flow is now the heat conduction λ [W/m] = $[(E/T)/L^2] / (K/L) = [E/(TKL)]$ and the storage is the heat capacity ρc [E/L³/K]. The dimension is again [L²/T] :

$$\mathbb{D} = \frac{\lambda}{\rho c} \left[\frac{E/(TKL)}{E/(KL^3)} \right] = \left[\frac{L^2}{T} \right]$$

(notice that in the dimension E = energy, T = time, L = length, K = temperature (from Kelvin)).

Because both the heat conduction and the heat capacity have a contribution from both the water and the grains (solids) of the aquifer we can compute them as the combination of these contributions. With ϵ for porosity we then have

$$\begin{aligned} \lambda &= \epsilon\lambda_w + (1 - \epsilon)\lambda_s \\ \rho c &= \epsilon\rho_w c_w + (1 - \epsilon)\rho_s c_s \end{aligned}$$

ρ [M/L³] is density and c [E/ (MK)], i.e. heat per kg solids per degree kelvin (= degree Celsius).

The heat capacity of saturated sandy soils is about $\lambda = 3 \text{ W/m/K} = 3 \text{ J/s/m/K}$. The specific heat capacity of water is $c_w = 4018 \text{ J/kg/K}$ and that of sand grains $c_s \approx 800 \text{ J/kg/K}$. With $\rho_s \approx 2650 \text{ kg/m}^3$ and $\epsilon \approx 35\%$ we get $\rho c = 2.85 \times 10^6 \text{ J/m}^3/\text{K}$.

The diffusivity then becomes

$$\mathbb{D} = \frac{\lambda}{\rho c} = \frac{3}{2.85 \times 10^6} = 1.06 \times 10^{-3} \text{ m}^2/\text{s} = 0.091 \text{ m}^2/\text{d}$$

From which we have

$$a = \sqrt{\frac{\omega}{2\mathbb{D}}} = \sqrt{\frac{\pi}{T\mathbb{D}}}$$

With these values it is possible to compute between what temperatures the temperature varies at different depth depending on the cycle time, i.e. due to daily, weekly, monthly or yearly temperature fluctuations at ground surface, the so-called temperature envelopes according to

$$T_{mean} - A \exp(-az) \leq temp \leq T_{mean} + A \exp(-az)$$

The monthly temperature in the Netherlands varies between 3.1C in January and 17.9 in July. The yearly amplitude is thus 7.4C with an average of 10.5C. Using this in the example, we can compute the temperature envelopes, that is, the lowest and highest temperatures lines between which the actual temperature will vary during one cycle time. Figure 5.2 shows the results, all computed for the same mean temperature and the same amplitude but for different cycle times as indicated in the legend. With the used data, the yearly temperature variation will barely reach 20 m below ground surface, a decade 50 m and 30 years 100 m. This implies that climate change may be measured using the change of the temperature at for instance 50 m below ground surface when measurements in the past are available, as is actually the case in the Netherlands.

5.3.3 Questions

1. Prove the correctness of the given solution yourself. As an extra exercise you could prove that equation 5.9 is correct by filling it into the partial differential equation for continuity $\frac{\partial Q}{\partial x} = -\frac{S}{kD} \frac{\partial s}{\partial t}$.
2. If the transmissivity if doubled, what is the effect on the drawdown?
3. When the ω is doubled, what is the effect on the drawdown?
4. Explain how the distance to where the fluctuation of the sea or lake reaches in the aquifer depends on the frequency of the wave.

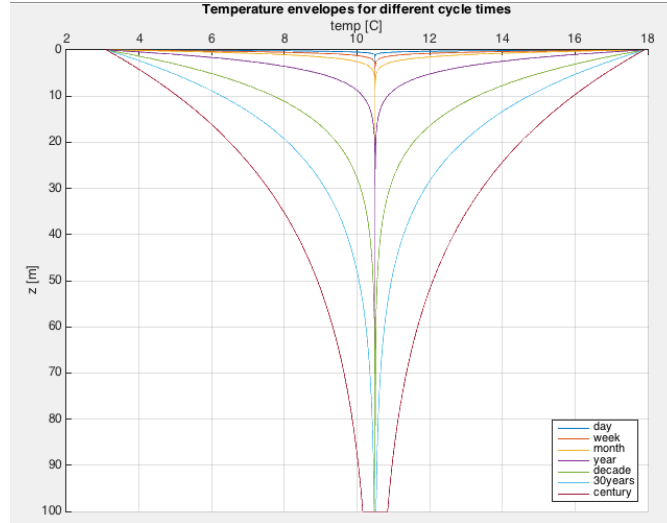


Figure 5.2: Temperature envelopes in the subsurface due to temperature fluctuations at ground surface with mean 10C and amplitude 7.4C. Envelopes depend on cycle time of the fluctuation (see legend).

5. What is the depth effect of waves on the beach with one cycle per second, tides with one cycle per 12 hours, moon-tides with one cycle per two weeks in an aquifer with transmissivity is 500 m²/d and a storage coefficient of 0.001 and 0.1 respectively?
6. Let the solution to the diffusion equation for the confined aquifer be $s(x, t) = A \exp(-ax) \sin(\theta_0 + \omega t - ax)$ and let $kD = 1000 \text{ m}^2/\text{d}$, $S = 10^{-3}$, and the amplitude $A = 2 \text{ m}$, and θ_0 is an arbitrary constant. Take time in days and show the head change $s(x, t)$ in Python or a spreadsheet.
7. Include the discharge $Q(x, t)$
8. Compute and also show the envelope of the wave as a function of x .
9. How far inland can we still measure the tide if our device allows us to see a variation of 1 cm?
10. What is the velocity of the wave?
11. What is the delay at 1000 m from the shore (or show the delay graphically as function of x)?
12. Add the case for a storage coefficient, $S_y = 0.2$. And show the relation between the case with $S = 0.001$ and $S_y = 0.2$.
13. Create a complex input using of 4 sines, each with a different initial angle θ_0 , amplitude A and angular velocity ω and show the result.

Copy your worksheet or Python code and alter the copy to answer the following question:

1. The head in a lake above a clay bottom varies daily 30 cm. How deep does this fluctuation penetrate the underlying clay layer with conductivity of 10^{-4} m/d and a specific storage coefficient of $S_s = 0.0001$ /m?
2. What if the variation is weekly, monthly and seasonally only?
3. If the sea is shallow and the clay layer is below the sea bottom, what will be the amplitude in the confined aquifer for the water compressibility $\beta_w = 5 \times 10^{-5}$ and porous matrix compressibility $\beta_s = 2 \times 10^{-5} \text{ m}^2/N$?
4. If the clay layer would be semi-pervious, what would this mean for the amplitude in the confined aquifer? Would it be greater, smaller compared with the case with a completely impervious layer?

Heat flow

1. What is the penetration depth of a diurnal, seasonal and centennial temperature wave at ground surface given and porosity of $\epsilon = 0.35$?
2. Heat flow and groundwater flow show the same partial differential equation except that drawdown is replaced by temperature change. They both have one coefficient called diffusivity. What is the dimension of this diffusivity?
3. Diffusivity consists of a part that expresses the ease of flow, λ , and a part that expresses the storage, ρc . What are these factors in the groundwater case and what are they in the heat flow case?
4. Show their dimensions and prove that the dimension of the diffusivity is the same in both cases.
5. Groundwater flow was ignored when we discussed heat flow. How would the temperature envelopes change due to upward groundwater seepage?
6. How would they change due to downward seepage? How much would you estimate the effect on the yearly temperature envelopes if the recharge is 333 mm per year and porosity is 33%?

5.4 Non-fluctuating interaction with surface water

5.4.1 Basins of half-infinite lateral extent

Consider a confined aquifer in direct contact with surface water as in figure 5.3. The aquifer thickness, transmissivity and storage coefficient are everywhere the same. The aquifer is half-infinite, which means that its right end extends to infinity. We consider the aquifer confined, because we will assume that its thickness is the same everywhere

and stays so to allow a closed analytical solution for the time-dependent groundwater flow. The aquifer being in direct contact the the surface water implies that there is no hydraulic resistance of any kind between the surface water and the aquifer.

We present here a basic analytical solution, which describes the change of head (and flow) caused by a sudden change of the surface-water level a an amount a.

In the confined case we use the elastic storage coefficient, $S = DS_s$ and in the unconfined case we use the specific yield, S_y . In cases where we consider unconfined aquifers, the effective thickness of the aquifer changes with the water table, and hence with the head. However, as long as the change of head is small compared to the thickness of the aquifer we may still apply the solution in practical cases and accept the small error that will cause the assumption of constant thickness in those cases.

Initially, the head is ϕ' in figure 5.3 and the head $\phi(x, t)$ varies in space and time due to a sudden change of head of the bounding surface water by a at $t = 0$. The surface-water head remains at $\phi' + a$ thereafter.

Because superposition applies (due to linear governing partial differential equation), we may just superimpose the change of head change $s(x, t) = \phi(x, t) - \phi'$, irrespective of the actual situation. The only thing that matters to us is the **change of head** s that is caused by the sudden change of the water level in the bounding surface water by the value a .

The case considered here is a base case. There exists a whole series of analytical solutions for different boundary conditions, which that are presented in the next section 5.4.3 for reference only, but they are not for the exam.

Consider a one-dimensional aquifer of infinity lateral extent as shown in figure 5.3 that is in direct contact with a fully penetrating water body at $x = 0$. Ignoring leakage and recharge, and assuming a constant transmissivity kD and storage coefficient S , the partial differential equation is the diffusion equation:

$$kD \frac{\partial^2 s}{\partial x^2} = S \frac{\partial s}{\partial t} \quad (5.11)$$

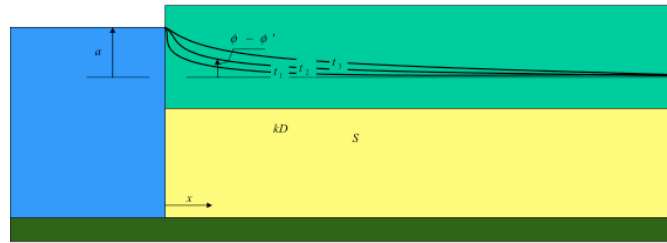


Figure 5.3: One-dimensional groundwater aquifer which extends to infinity to the right, and has constant transmissivity kD and storage coefficient S , while it is in direct contact with surface water at $x = 0$ in which the water level is suddenly changed by a at $t = 0$

One well-known solution is for the case in which the head at $x = 0$ is suddenly raised by a value, A , and maintained from that time on, while the initial head is zero throughout (Figure 23).

The solution is

$$s(x, t) = \phi(x, t) - \phi_0 = A \operatorname{erfc}(u), \quad u = \sqrt{\frac{x^2 S}{4kDt}}$$

Where $s(x, t)$ is the head change, $\phi(x, t)$ the head and $\phi_0(x)$ the initial head that may be a function of x , because that does not interfere with the principle of superposition.

By definition

$$\operatorname{erfc}(z) = \frac{2}{\sqrt{\pi}} \int_z^{\infty} e^{-y^2} dy \quad (5.12)$$

and so its derivative is

$$\frac{d \operatorname{erfc}(z)}{dz} = -\frac{2}{\sqrt{\pi}} e^{-z^2}$$

Therefore, the discharge is

$$Q = -kD \frac{\partial s}{\partial x} = A \sqrt{\frac{kDS}{\pi t}} \exp\left(-\frac{x^2 S}{4kDt}\right)$$

and, for $x = 0$

$$Q_0 = A \sqrt{\frac{kDS}{\pi t}}$$

The function $\operatorname{erfc}(-)$ is the so-called complementary error function. Abramowitz & Stegun (1964) provide tables and expressions to compute this function in several ways. The erfc function is also one of the functions present in Excel. Its graph is shown in figure 5.4

Hence the solution of head change versus distance to shore always has the shape of this curve, be it that the horizontal axis will be squeezed or stretched depending on the values of the parameters in u . The shorter the time, the larger u , the more compressed is the horizontal axis. A small kD or large S also has the effect of compressing the horizontal axis.

For the understanding it is convenient to express $u = x/L$ so that $L = \sqrt{4kDt/S}$, which is a constant for any fixed t . For this fixed t , L may be considered a characteristic distance, as it scales x . For instance, half of the initial head change has been reached when $u = 0.5$ that is at a distance $x = 0.5L$. Also, the head change is about 10% of a at $u = 1$, that is at $x = L$ with L fixed for the time of observation. No head rise has yet occurred for about $u = 2.5$ hence for $x > 2.5L$. This is all practical information when judging an actual situation, without the need for a computer.

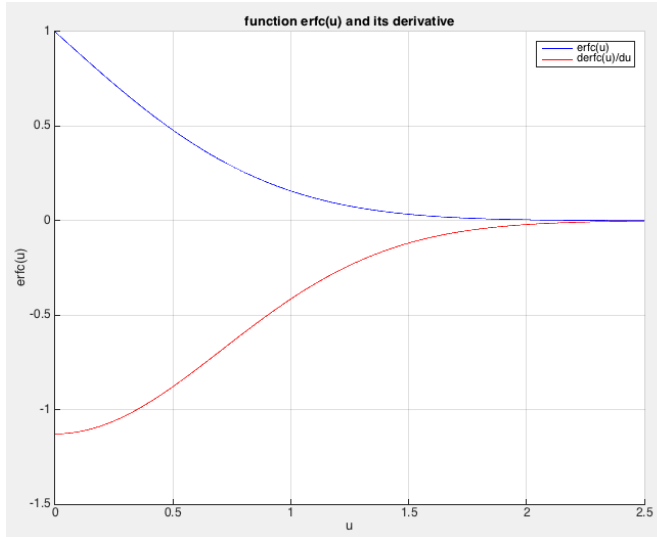


Figure 5.4: $\text{erfc}(u)$ and its derivative $-(2/\sqrt{\pi}) \exp(-u^2)$

It is also possible to plot $\text{erfc } u$ and its derivative versus $1/u$. To make the graph meaningful, we have to use a logarithmic scale for $1/u$ as is shown in figure 5.5. The time scale is then proportional to \sqrt{t} . We can write $u = \sqrt{t/T}$ with $T = 4kD/x^2S$ where T can be considered a characteristic time for fixed distance x . We see that for $t/T \approx 2$ about half the final (maximum) head change has been reached. It is useful and practical to consider this graph from the perspective of t/T and not t . Taking this perspective one only needs one graph; it covers all possible cases, the only thing that changes when choosing another observation point is the value of T . T can really be considered characteristic for the situation at a chosen distance x . The graph also shows that some time elapses before the influence of the river reaches the observation point. This value of $1/u$ for this time is about 0.4 as shown in figure 5.5. Hence $\sqrt{1/T} = 0.4$ so $t = 0.16T$. The result is also universal. 90% of the final head is reach at about $1/u = 10$ so $\sqrt{t/T} = 10$, so $t = 100T$. And so forth.

For the discharge we need the derivative, which is also shown in both figures (in red).

Exercise: Proof that equation 5.12 fulfills the partial differential equation 5.11.

5.4.2 Questions

1. All drawdowns due to a sudden change of river stage are expressed in a simple erfc-function. Can you express the argument u using a ratio of the distance x from the river and some characteristic distance X that is valid for a fixed time?
2. What is the ratio x/X for $s = 0.5s_0$?

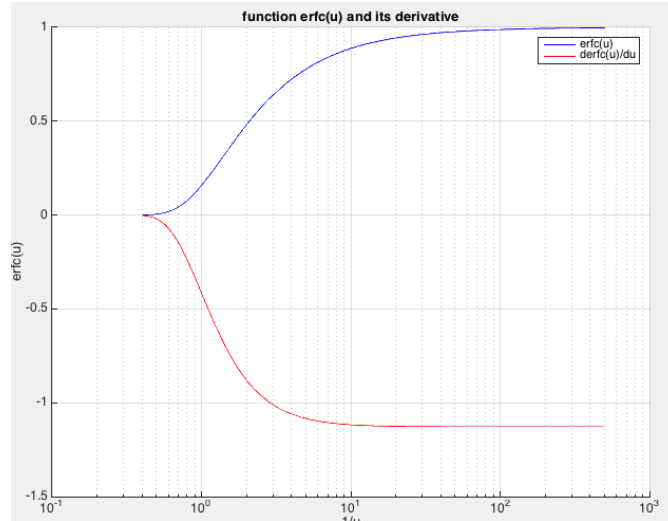


Figure 5.5: $\text{erfc}(u)$ and its derivative as a function of $1/u$ instead of u

3. Alternatively, how could you express the drawdown as a ratio between time and a characteristic time T for a fixed distance?
4. What is then the ratio t/T for $s = 0.5s_0$?
5. At what time expressed at t/T would you expect to head to start changing at some given fixed distance x after a sudden change of river stage at $x = 0$?
6. Given the mathematical expression for the drawdown, derive yourself the expression for the discharge $Q(x, t)$.
7. What is the discharge at $x = 0$ mathematically?
8. An aquifer ($kD = 400 \text{ m}^2/\text{d}$, $S = 0.1$) in good contact with a river. The water level in the river changes 2 m in a very short time. Show the effect of this change for a point at 10, 100 and 1000 m?
9. How long does it take that the head change in the three points is 10 cm?
10. Show the head over time in these points.
11. Show the discharge over time in these points.
12. How long will it take until the head in the center of a 10 m thick aquitard with resistance $c = 5000 \text{ d}$ has reached half the head change suddenly applied at both its top and bottom at $t = 0$?

A canal in a dune area is used to provide storage for drinking water in the case of an emergency. $kD = 100 \text{ m}^2/\text{d}$, $S = 0.2$. During such an emergency, the water level in the canal is suddenly lowered by 5 m.

1. How much water will flow into the storage canal from two sides in 1 day, 1 week, 6 weeks?
2. What will be the drawdown over time at 10, 100, 300, 1000m (the storage in the canal itself)?
3. How long may the extraction continue if the maximum drawdown is 5 m?
4. How much groundwater has been extracted when this drawdown has been reached?
5. We neglected the volume in the canal itself. What percentage is the canal volume compared to that of the groundwater entering the canal from the sides? Assume the canal is 20 m wide?
6. Compute the flow to the canal in 6 weeks if there is a fixed-head boundary condition at 70 m distance.

5.4.3 Higher-order solutions (not for exam)

The previous well-known basic solution is the first of an infinite series of solutions of the same partial differential equation but different boundary conditions, namely $s(0, t) = a t^{n/2}$ with a a constant and $n \geq 0$. The solution given above is for $n = 0$. The entire series of solutions is given as

$$s(x, t) = A t^{n/2} \frac{i^n \operatorname{erfc} u}{i^n \operatorname{erfc} 0}, \quad u = \sqrt{\frac{x^2 S}{4kDt}}$$

where $i^n \operatorname{erfc} u$ is the n^{th} repeated integral of the complementary error function (see Abramowitz & Stegun, 1964, section 7.2). A number of these functions is shown in figure 5.6.

By definition

$$i^n \operatorname{erfc} z = \int_z^\infty i^{n-1} \operatorname{erfc}(\zeta) d\zeta$$

with

$$i^0 \operatorname{erfc} z = \operatorname{erfc} z$$

and

$$i^{-1} \operatorname{erfc} z = \frac{2}{\sqrt{\pi}} e^{-z^2}$$

Higher order functions may be computed by the recursive relation

$$i^n \operatorname{erfc} z = \frac{-z}{n} i^{n-1} \operatorname{erfc} z + \frac{1}{2n} i^{n-1} \operatorname{erfc} z$$

By applying Darcy's law, we find the discharge

$$Q(x, t) = \frac{\sqrt{kDS}}{2\sqrt{t}} A t^{n/2} \frac{i^{n-1} \operatorname{erfc} u}{i^n \operatorname{erfc} 0}$$

The other way around when we write

$$Q(0, t) = A t^{n/2}, \quad n \geq 0$$

it is directly found that

$$Q(x, t) = A t^{n/2} \frac{i^{n-1} \operatorname{erfc} u}{i^n \operatorname{erfc} 0}$$

with

$$s(x, t) = \frac{2}{\sqrt{kDS}} A t^{n/2} \frac{i^n \operatorname{erfc} u}{i^n \operatorname{erfc} 0}$$

A basic solution is immediately obtained for $n = 0$, so that $Q(0, t)$ is constant.

These functions may be used to compute the head and flow due to either a constant or changing head at $x = 0$ or to either a constant or changing flow at $x = 0$. Computations are easily done in Excel after the functions have been implemented as User Defined Functions in Visual Basic.

Example: For instance, the water level in Lake Nasser in Egypt has risen by 60 m between 1971 that the dam at Aswan was closed and 1991 when the lake was full. This boils down to 3 m/year. Assume further that the bordering aquifer is 200 m thick and that it has a conductivity $k = 1 \text{ m/d}$ and a specific yield $S_y = 0.1$. One could then ask the question, how far the effect of the filling of the lake would be measurable in the bordering groundwater, and hence how much lake water would have been stored in that same period.

Hence we have:

$$s(x, t) = A t^{n/2} \frac{i^n \operatorname{erfc} u}{i^n \operatorname{erfc} 0}, \quad u = \sqrt{\frac{x^2 S}{4kDt}}, \quad A = 3 \text{ m/y}, \quad n = 2$$

and

$$s(x, t) = A t \frac{i^2 \operatorname{erfc} u}{i^2 \operatorname{erfc} 0}, \quad Q(x, t) = \sqrt{\frac{kDS}{4t}} A \frac{i^1 \operatorname{erfc} u}{i^2 \operatorname{erfc} 0}$$

with proper values of kD and S , a graph can be made for s and Q as a function of x for given times or for the head as a function of time for given values of x . This exercise is left to the reader.

Figure 5.6: $i^n \operatorname{erfc}$ functions

5.4.4 Questions

1. What is the mathematical expression for the head $s(x, t)$ and the discharge $Q(x, t)$ for the case in which the river stage increases linearly with time?
2. The same for the case when the discharge increases linearly with time.
3. Let a lake (like Lake Nasser) have a water level that linearly raised between 1971 and 1991 by 60 m. Compute the change of head in the aquifer at 1 km adjacent to the lake. Assume the $kD = 1000 \text{ m}^2/\text{d}$ and $S = 0.1$.
4. Compute the total amount of water that infiltrated over this period.
5. Assume the aquifer has constant thickness and its porosity is 35%. With this information compute how far the lake water penetrated the aquifer during this period.
6. When, after 1991, the water level has been more or less constant, then how much is the infiltration $Q(0, t)$ at the lake shore in 2021? by how much has it declined since 1991?

5.4.5 Superposition in time, half-infinite aquifer

Consider a half-infinite aquifer that is in direct connection with surface water at $x = 0$. The analytical solution of the change of the groundwater head $s(x, t)$ caused by a sudden change of the surface water level by an amount A m at $t = 0$ was given earlier in this chapter:

$$s(x, t) = A \operatorname{erfc} \sqrt{\frac{x^2 S}{4kDt}}, \quad t \geq 0, \quad s(x, t) = 0 \quad t < 0$$

The head change $s(x, t)$ due to an arbitrary number of such sudden changes of the surface water level A_i can be obtained by superposition as usual. Using i as event index, we then get

$$s(x, t) = \sum_{i=1}^N \left\{ A_i \operatorname{erfc} \sqrt{\frac{x^2 S}{4kD(t - t_i)}} \right\}, \quad t \geq t_i$$

Each term is nonexistent, hence zero for $t < t_i$. The surface-water level at any time is $s(0, t) = \sum_1^N A_i$, $t > t_i$, because each change of water level is supposed to last forever after it started at t_i . This way one can compute the head change and the flow in an aquifer due to an arbitrary variation of the surface water level as a boundary condition of the groundwater system; if the fluctuation is frequent, then we need to split up the time-elevation curve of the surface water in more and smaller pieces to allow accurate-enough calculation. Of course, if the the level has a stable fluctuation, one would rather use the solution for a sine boundary head to simplify the computations; even a combination is possible, because superposition applies. The problem one encounters in practice would

be to follow a detailed irregular fluctuation pattern. This generates large sums of erfc functions to carry along, which will become a pain if the number increases beyond say ten. For such cases, one could (would rather) look for convolution as the most efficient method (see description elsewhere in this syllabus).

In the following sections we concentrate on superposition in space of obtain a solution for a specific time. But it should be clear from the beginning that superposition can be combined with superposition time to adhere both to more complex boundary conditions in space and time.

Question: Consider a situation with $kD = 400 \text{ m}^2/\text{d}$ and $S_y = 0.1$. The water level $A = [1.0, -0.5, +0.5, -0.25]$ at $t = [0.5, 0.8, 1.0, 2.0]$. Show the groundwater level as a function of time for $x = 50 \text{ m}$ for $0 \leq t \leq 5 \text{ d}$. Figure 5.7 gives the outcome.

5.5 Groundwater basins as land strips of limited width between straight head boundaries

5.5.1 Introduction

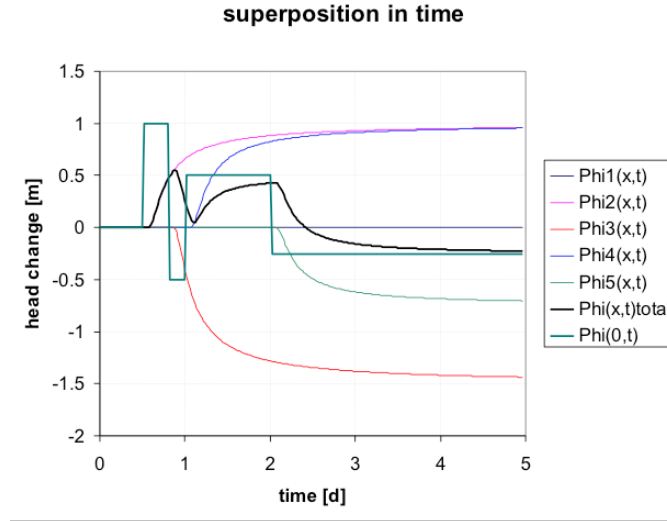
In many practical situations basins will be limited in size instead of being half-infinite. Examples are groundwater basins bounded by fixed head boundaries on either side. This includes basins that are closed on one side, since this line of no flow is just the water divide, so that such a basin is equivalent to a symmetrical one of double width. Often watersheds can be regarded as a set of sub-basins bounded by river branches on either side of the water divide between them. The basins considered here may be as narrow as a parcel of arable land or meadows between ditches as one can find anywhere in the Netherlands of perhaps 100 m wide, but just as well land between brooks of several km apart, between river branches tens of km apart or in deserts even more than that.

Even though many basins are two dimensional, we limit ourselves to one-dimensional cases, in which the head only depends on x and t . We learn to compute the variation of head and flow in such basins as they are affected by the changes of the head boundary condition at one or both sides.

We first consider the case where the left-bounding head suddenly rises by a fixed amount, while the right-hand boundary head is kept the constant. We will show that the superposition of the effect of an infinite number of “mirror” strips of land is necessary to fulfill the boundary head condition at all times. Then we consider a given change of head on either side of the strip, which also yields a solution by superposition of an infinite number of equal land strips. The case with sudden head change that is the same on either side of the land strip, is just a special case. We will compare that with a different general solution for the same situation, that we well then analyze to deduce the characteristic time of groundwater basins that can be regarded or approximated as strips. This results in simple an practical insight into the dynamic behavior of such groundwater basins.

The mentioned superposition of an infinite number of strips leads to superposition

Figure 5.7: Superposition in time example



patterns that are shown below the respective figures. These patterns allow immediate recognition of the boundaries that apply on the strip between points A and B, that we want to analyze.

5.5.2 Water level at the left hand side suddenly rises by a height a , the level at the right-hand side remains at zero

Figure 5.8 shows a groundwater basin with constant transmissivity kD and storage coefficient S . It has a width L and is bounded on either side by surface water in direct contact with the confined aquifer. The water level at the left changes suddenly by height a . How can we solve this, given the solution for the half space that we already have?

The answer is: by using mirror “ditches”.

The infinite half-space solution will cause a change of head at the right side (point B). To avoid this, a change of $-a$ is applied at $x = 2L$. This by itself will cause an unwanted head change at point A , which may be canceled by placing a positive head change at $x = 2L$ and so on as indicated at the scheme below the cross section. We need an infinite number of mirror changes. The end effect is that the change at point A is indeed a while that at point B remains zero.

That this is correct may be seen as follows. The scheme of head changes around point B is anti-symmetrical. Its net effect must, therefore, be zero. On the other hand, the mirror scheme around point A is symmetrical as well, except for the head change at A itself. Therefore, the net effect at point A is caused by the head change at A only, as the other changes cancel out.

Because the scheme is anti-symmetrical around B , point B is the most convenient location to start the x -axis. Then the effect of all the head changes summed will be

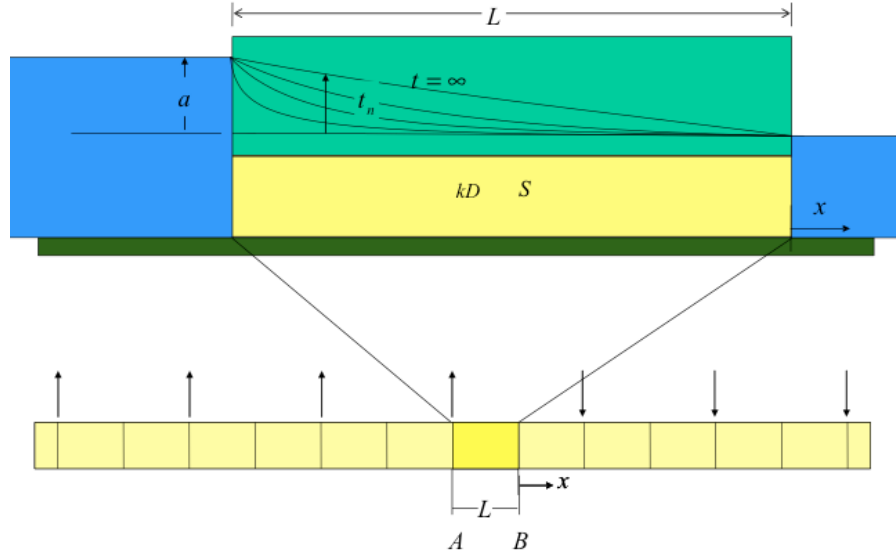


Figure 5.8: Confined groundwater basin to the left and right bounded by surface water in direct contact with the aquifer, where the water level at the left boundary is suddenly raised by A at $t = 0$ and that at the right side remains unchanged. The lower picture shows the superposition scheme; the arrows show where the water level is suddenly raised or lowered.

$$s(x, t) = A \sum_{i=1}^{\infty} \left\{ \operatorname{erfc} \left[\{(2i-1)L + x\} \sqrt{\frac{S}{4kDt}} \right] - \operatorname{erfc} \left[\{(2i-1)L - x\} \sqrt{\frac{S}{4kDt}} \right] \right\}$$

5.5.3 Shifting the zero point of the x -axis.

We may shift the zero point of the x -axis to the center of the strip by replacing x by $x' = x - \frac{L}{2}$

Thus

$$s(x', t) = A \sum_{i=1}^{\infty} \left\{ \operatorname{erfc} \left[\left\{ (2i-1)L + x' - \frac{L}{2} \right\} \sqrt{\frac{S}{4kDt}} \right] - \operatorname{erfc} \left[\left\{ (2i-1)L - x' + \frac{L}{2} \right\} \sqrt{\frac{S}{4kDt}} \right] \right\}$$

5.5.4 Arbitrary non-symmetrical case

Hence to compute the head change for a strip where the water on the left-hand side is raised by A while that on the right side is raised by B , we have to superimpose the two

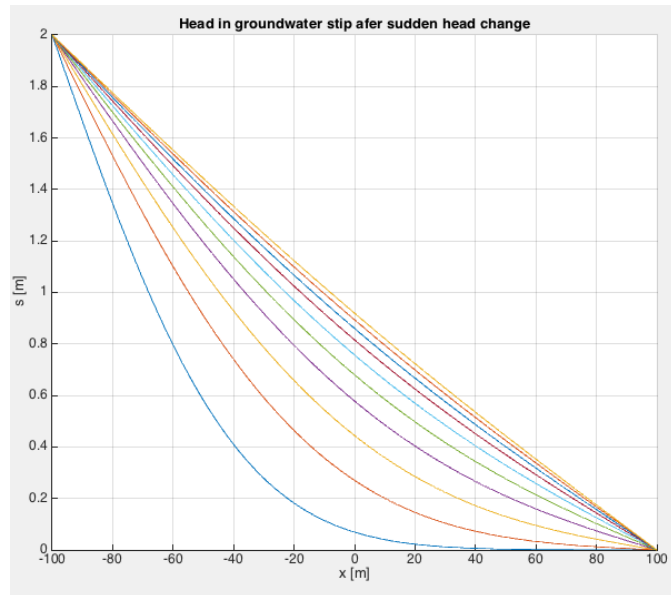


Figure 5.9: Head after sudden head rise at $x = -L/2$ for various times, $kD = 400 \text{ m}^2/\text{d}$, $Sy = 0.1$, $L = 200 \text{ m}$, $t = [0.28, 0.56, 0.84, 1.12, 1.40, 1.68, 1.96, 2.24, 2.52, 2.80] \text{ d}$.

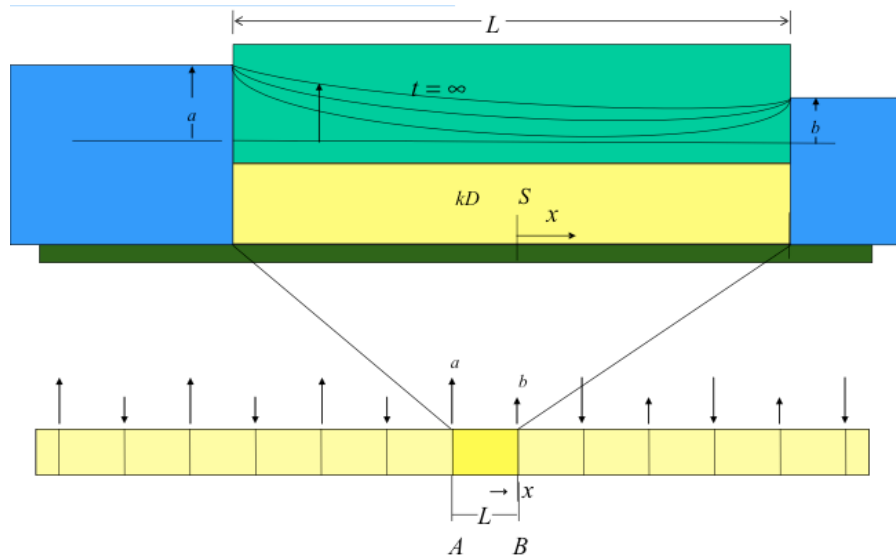


Figure 5.10: As figure 5.8 but the water level is raised independently on the left and right side by A and B respectively, and the x -axis is now centered in the center of the strip. The lower picture shows the superposition scheme; the arrows show where the water level is suddenly raised or lowered.

cases (see figure 5.10). For the right-hand side rise, we have to replace x' by $-x'$ to indicate the same point in the strip. This yields

$$s(x', t) = \dots$$

$$A \sum_{i=1}^{\infty} \left\{ \operatorname{erfc} \left[\left\{ (2i-1)L + x' - \frac{L}{2} \right\} \sqrt{\frac{S}{4kDt}} \right] - \operatorname{erfc} \left[\left\{ (2i-1)L - x' + \frac{L}{2} \right\} \sqrt{\frac{S}{4kDt}} \right] \right\} + \dots$$

$$\dots + B \sum_{i=1}^{\infty} \left\{ \operatorname{erfc} \left[\left\{ (2i-1)L - x' - \frac{L}{2} \right\} \sqrt{\frac{S}{4kDt}} \right] - \operatorname{erfc} \left[\left\{ (2i-1)L + x' + \frac{L}{2} \right\} \sqrt{\frac{S}{4kDt}} \right] \right\}$$

An example result is shown in figure 5.11

5.5.5 Symmetrical case, $A = B$

Figure 5.12 shows the same basin as before, with a symmetrical simultaneous rise of the water table by A on both sides. This is solved by superposition like before. The solution for $A = B$ may explicitly be written in a somewhat simpler form as (See also Carslaw and Jaeger, p97, eq 9)

$$s(x, t) = A \sum_{i=1}^{\infty} \left\{ (-1)^{i-1} \left[\operatorname{erfc} \left(\left[\left(i - \frac{1}{2} \right) L + x \right] \sqrt{\frac{S}{4kDt}} \right) + \operatorname{erfc} \left(\left[\left(i - \frac{1}{2} \right) L - x \right] \sqrt{\frac{S}{4kDt}} \right) \right] \right\} \quad (5.13)$$

To use this equation to compute the drainage of a groundwater basins one may write $s(x, t) = A(1 - \sum ..)$. This expression tells what happen after the groundwater as at $s = \phi_0 + A$ at $t = 0$ and drains toward $s = 0$ thereafter. One can imagine this situation to occur after a sudden large shower, that immediately raises the head by a uniformly over the entire basin, which start draining thereafter. The head rise due to such a shower would be $A = N/S_y$.

The discharge at any point x is obtained as usual by using Darcy's law, i.e. $Q = -kD(\partial s/\partial x)$:

$$Q(x, t) = -A \sqrt{\frac{kDS_y}{\pi t}} \times \dots$$

$$\dots \times \sum_{i=1}^{\infty} \left\{ (-1)^{i-1} \left[\exp \left(- \left[\left(i - \frac{1}{2} \right) L + x \right]^2 \frac{S}{4kDt} \right) - \exp \left(- \left[\left(i - \frac{1}{2} \right) L - x \right]^2 \frac{S}{4kDt} \right) \right] \right\} \quad (5.14)$$

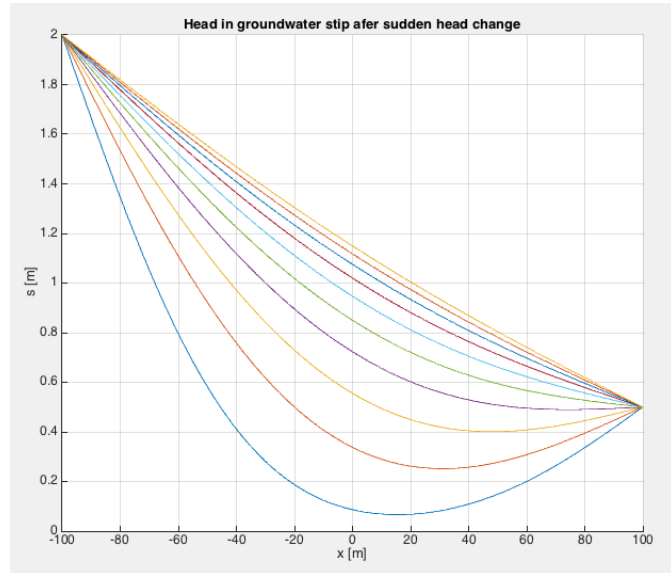


Figure 5.11: Head after sudden head rise of $A = 2$ m at $x = -L/2$ and $B = 0.5$ m at $x = +L/2$ for various times, $kD = 400 \text{ m}^2/\text{d}$, $Sy = 0.1$, $L = 200 \text{ m}$, $t = [0.28, 0.56, 0.84, 1.12, 1.40, 1.68, 1.96, 2.24, 2.52, 2.80] \text{ d}$.

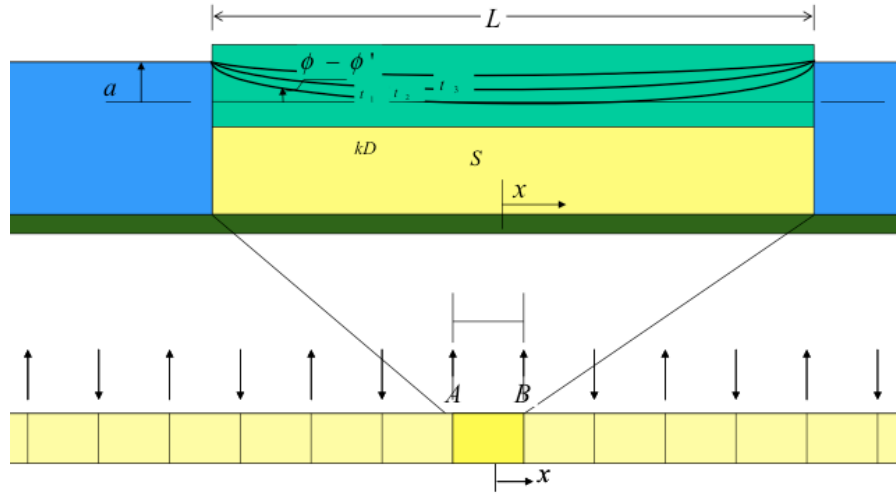


Figure 5.12: Groundwater basin bounded by surface water in direct contact on either side in which the water level is raised by A on both sides. The lower picture shows the superposition scheme with the errors indicating where the water level is raised or lowered for the superposition.

As can be seen, immediately after the head change, the water table drops very fast near the edges of the strip. Very soon, however, the head takes the shape of a cosine and the strip drains gradually until its final equilibrium is reached.

The cosine shape at later drainage stages follows from another form of analytical solution of the same strip, as will be discussed in the next section.

An example is shown in figure 5.13. In this case the so-called half times are used as times. The halftime is $n\Delta t$, with $\Delta t = 0.28 \times (L/2)^2 S/kD$, see next section. After each halftime, the difference between the head and the equilibrium final head is halved.

5.5.6 Questions

1. Set up a mirror scheme for the case of a strip of land bounded by straight surface water on either side, where the surface water stage of the right-hand side canal suddenly changes by a fixed value.
2. Show, explain on the hand of the obtained mirror scheme that the result is correct, i.e. that the result with all the mirror strips match the boundary conditions exactly.

5.6 Symmetrical drainage from a land strip bounded by straight head boundaries (characteristic time of flow basins)

Here we introduce a solution for the drainage of a land strip that initially has uniform head $s(0, x) = A$ and is bounded by two straight head boundaries at $x = \pm b$ with head at $s(\pm b, t) = 0$. This solution seems completely different from the one we obtain by infinite mirroring of strips of land as we did in the previous sections, yet provides the same result for the symmetrical case. The advantage of this form of the solution is that it can be further analyzed to deduce general drainage patterns and their time scale.

5.6.1 Analytical solution

In the previous section, we solved the symmetric one-dimensional basin by superposition of an infinite number of solutions for the half strip. While this is perfectly o.k., other solutions exist. These other solutions may look quite different, but are mathematically the same. For instance one by Kraaijenhoff van der Leur, see (Verruijt, 1999), p87), which is the same as that of Carslaw and Jaeger (1959, p97, eq. 8), reading

$$s(x, t) = A \frac{4}{\pi} \sum_{j=1}^{\infty} \left\{ \frac{(-1)^{j-1}}{2j-1} \cos \left[(2j-1) \left(\frac{\pi}{2} \right) \frac{x}{b} \right] \exp \left[- (2j-1)^2 \left(\frac{\pi}{2} \right)^2 \frac{kD}{b^2 S} t \right] \right\} \quad (5.15)$$

$s(x, t)$ is the head relative its equilibrium value, which is $s(x, \infty) = 0$. The x -axis is taken such that $x = 0$ in the center and $x \pm b$ corresponds to the sides with fixed

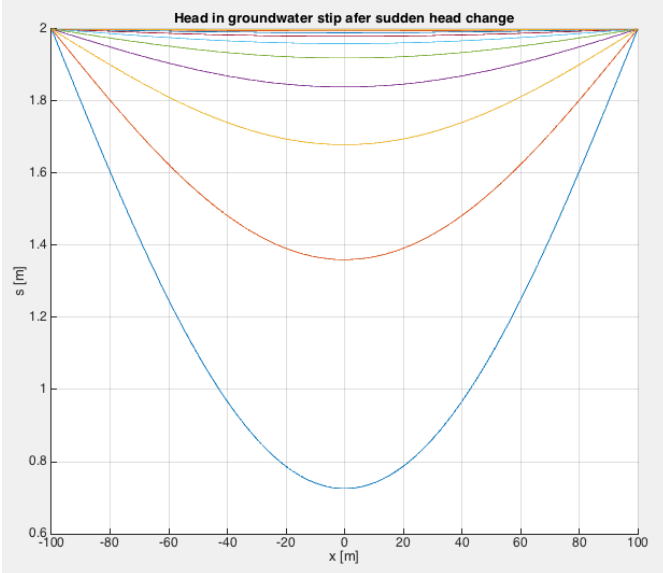


Figure 5.13: Head after sudden head rise of $A = 2$ m at $x = -L/2$ and $B = 0.5$ m at $x = +L/2$ for various times, $kD = 400 \text{ m}^2/\text{d}$, $Sy = 0.1$, $L = 200 \text{ m}$, $t = [0.70, 1.40, 2.10, 2.80, 3.50, 4.20, 4.90, 5.60, 6.30, 7.00] \text{ d}$

boundary conditions $s(\pm b, t) = 0$. The initial head is $s(x, 0) = A$ inside the section, $-b < x < b$. The formula describes the drainage that follows after the initial situation.

This behavior is characteristic for a field after a sudden shower causing the head in the field to suddenly change everywhere by the same amount, while the level in the ditches at both sides is kept the same. After the shower, the drainage occurs gradually until equilibrium is finally reached (which theoretically takes infinite time).

This formula yields the same head as was obtained previously with superposition of an infinite number of erfc-functions. Even though the solution presented here looks mathematically completely different, the numerical outcomes are, however, equivalent. We will use this solution to derive drainage characteristics that can be applied in practice on different scales.

Figure 5.14 gives the results as an example. The lines are the same as in figure 5.13 and the circles are the results of equation 5.15 for the same times. One sees that the first lines are A minus line marked by the circles.

Exercise: Implement equation 5.15 together and show that its outcomes are equivalent to that obtained by the erfc-solution for suddenly lowering of the surface water level on both sides of a strip of land.

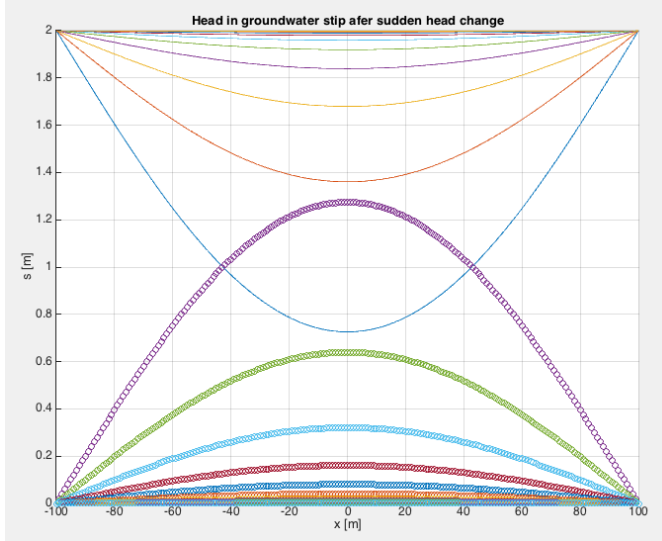


Figure 5.14: Head after sudden head rise of $A = 2$ m at $x = -L/2$ and $B = 0.5$ m at $x = +L/2$ for various times, $kD = 400 \text{ m}^2/\text{d}$, $Sy = 0.1$, $L = 200$ m, $t = [0.70, 1.40, 2.10, 2.80, 3.50, 4.20, 4.90, 5.60, 6.30, 7.00] \text{ d}$. Lines are the same as in figure 5.13 the circles are the results of equation 5.15. The first are a minus the second. Halftimes are used.

5.6.2 Long-term drainage behavior, characteristic drainage time

Expression 5.15 looks complicated at first, but it can be broken down to yield useful and practical insights. For that purpose, we analyze the kernel under the summation.

The $2j - 1$ is just the series 1, 3, 5, 7, ... and $(-1)^{2j-1} = +1, -1, +1, -1, \dots$. Next we have a product of a cosine and an exponent. The cosine will fluctuate between -1 and +1. Then notice the exponent and for simplicity write it as

$$\exp \left[- (2j - 1)^2 \left(\frac{\pi}{2} \right)^2 \frac{t}{T} \right]$$

where $T = \frac{b^2 S}{k D}$ may be regarded as a characteristic time of the drainage. The exponent terms now become

$$\exp \left(- \left(\frac{\pi}{2} \right)^2 \frac{t}{T} \right), \exp \left(-9 \left(\frac{\pi}{2} \right)^2 \frac{t}{T} \right), \exp \left(-25 \left(\frac{\pi}{2} \right)^2 \frac{t}{T} \right), \dots$$

Because $\frac{t}{T} > 0$ the second and higher terms will finally become much smaller than the first and may, therefore, be neglected when $t > t_n = nT$ where n needs to be estimated. So let us see when the second term is much less than the first so that only the first term matters:

$$\exp \left(-9\pi^2 \frac{t}{T} \right) \ll \exp \left(-\pi^2 \frac{t}{T} \right)$$

or

$$\exp\left(-9\left(\frac{\pi}{2}\right)^2 \frac{t}{T}\right) = \epsilon \exp\left(-\left(\frac{\pi}{2}\right)^2 \frac{t}{T}\right)$$

where one may choose $\epsilon = 0.01$ for example. Taking the log at both sides yields

$$-9\left(\frac{\pi}{2}\right)^2 \frac{t}{T} = \ln \epsilon - \left(\frac{\pi}{2}\right)^2 \frac{t}{T}$$

hence

$$\ln \epsilon = -8\left(\frac{\pi}{2}\right)^2 \frac{t}{T}$$

$$\frac{t}{T} = -\frac{\ln \epsilon}{8\left(\frac{\pi}{2}\right)^2}$$

For the chosen $\epsilon = 0.01$, so that $-\ln \epsilon / \left(8\left(\frac{\pi}{2}\right)^2\right) = 0.23$. Therefore, we conclude that all higher terms are negligible when $t > 0.23T$.

This means that when $t > 0.23T$ the expression given above reduces to

$$s(x, t) = A \frac{4}{\pi} \cos\left(\frac{\pi x}{2b}\right) \exp\left(-\left(\frac{\pi}{2}\right)^2 \frac{t}{T}\right), \quad t > 0.23T, \quad T = \frac{b^2 S}{kD}$$

This is a simple-to-understand expression. It is a cosine with its top equal to $a_{\pi}^{\frac{4}{\pi}}$ occurring in the center where $x = 0$ and zero where $x = \pm b$. This cosine shaped groundwater mound gradually declines according to the exponent.

An exponential decline can always be characterized by its halftime, i.e. the time in which the head by half. So if t increases by the halftime $\Delta t_{50\%}$, the $s(x, t)$ is reduced by a factor 0.5:

$$0.5 \exp\left(-\left(\frac{\pi}{2}\right)^2 \frac{t}{T}\right) = \exp\left(-\left(\frac{\pi}{2}\right)^2 \frac{t + \Delta t}{T}\right)$$

taking the log on both sides yields

$$\ln 0.5 - \left(\frac{\pi}{2}\right)^2 \frac{t}{T} = -\left(\frac{\pi}{2}\right)^2 \frac{t + \Delta t}{T}$$

and so

$$\begin{aligned} \ln 0.5 &= -\left(\frac{\pi}{2}\right)^2 \frac{\Delta t}{T} \\ \frac{\Delta t}{T} &= \left(\frac{2}{\pi}\right)^2 \ln 2 \approx 0.28 \end{aligned}$$

This implies that when time progresses by $\Delta t = 0.28T$ the drawdown is halved (under the condition that $t > 0.23T$).

This result allows us to immediately compare the halftimes of the drainage of groundwater basins of widely different size and aquifer properties. The size of the basin is expressed as its half width b . Of course, when a groundwater basin does not have this form, one should estimate a reasonable size measure based on the distance from the water divide to its drainage base, which may be rivers or the coast.

Table 5.1 gives the characteristic time $T = b^2 S_y / kD$ of some groundwater basins and their computed characteristic times and half times ($0.28T$).

5.6.3 Questions

1. Show on the hand of equation 5.15 what the half-time of the drainage of this system is. Derive it yourself.
2. How does the characteristic time relate to halftime? Show this mathematically?
3. Implement equation 5.15 and make a graph of some of the first terms of the series and of its sum.
4. Show that equation 5.15 equals equation 5.13 by implementing both in the same spreadsheet. Notice that the *first* = 1 – *second*.
5. Derive the discharge from equation 5.15 and show that it is the same as that in equation 5.14 by implementing both in the same spreadsheet.
6. Show some of the first terms of the series in equation 5.13 in Excel.

Situation	Country	kD m ² /d	S_y [J]	b m	T d	$T_{50\%}$ d	T yr	$T_{50\%}$ yr
Nubian Sandstone	Egypt	500	0.001	5.00E+05	500000	140000	384	418
Kalahari	Botswana	500	0.1	3.00E+05	18000000	5040000	13808	15051
Veluwe area	Netherlands	6000	0.27	20000	18000	5040	14	15
Dunes	Netherlands	200	0.22	2000	4400	1232	3	4
Power bulb parcel	Netherlands	200	0.1	50	1.25	0.35	0.001	0.001

Table 5.1: Characteristic times $T = b^2 S_y / kD$ and halftimes $\Delta t_{50\%} = 0.28T$ of the drainage of various groundwater systems

6 Transient flow to wells

6.1 Introduction

This chapter deals with the flow to wells in aquifers. The flow to a well is treated as actually symmetric and horizontal. Resistance of to flow due to vertical components is neglected. This is the usual Dupuit-Forchheimer approximation. It is one of the most useful approximations that exist; it allows computing groundwater flow very accurately as horizontal, without having to deal with head losses due to vertical components. Important vertical components may, however, occur in the vicinity of wells that only partially penetrate the aquifer. Disturbances of the essentially horizontal flow due to partial penetration of well screens is only important in the vicinity of the wells and can be dealt with by a correction on the drawdown as outlined below.

More complicated situations, such as well fields and wells near specific boundaries, are dealt with through superposition.

We start with an overview of the analytical solutions that we will deal with and their related steady-state versions.

In the past groundwater flow solutions and equations were computed by looking up values in tables. Nowadays everyone has access to Excel or Python and, therefore, we will compute the values of the different well functions rather than looking them up. However not all required mathematical functions are always present, especially not in Excel. Therefore we will implement their mathematical formulas as user defined functions in Excel. This provides the user with these functions so that he/she can use them in Excel just like other native functions that Excel provides as standard. The implementation will be in Visual Basic. Generally only a few lines are needed to implement the most important transient groundwater flow solutions.

6.2 Wells and well functions overview

The next three figures give an impression of what wells are, without entering in the details of their construction and the installation of pumps, pump cellars, electricity and so on. What matters is the position of the screen inside the aquifer. There exist numerous types of wells: open wells, dug wells, drilled wells, tube wells, horizontal wells and more. In this course we limit ourselves to those that are essentially of small diameter, i.e. of small well radius indicated as r_0 . This limitation suffices for most practical situations. For special cases not covered, one has to refer to the literature for analytical solutions or rely on a numerical model. Kruseman & De Ridder (1994) is probably the most renowned book on the analysis of pumping test hand has been used in all continents for about four

Figure 6.1: Large-diameter open well in India (copied from Newspaper NRC)



decades (the first issue is of 1970). This book, 1994 issue, can be found and downloaded from the Internet for free, it is a very good reference that covers the relevant literature in a practical way and also provides tables with the values for many of the analytical groundwater functions. The latter is an advantage, because some are quite complicated to implement yourself.

One special solution is just given for reference and will not be part of the course. It is the solution for large diameter wells, such as the one shown in figure .. The implementation of that solution is also provided in the concerned section of this syllabus.

Figure 6.2 is a sketch of a well in an unconfined aquifer (synonymous with “water-table aquifer” and “phreatic aquifer”) and opposite to “confined aquifer” of which a sketch is given in figure 6.3. The screen, i.e. the perforated portion of the well is fully penetrating the (wet) section of the aquifer in figure 6.2, while it is not completely penetrating the aquifer in figure 6.3. Very often the penetration of the aquifer by the screen is only minor where aquifers are thick. It should be noted that due to partial penetration of a well screen, the streamlines are no longer horizontal near the well, say less than one aquifer thickness from the well. The concentration of the streamlines towards a partially penetrating screen cause extra head loss relative to the situation with a fully penetrating screen. This head loss can be taken into account when necessary.

The right-hand side of figure 6.3 shows the streamlines in the case of a completely confined aquifer, one without vertical leakage. The left-hand side of figure 6.3 show the streamlines in a semi-confined aquifer, that is recharged by seepage from an overlying layer or aquifer. Of course, seepage may also occur from underlying layers, but we will not deal with such multilayer groundwater flow systems in this syllabus.

Transient flow due to an extraction by a well in a water table or perfectly confined aquifer of infinite lateral extent, will never reach steady state; the decline of the water level

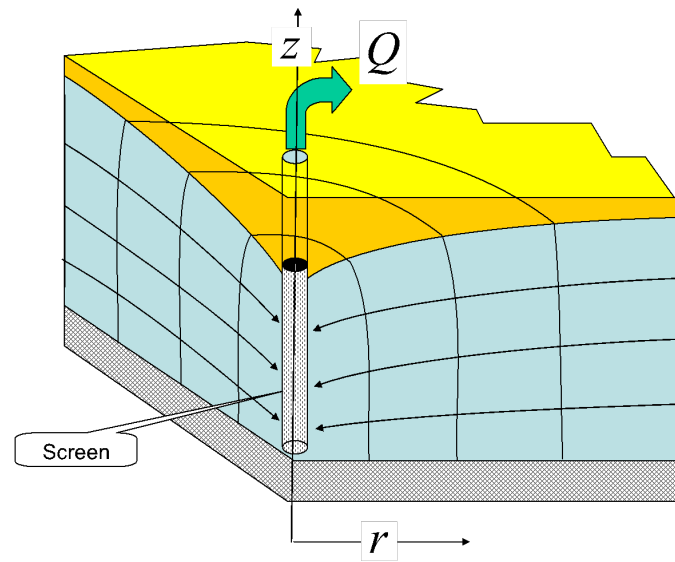


Figure 6.2: A tube well in an unconfined aquifer

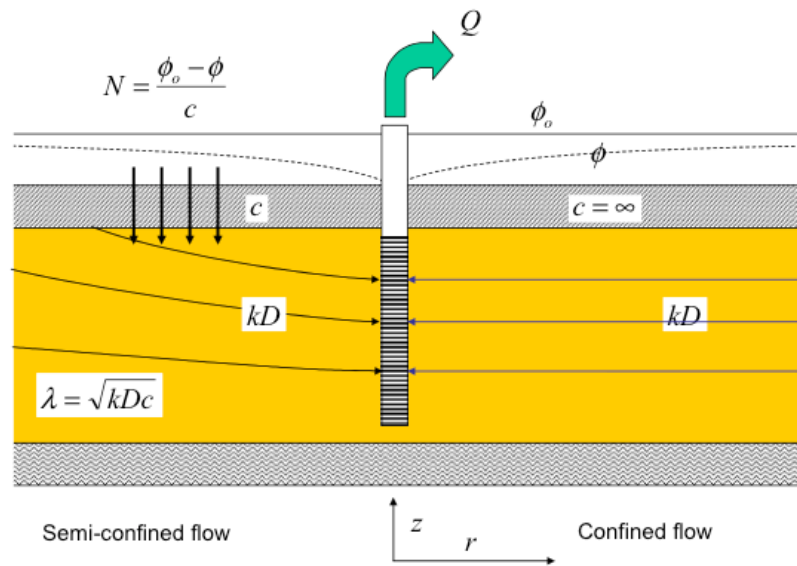


Figure 6.3: Tube well with stream lines in a semi-confined and a confined aquifer

in the well will never stop, that is, until the pump can no longer reach it or when the well becomes dry inside. To the contrary, transient flow in semi-confined aquifers will reach a steady state after some time, depending on the transmissivity and the storativity of the aquifer and the vertical resistance of the overlying (and or underlying) semi-pervious layer, the aquitard, that confines the aquifer.

Governing equations are important as they stage the physical foundation and the approximations made to solve a problem analytically. They will be presented in the sections that present a specific solution. However, the general relation between solutions for a water table aquifer and confined aquifers is presented here.

The transmissivity in a water-table aquifer is given by $T = kh$ where h is the distance from the water table to the bottom of the aquifer, which is assumed to be horizontal. That of a confined aquifer is $T = kD$ with D the thickness of the confined aquifer. h depends on the water table, which is variable as it changes due to the pumping and perhaps other factors such as varying boundary conditions. Notice that there are not analytical solutions dealing with a time-variable water table; they all nearly the solution by taking $D \approx h$, where h may be chosen a suitable average of the area of interest. As always, the partial differential equation is linearized before solving it. This means that superposition can be applied, so that we may add an arbitrary number of different solutions to the same groundwater system simultaneously. It also means that there is no impact from any factor or boundary condition as long as it is not influenced by the wells considered. This means that precipitation and evaporation play no role when it comes to compute the changes of the groundwater head caused by wells. This simplification may fail, however, when the groundwater system does not obey to the assumptions underlying the solved partial differential equation. This is the case, for example, when plant evaporation is reduced in a nonlinear fashion due to the drawdown of the water table caused by the well. One should also keep such exceptions in mind when solving practical problems and stay aware of the limitations to the calculation methods and formulas applied. The same is true when applying groundwater models.

The table 6.1 shows the most important, and always applied, groundwater well solutions. Only the first one deals with a water-table aquifer, while all others require the transmissivity to be constant. To use these solutions for water-table aquifers, the drawdown should remain small compared to the wet aquifer thickness. However, one may often overcome such conditions by using a proper average for the aquifer thickness. The water-table solution always depends on the dynamic thickness of the aquifer h , while this is not the case for the other solutions; they all compute the head change or (equivalently) the drawdown, independently of the aquifer head or groundwater level. The first two solutions are related as follows

$$h^2 - H^2 = (h - H)(h + H) \approx 2sH = 2sD \quad (6.1)$$

Replacing $h^2 - H^2$ in the first solution by $2sH$ immediately yields the second. Equation 6.1 also gives a clue to the accuracy of using a confined-case solution for an unconfined case, as we will often do in practice. It requires that $h + H \approx 2D$. A head change of h of 20% of H then causes an error in the computed drawdown of about 10%, which is

acceptable in most circumstances.

Clearly, the second Thiem solution is directly related to the transient Theis solution, but they are not equivalent because the Theis solution has not steady state. However, the difference between the transient heads at different finite distances from the well does become steady state, and that steady state is equivalent to the Thiem solution for constant aquifer thickness. The steady-state solution for flow to a well in a leaky aquifer, De Glee (1930), is the steady state of the Hantush (1955) transient solution of the same situation. Also carefully notice that all steady-state solutions have a 2 in the denominator of the factor multiplying the well function or logarithm, while all transient solutions have a 4 at that position. From this it immediately follows that the Hantush solution for $t \rightarrow \infty$ is

$$\frac{Q}{4\pi kD} W\left(u_{t \rightarrow \infty}, \frac{r}{\lambda}\right) = \frac{Q}{2\pi kD} K_0\left(\frac{r}{\lambda}\right)$$

so that

$$W\left(u_{t \rightarrow \infty}, \frac{r}{\lambda}\right) = 2K_0\left(\frac{r}{\lambda}\right)$$

6.3 Theis: transient well in an infinite aquifer with constant transmissivity and storativity

Theis (1935) published a new solution for the dynamic change of head caused by a well pumping at a constant rate from $t = 0$ from an infinite aquifer with uniform transmissivity and storativity.

The solution by Theis is one of the major breakthroughs in groundwater hydrology. For the first time it was possible to analyze the dynamics of the heads and flows caused by extracting wells. Before Theis only steady-state flow solutions for the groundwater flow problem existed, which very much limited possible analysis of actual pumping regimes. Theis introduced just this, dynamics of groundwater flow. According to Theis, when a well pumps from an aquifer of infinite extent, all water must come from storage; there are no extra sources. Clearly, the flow to a non-extracting well in an infinite aquifer is

Name	Water table?	Leakage?	Transient?	Solution
Thiem	yes	no	no	$h^2 - H^2 = \frac{Q}{\pi k} \ln \frac{R}{r}$
Thiem	no	no	no	$s = \frac{Q}{2\pi kD} \ln \frac{R}{r}$
De Glee (1930)	no	yes	no	$s = \frac{Q}{2\pi kD} K_0\left(\frac{r}{\lambda}\right)$
Theis (1935)	no	no	yes	$s = \frac{Q}{4\pi kD} W(u)$
Hantush (1955)	no	yes	yes	$s = \frac{Q}{4\pi kD} W(u, \frac{r}{\lambda})$

Table 6.1: Overview of the most important groundwater-well solutions. In all formulas $\lambda = \sqrt{kDc}$ and $u = \frac{r^2 S}{4kDt}$

axial-symmetric. Therefore, only the distance to the well, r , and time matter as the two independent variables. To analyze the flow to such a well we consider continuity of a ring with thickness dr between r and $r + dr$ from the well. The situation is given in figure 6.4. Notice that that this figure show a cross section through an axially symmetric groundwater system. Also notice that in the figure the thickness of the aquifer is the height of the water table above the base of the aquifer. However we assume here that this thickness is constant and equal to D , which is valid as long as the drawdown is small relative to the thickness of the aquifer. Also the storativity, S , is constant. The head in the aquifer was initially ϕ_0 . The drawdown, s , is therefore $\phi_0 - \phi$, when we consider drawdown positive. We may also define the head change and use $\phi - \phi_0$ instead. The only difference is the sign.

To see what's in Theis' solution, we look first at the partial differential equation that he solved. The first thing to derive such a governing PDE, we just consider continuity, which is the water budget of a small concentric ring of width dr around the well disregarding any physical laws except continuity. The water budget of the ring at time t reads

$$q(2\pi r) - \left(q + \frac{\partial q}{\partial r} dr \right) (2\pi(r + dr)) = S \frac{\partial \phi}{\partial t} (2\pi r) dr$$

This equation can be simplified

$$\begin{aligned} q(2\pi r) - \left(q + \frac{\partial q}{\partial r} dr \right) (2\pi r) - \left(q + \frac{\partial q}{\partial r} dr \right) 2\pi dr &= S \frac{\partial \phi}{\partial t} (2\pi r) dr \\ -\frac{\partial q}{\partial r} - \left(q + \frac{\partial q}{\partial r} dr \right) \frac{1}{r} &= S \frac{\partial \phi}{\partial t} \end{aligned}$$

Letting $dr \rightarrow 0$ we obtain our continuity or water balance equation

$$-\frac{\partial q}{\partial r} - \frac{1}{r} q = S \frac{\partial \phi}{\partial t}$$

At this point we switch to a physical law, namely that of Darcy by writing

$$q = -kD \frac{\partial \phi}{\partial r}$$

So that if we combine Darcy's law with continuity, we get

$$-\frac{\partial}{\partial r} \left(-kD \frac{\partial \phi}{\partial r} \right) - \frac{kD}{r} \frac{\partial \phi}{\partial r} = S \frac{\partial \phi}{\partial t}$$

And because it was assumed that kD is constant, this simplifies to

$$\frac{\partial^2 \phi}{\partial r^2} + \frac{1}{r} \frac{\partial \phi}{\partial r} = \frac{S}{kD} \frac{\partial \phi}{\partial t}$$

which is the PDE that Theis solved for the following initial and boundary conditions.

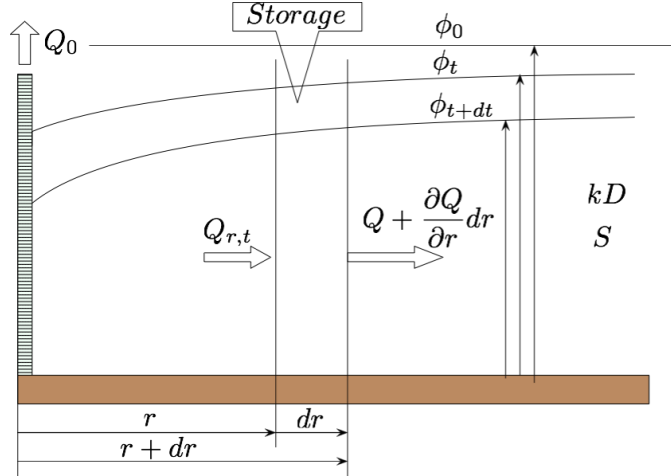


Figure 6.4: Scheme axial symmetric flow to an extraction well according to Theis

$$\begin{aligned}\phi_{r,0} &= \phi_0 \\ \phi_{\infty,t} &= 0 \\ Q_0 &= -2\pi r k D \left(\frac{\partial \phi}{\partial r} \right)_{r \rightarrow 0}\end{aligned}$$

With as solution

$$s = \phi - \phi_0 = \frac{Q}{4\pi k D} W(u), \quad u = \frac{r^2 S}{4k D t}$$

Notice that not the head is important but only the difference from the initial head matters, hence the head-change of the drawdown. Also notice that all steady-state well formulas have the factor $2\pi k D$ while the transient solution all have $4\pi k D$. Finally notice that the well function W does not depend on r or t separately but on a variable, called u , which combines r and t together with S and $k D$ in a specific way. All formulas describing transient flow to wells have this variable u .

The function W is known as Theis' well function among hydrologists, however, mathematicians knew that function long before Theis; they have a name for it, the exponential integral

$$\text{expint}(u) = E_1(u) = \int_u^\infty \frac{e^{-y}}{y} dy \quad (6.2)$$

Python and Matlab. Clearly the well function has is given in tables in book on pumping test analysis like Kruseman & De Ridder (1972, 1994, free on the Internet) and in mathematical table books like Abramowitz & Stegun (1964). Nowadays this function

is readily available in software such as Python and Matlab, but in Excel it has to be implemented, preferably in Visual Basic to use it easily in computations.

Next to the integral representation, the exponential integral can be expressed as a power series that will reveal useful when studying the behavior of the well function. The power series representation is

$$\begin{aligned} W(u) &= -\gamma - \ln u + u - \frac{u^2}{2 \times 2!} + \frac{u^3}{3 \times 3!} - \frac{u^4}{4 \times 4!} + \dots \\ \gamma &= 0.577216\dots \end{aligned} \quad (6.3)$$

where γ is the so-called “Euler’s constant”, similar like other constants in mathematics like π and e , only less known by the wider public.

Unconfined flow approximation by Theis: Although the solution as it was presented holds for confined flow or for unconfined aquifers where the drawdowns varies only little compared to the thickness of the aquifer, Theis himself used linearization as described in equation 6.1, writing $2sD = h^2 - D^2$ and $u = \frac{r^2 S}{4k\bar{h}}$ with $\bar{h} = 0.2(h + D)$. Hence

$$h^2 - D^2 = \frac{Q}{2\pi k} W(u), \quad u = \frac{r^2 S}{4k\bar{h}t}$$

6.3.1 Implementation of the Theis well function in Excel

We have two representations of the Theis well function, or the exponential integral, as given above. We will implement both in Visual Basic. For who wants, a Python implementation is left as an exercise.

The integral can be numerically computed. Because u will span many orders of magnitude in practice, it is wise to carry out the integration on a logarithmic axis. As $dy/y = d\ln y$ we may write the integral as follows

$$W(u) = \int_{\ln u}^{\infty} e^{-y} d(\ln y)$$

writing $\ln y = \nu$ so that $y = e^\nu$ changes the integration into

$$\begin{aligned} W(u) &= \int_{\ln u}^{\infty} e^{-e^\nu} d\nu \\ &\approx \int_{\ln u}^{20} e^{-e^\nu} d\nu \\ &\approx d\nu \sum_{\ln u}^{20} e^{-e^\nu} \end{aligned}$$

where we replaced ∞ by a practical upper limit of 20, which corresponds to $e^{20} \approx 5 \times 10^8$. In the practical summation, we choose $d\nu$ as a small fraction of a log cycle, say $d\nu = 0.01$.

The figure gives the implementation as user defined function in Visual Basic in Excel.

The power series implementation is almost straightforward. But the easiest way to sum the terms is to circumvent having to compute the factorials. The way to do is to express term $n + 1$ in term n so that a next term is easily computed from the previous.

$$\begin{aligned} Term_{n+1} &= Term_n \times Factor \\ \frac{u^{n+1}}{(n+1)(n+1)!} &= \frac{u^n}{n \times n!} \times -\frac{n u}{(n+1)^2} \end{aligned}$$

So that the sought factor equals

$$Factor = \frac{n}{(n+1)^2} u, \quad n = 1, 2, 3, \dots$$

Exercise: now that we have the two implementations, show that their outcomes are the same.

6.3.2 Type-curve for the Theis well function

All books on groundwater pumping tests show the Theis type curve (Figure 6.7). The type curve is the well function plotted on double logarithmic scale in a way that it is directly comparable with an actual drawdown curve on double log axes; it looks like the drawdown shown vertically upward and time on the horizontal axis. Hence the type curve shows the well function vertical and $1/u$ on the horizontal axis, because $1/u = \frac{4kDt}{r^2S}$ is proportional to time. This type curve can be used to read values of the well function for given values of $1/u$ but also for the analysis of a pumping in an aquifer that fulfills the assumptions that underlie the derivation of the Theis solution. These assumptions are:

1. The aquifer has uniform transmissivity and uniform storativity (either elastic when confined, or specific yield when phreatic). In case of a phreatic aquifer, the drawdown should be small so that the transmissivity is not changed much relative to the aquifer depth by the decline of the water table.
2. The aquifer extends to infinity. In practice this means far enough such that the pumping test is not affected by boundaries of the groundwater system.
3. The well is pumped at a constant rate from a given point in time, which is set to $t = 0$ in the formula.
4. The diameter of the well is small.

```

Public Function Expint(u As Double) As Double
'Exponential integral (Theis well function computed by integration)
'TO 151211

Dim dlny, y, w, lnINF As Double

lnINF = 20           'end of integration
dlny = 0.01          'step size for integration, small part of log cycle
lny = Log(u) + 0.5 * dlny   'first location on log axis, use +0.5dlny to move to center of steps

w = 0               'Initialize and loop till lnINF wasreached
While lny < lnINF
    y = Exp(lny)
    w = w + Exp(-y)
    lny = lny + dlny
Wend

'finally multiply by the step size, all at once is more efficient than while looping
Expint = w * dlny

End Function

```

Figure 6.5: Theis well function (expint) implemented in Visual Basic for Excel

```

Function Wtheis(u As Double) As Double
'Theis well function implemented as a power series
Dim gamma, deltaStop, term, term1, term2 As Double
Dim N, NMax As Integer

If u >= 10 Then
    Wtheis = 0#
Else
    gamma = 0.577216 'Euler's constant

    deltaStop = 1e-06
    NMax = 100: N = 1
    term = u: term1 = term: term2 = term
    w = -gamma - Log(u) + term

    While (Abs(term1 + term2) > deltaStop) And (N <= NMax + 1)
        term = -term * u * N / ((N + 1) * (N + 1))
        w = w + term: N = N + 1
        term2 = term1: term1 = term
    Wend

    Wtheis = w
End If

```

Figure 6.6: Theis well function as power series implemented as User Defined Function in Visual Basic for Excel

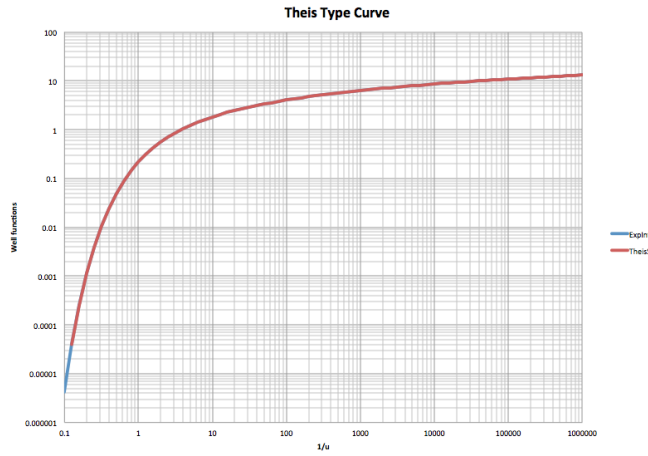


Figure 6.7: Theis type curve in Excel. The two implementations have been plotted one over the other; they perfectly overlap.

6.3.3 Theis classic pumping-test analysis

In a pumping test a well pump is switched on and continues to pump at a virtually constant flow, i.e. to the extent that it is possible given the pump and the drawdown; the analysis, at least assumes that the flow from the well is constant. The test needs to be done in either a confined or unconfined aquifer without leakage from overlying or underlying layers. In the case of a water table aquifer, the drawdown should remain limited to say about 20% of the aquifer thickness to not violate the assumption of a constant uniform transmissivity. The aquifer needs to be extended enough so that possible flow boundaries do not interfere with the drawdown during the time that the test lasts. Further, the head is measured in one or more piezometers placed at different distances and also in different directions from the well. At least three different directions are necessary to discover whether or not the aquifer is anisotropic in the horizontal plane. This is not so often the case, but it should be checked whenever possible to prevent misinterpretations. The heads in the piezometers are measured from some time before the pumping test starts and frequently during the test such that the evolution of the drawdown can be established accurately when the points are later on plotted on a logarithmic time scale. If possible, two to three log-cycles should be covered; three or four log cycles would be: the first measurement after one minute, the last one after 1000 minutes or 10000 minutes. The initial measuring period before the start of the pumping test is to establish the initial head, which we need to compute the drawdown as the measured head minus the initial head (or the initial head minus the measured head if one so desires, only the sign changes, not the interpretation).

After the test has finished and the data collected, it's time to plot the data. One could of course plot drawdown versus time, but that yields a different curve for each piezometer, which than would have to be interpreted one by one individually. However, the type curve is a function of $1/u = \frac{4kD}{S} \frac{t}{r^2}$. This implies that if we plot the drawdown

versus t/r^2 instead of just versus t , the data of all piezometers should just fall on the same graph. Now the interpretation.

With the type curve we have on the vertical axis $W(u)$ and on the horizontal axis $\frac{1}{u} = \frac{4kD}{S} \frac{t}{r^2}$. On the curve with the measurements we have on the vertical axis the drawdown $s = \frac{Q}{4\pi k D} W(u)$ and on the horizontal axis $\frac{t}{r^2}$. We see that the vertical axes of the two figures differ by a factor $Q/(4\pi k D)$ and that the horizontal axes differ by a factor $4kD/S$. On a logarithmic scale, multiplication becomes addition, i.e. vertical shift by $\log\left(\frac{Q}{4\pi k D}\right)$ and so for the horizontal logarithmic axis the difference is a factor $4kD/S$, hence a horizontal shift equal to $\log\left(\frac{4kD}{S}\right)$. What happens is that the measured drawdown curve on double log scales has exactly the same shape and size as the type curve. If one is plotted on transparency, it can be shifted parallel to the vertical and horizontal axes, until the measured drawdown and the type curve fit. Then the ratio of the matching values on the vertical axes is $Q/(4\pi k D)$ and that of the horizontal axis is $4kD/S$. Hence these two factors have thus been determined. And because Q is known, we now have the value for both the transmissivity and the storativity, hence we have interpreted the pumping test to determine the two aquifer parameters.

6.3.4 Standard behavior obtained from simplified Theis well function

Already the type curve of the Theis solution on linear vertical and logarithmic horizontal scale reveals much of the behavior. It shows that for a point at some distance it takes some time before the drawdown sets on. Then after some time the drawdown becomes linear on this half-logarithmic graph. We can analyze this behavior and draw some important consequences from a simplification of the Theis type-curve that lends itself for easier analysis.

Given the power series representation in equation 6.3, and noting that for small values of u , say $u < 0.1$ only the first two terms matter, we can simplify the Theis solution for such cases. To show this in a few steps:

Start with the power series representation and ignore all terms with u

$$W(u) \approx -577216 - \ln u + \dots$$

which is valid for sufficiently small u (i.e. for large times and small r). Then turn the constant into a logarithm, use $u = r^2 S / (4kDt)$ and combine the two logs.

$$\begin{aligned} W(u) &\approx -\ln(1.7811) - \ln\left(\frac{r^2 S}{4kDt}\right) \\ &\approx -\ln\left(\frac{r^2 S}{2.25kDt}\right) \end{aligned}$$

Finally, reverse the sign:

$$W(u) \approx \ln\left(\frac{2.25kDt}{r^2S}\right)$$

The latter may also be written as

$$W(u) \approx \ln\left(\frac{0.563}{u}\right)$$

Here we see that for small u the well function can be approximated by this simple logarithm.

6.3.5 Derived behavior using the logarithmic approximation of $W(u)$

Behavior with respect to time is easily demonstrated by splitting the log in a part with and without time

$$W(u) \approx \ln\left(\frac{2.25kD}{r^2S}\right) + \ln(t) \quad (6.4)$$

Hence, the well function is a constant, i.e. its value at $t = 1$ plus the log of t . For each different distance to the well, the constant is different, but the $\ln t$ term is the same. Hence, the time drawdown curves of points at different distance from the well are all parallel, they are only shifted along the horizontal time axis. This is shown in figure 6.8. As can be seen from the figure, the drawdown according to Theis sets in after some time and after some transition period it becomes linear on logarithmic axis. The thin lines show the logarithmic approximation. The first term in equation 6.4 is the value that each straight drawdown line intersects at $t = 1$, which is at the black circles that are also plotted in figure 6.8. Also notice how the drawdown curves of all the piezometers fall on the same line if plotted versus $1/u$ instead of t or versus t/r^2 instead of time. This is illustrated in figure ..

How the well function increases per log-cycle of time is also interesting. That is

$$W\left(\frac{r^2S}{4kD10t}\right) - W\left(\frac{r^2S}{4kDt}\right) = \ln 10 = e \approx 2.7$$

is always the same, irrespective of the properties of the subsoil and of distance from the well. This allows for a very simple analysis of a pumping test. Let's assume the time is large enough such that the drawdown is linear on half-logarithmic scale. Then

$$s = \frac{Q}{4\pi k D} \ln\left(\frac{2.25kD}{r^2S}t\right)$$

So that the extra drawdown over one log-cycle of time is

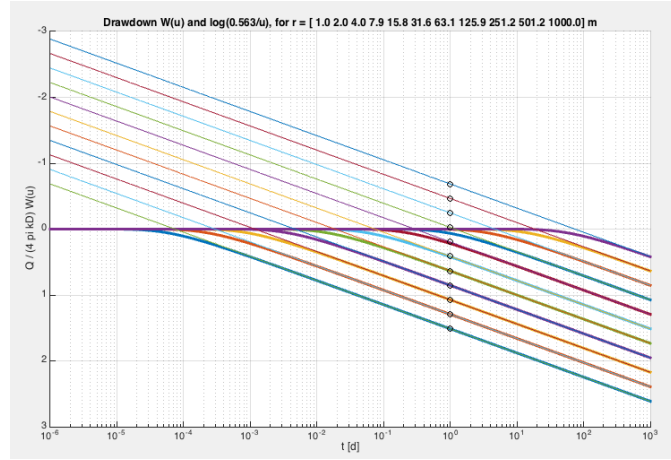


Figure 6.8: Drawdown (notice that positive drawdown is plotted downwards) versus time according to Theis (thick lines) and logarithmic approximation (thin lines) for different distances as given in the head of the picture. $Q = 2400 \text{ m}^2/\text{d}$, $kD = 1200 \text{ m}^2/\text{d}$ and $S = 0.2$. The circles are the first log term in equation 6.4.

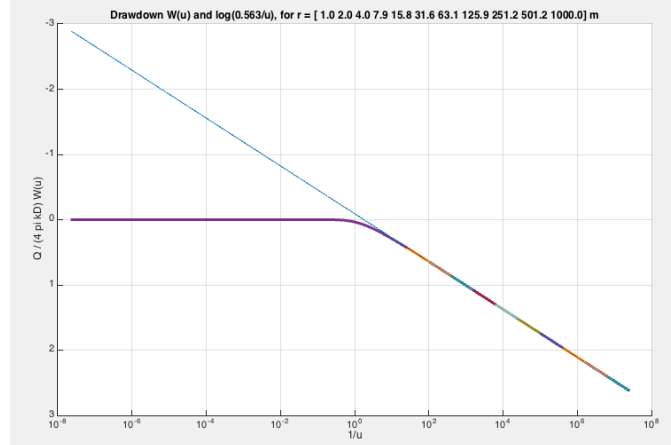


Figure 6.9: Same as figure 6.8, but now plotted versus $1/u$ instead of t . A similar results is obtained if plotted versus t/r^2 instead of time. The drawdown curves of different piezometers fall all on the same line.

$$\Delta s_{logcycle} = s_{10t} - s_t = \frac{Q}{4\pi kD} \ln 10$$

Given that we know the extraction Q and that we measured the $\Delta s_{logcycle}$, we can immediately compute the transmissivity of the aquifer from

$$\begin{aligned} kD &= \frac{Q}{4\pi} \frac{e}{\Delta s_{logcycle}} \\ &\approx 0.21 \frac{Q}{\Delta s_{logcycle}} \end{aligned}$$

This simple analysis is always applicable when $u < 0.1$, hence for large t and small r . This therefore, becomes particularly interesting for the analysis of pumping tests where the only measurements available are those of the drawdown in the well itself, i.e. for very small r ! Such a test is called a well test. The r in a well test is so small that the logarithmic approximation of the drawdown sets in very early. This implies that even relatively short well test is enough to determine the transmissivity of the aquifer. This is an advantage also in semi-confined aquifers, in which the drawdown becomes steady after some time, so that the Theis solution fails. However shortly after the pump was switched on the drawdown does behave like that envisioned by Theis. So this method tends to be valid and practical.

A problem with interpretation of the drawdown in the well bore is extra drawdown when the screen only partially penetrates the aquifer, and an extra drawdown due to a skin on the bore face due to left-overs of for instance drilling mud or from clogging. Both these extra drawdowns are or become stationary very soon after onset of the pump. When skin and drawdown due to partial screen penetration are constant, they do not influence the drawdown difference at different points in time, and, therefore, the drawdown per log-cycle remains exactly the same. This implies that problems that occur with for instance steady-state interpretation of drawdown in and near the well bore (skin and partial penetration and vertical anisotropy), that need to be corrected for in such an analysis, do not play any role in the drawdown per log cycle, and, therefore in the determination of the transmissivity of the aquifer, without the need for extra piezometers.

To determine the storage coefficient from a well test, we need an absolute value of the drawdown from a time and distance when the logarithmic approximation holds true. A difference in drawdown between two points in time or two distances that the same time, will not work because the $kD/(4S)$ drops out of the argument of the logarithm when subtracting two logs. An absolute drawdown, however is influenced by a well skin, partial penetration and vertical anisotropy (in the case of partial penetrating well screen). The skin and the vertical anisotropy are generally not known and even the depth of the aquifer is not always known, especially when drilling was stopped before reaching the bottom of the aquifer, which is generally the case. Therefore, from a well test alone, one can generally not determine the storage coefficient of the aquifer. For this a piezometer at some distance is required. The drawdown in this piezometer is not affected in any way by a skin because no water is extracted from it. And also if the distance is more

than about 1.5 times the aquifer thickness from the well, partial penetration may be neglected. Notice that if the aquifer is vertically anisotropic the required distance from the well is larger by a factor $\sqrt{k_r/k_z}$. Of course, a well at a larger distance from the well takes longer for the approximation of the well function to be valid, and, therefore, in a semi-confined (i.e. leaky) aquifer, the deviation from the Theis situation may affect the shape of the drawdown and hinder proper analysis by this simple method.

6.3.6 Drawdown at a fixed time at different r

The counterpart of the drawdown versus time at a given location is the drawdown versus distance at a given time. In general, this drawdown is much more difficult to observe because it requires having multiple piezometers at different distances, which are, obviously almost never available in practice. Another difficulty counteracting the interpretation of such a multiple piezometer pumping test with the simplified well function is, that piezometers at larger distances will not yet behave according to the approximation because their value of u is still too large. Finally, their drawdown may be impacted by deviating drawdown behavior in case of leakage from overlying or underlying layers.

Nevertheless some insight in the behavior can still be obtained from the approximation. Making r explicit yields

$$W(u) \approx \ln\left(\frac{2.25kDt}{S}\right) - 2\ln r \quad (6.5)$$

The first log is a constant at any fixed point in time for every piezometer, irrespective of its distance to the well. The impact of the distance to the well is completely confined to the second term. We see that the drawdown is proportional to $\ln r$ and hence gives a straight line on the drawdown versus log distance graph. The drawdowns versus r at different times are all parallel like it was the case with the drawdowns versus time that we discussed before. Only the drawdown versus distance curves are twice as steep the half log chart than those versus time.

Figure ... shows the drawdowns as a function of r at different times as indicated in its header. The same extraction and aquifer properties were applied as before. The first log term in equation 6.5, these are the intersections of the logarithmic approximation with the vertical line where $r = 1\text{m}$; these intersections are indicated in the figure as black "o's". Again, the drawdown was plotted with the positive axis downward so it complies more intuitively with the concept of a reduced groundwater head caused by pumping. Here, too, all lines fall on the same graph when plotted versus u instead of versus r or, equivalently when plotted versus r^2/t instead of just r , which is shown in figure ...

If we have the measured drawdowns in two piezometers with r_1 and r_2 respectively at a fixed time we may interpret them as follows

$$\Delta s_{r_2, r_1} = s_{r_2} - s_{r_1} = -\frac{Q}{2\pi k D} \ln \frac{r_2}{r_1}$$

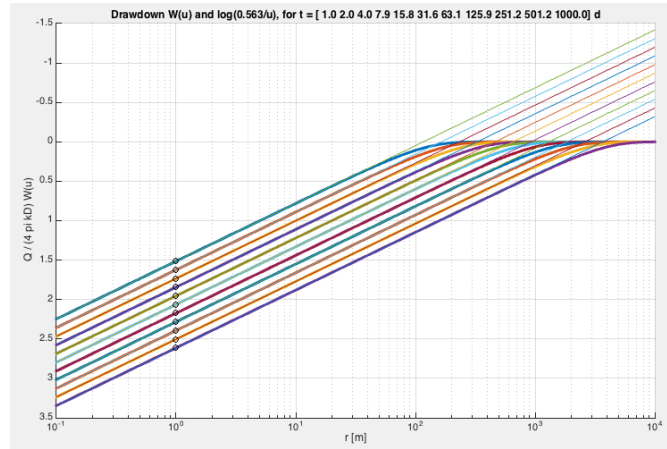


Figure 6.10: Drawdown (notice that positive drawdown is plotted downwards) versus distance r according to Theis (thick lines) and logarithmic approximation (thin lines) for different distances as given in the head of the picture. $Q = 2400 \text{ m}^2/\text{d}$, $kD = 1200 \text{ m}^2/\text{d}$ and $S = 0.2$. The circles are the first log term in equation 6.5.

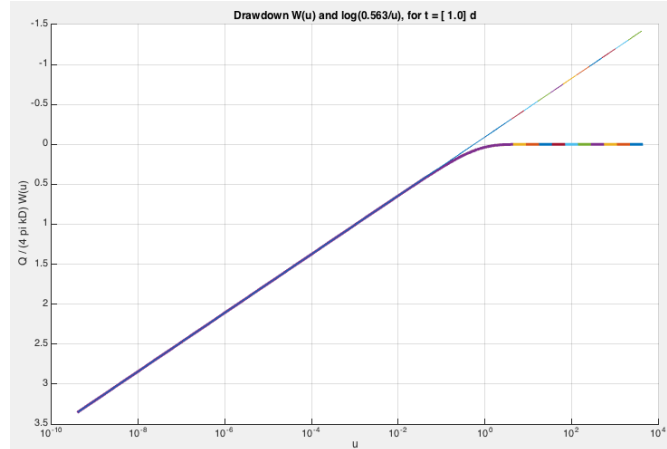


Figure 6.11: Same as figure 6.10, but now plotted versus u instead of versus r . A similar results is obtained if plotted versus r^2/t instead of r . The drawdown curves of different piezometers fall all on the same line.

(notice the 2 instead of the 4 in the denominator). And so

$$kD = \frac{Q}{2\pi} \frac{\ln(r_2/r_1)}{\Delta s_{r_1,r_2}}$$

This interpretation is, however much more apt to difficulties than the one dealt with in the previous paragraph, because the closest piezometer may be influenced by partial penetration, and if the closest piezometer is the well itself, also by the well skin, and, further, the drawdown in the farthest piezometer not obey the approximation of the Theis well function.

6.3.7 Radius of influence

The well function clearly shows that it take some time for the drawdown to reach a piezometer at distance. Therefore, we may talk about a “radius of influence” which is dynamic and indicates to how far from the well the drawdown is perceived. It is an important insight. Clearly, we can define the radius of influence in different ways. For instance, we could say the radius of influence is the distance where the drawdown is 1 cm, 10 cm or whatever case appropriate choice is made. However we could, and we do that here, opt for a more general notion. If we look at the logarithmic approximation of the Theis well function we notice that the drawdown is always a straight line in the drawdown versus log time scale. We now define the radius of influence in a general way as the distance at which the straight drawdown line intersects drawdown $s = 0$.

The analysis is then straightforward. Starting with the approximation

$$W(u) \approx \ln\left(\frac{2.25kDt}{r^2S}\right) = 0$$

So that

$$\frac{2.25kDt}{r^2S} = 1$$

and so

$$r = \sqrt{\frac{2.25kDt}{S}}$$

This radius is, therefore proportional with \sqrt{t} . It is, obviously, also larger when the transmissivity is larger, so that influence can spread faster, and smaller when the storage coefficient is larger, which reduces the spreading of influence. This simple equation is very practical to state how far the influence of a well under the conditions envisioned by Theis reaches as a function of time.

Of course, one may adopt the relation such that it gives a certain drawdown s_{min}

$$s_{min} \approx \frac{Q}{4\pi kD} \ln \frac{2.25kDt}{r^2S}$$

Which can be manipulated to

$$r \approx \sqrt{\frac{2.25kDt}{S} \exp\left(\frac{4\pi kD}{Q} s_{smin}\right)}$$

But it does not bring a proper answer, because the approximation of the well function is not valid for small drawdowns. What we, therefore should do instead is use the actual well function

$$s_{min} = \frac{Q}{4\pi kD} W(u)$$

then determine the value of $W(u)$ that given the answer

$$W(u)_{min} = s_{min} \frac{4\pi kD}{W}$$

Then determine the value u_{min} that belongs to the wanted $W(u)_{min}$, so that

$$u_{min} = \frac{r^2 S}{4kDt}$$

and, finally,

$$r = \sqrt{\frac{4u_{min}kDt}{S}}$$

If we compare this with our first approach, we have here $4u_{min}$ instead of 2.25. Both approaches are valid, but the latter is exact in terms of the drawdown that is used as a threshold to determine the radius of influence.

6.3.8 Relation with the solution for the steady-state situation

We obtain a steady-state situation when we use a well an a negative mirror well at some distance $2R$.

Let's use the simplified Theis solution to compute the result.

$$s = s_1 + s_2 = \frac{Q}{4\pi kD} \ln\left(\frac{2.25kDt}{r_1^2 S}\right) - \frac{Q}{4\pi kD} \ln\left(\frac{2.25kDt}{r_2^2 S}\right)$$

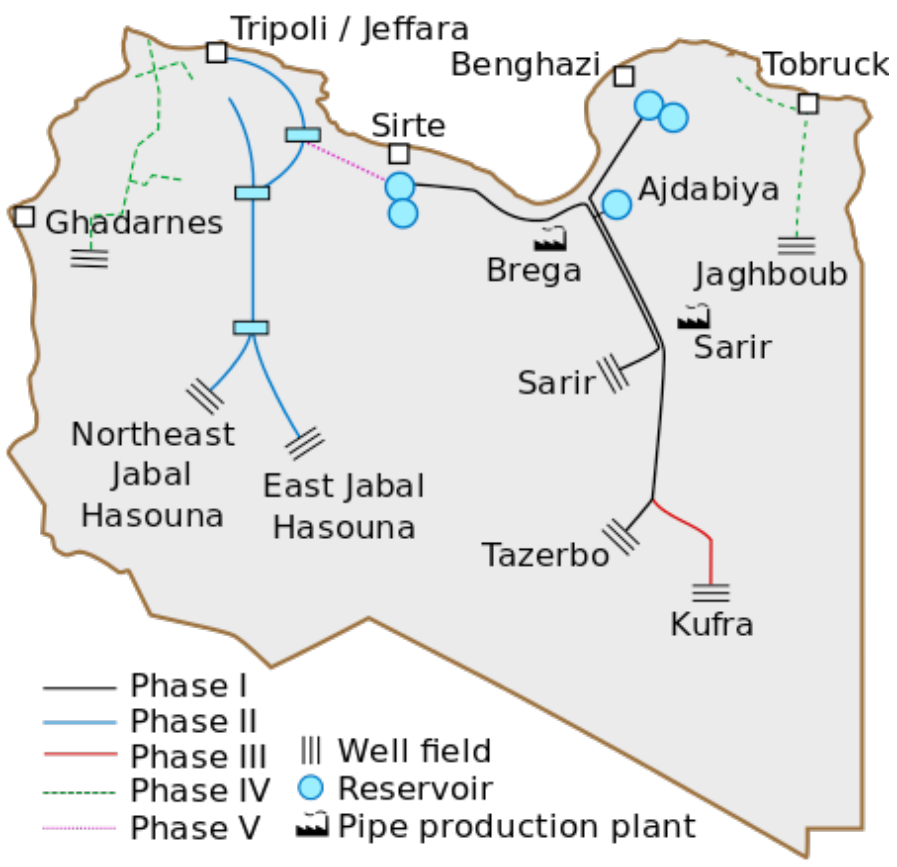
For the drawdown in the well, we have $r_1 = r_w$ and $r_2 = 2R$, hence

$$\begin{aligned} s &= \frac{Q}{4\pi kD} \ln\left(\frac{(2R)^2}{r_w^2}\right) \\ &= \frac{Q}{2\pi kD} \ln\left(\frac{4R}{r_w}\right) \end{aligned}$$

This implies that the drawdown in this well is the same as that in a well in a circular island with a radius equal to 2 times the distance between the well and its mirror well and that this drawdown will be constant after sufficiently long time, such that the logarithmic approximation of the Theis drawdown formula applies. Note that the square under the logarithm leads to $2\pi kD$ (steady) instead of $4\pi kD$ (transient).

6.3.9 Exercises

1. An unconfined aquifer has a transmissivity of $500 \text{ m}^2/\text{d}$ and a specific yield of 0.15 and is situated above an impervious base. Groundwater is abstracted during 2 weeks. During the first 10 days, the abstraction rate is $1000 \text{ m}^3/\text{d}$; during the last 4 days, the abstraction is $3000 \text{ m}^3/\text{d}$. What is the drawdown at the end of this 2 week period at a distance of 80 m from the well?
2. A square building with sides of 50 m pit needs its floor at 7 m below ground surface dry. The water table is initially at 4 m below ground surface. The aquifer is unconfined with its bottom at 50 m below ground surface. The hydraulic conductivity is estimated at 20 m/d and the specific yield is 0.25. The works at the dry bottom need to start in 4 weeks. It takes one week to install a well at each corner of the building pit. At what capacity must these wells pump to realize a groundwater level that is 50 cm below the excavated floor in 4 weeks?
3. The Nubian sandstone aquifer is the world's largest known aquifer system (See Wikipedia). Two million km² in size it NW Sudan, NE Chad, SE Libya and most of Egypt containing an estimated 150000 km³ of fossil groundwater. It may be considered confined with a transmissivity of $600 \text{ m}^2/\text{d}$. Libya under Ghadafy created the so-called Great Man-Made River Project. It began extracting $2.4 \text{ km}^3/\text{year}$ ($6.6 \text{ million m}^3/\text{d}$ or $275000 \text{ m}^3/\text{h}$ or $76 \text{ m}^3/\text{s}$). The wells of Tazerbu can be easily found on Google Earth, they are 400 km away from the Egyptian border. Assume that the wells in Tabarzu extract $15 \text{ m}^3/\text{s}$ from the aquifer; how will the drawdown develop at the border between Egypt and Libya?
5. Groundwater is extracted from an unconfined aquifer to irrigate crops by means of a pivot. A well will supply the pivot has 50 ha. 50% of the irrigated waters is consumed by the crop and hence evaporated; the remaining 50% is water that returns to the aquifer. A crop consumes a water volume equivalent to a layer of 75 cm. Two crops can be harvested in a year. What is the required pumping capacity of the well and how will the groundwater head below the pivot develop. Compute the drawdown over time at the following distances from the well a) 0.2 m (=inside the well, required to see if it falls dry), b) at the edge of the irrigated 50ha circular are served by the well, c) at 2 and 5 times this distance to estimate its impact on neighboring wells.
6. An area in Morocco irrigation is done by means of drainage tunnels (qanats, or khettaras). The water to this aquifer is rainwater captured in the hills and mountains nearby. The general groundwater flow away from the foot of the mountains causes a gradient of the natural groundwater, which is used by the drainage tunnels. These tunnels run from their outcrop in the villages with a small upward gradient towards the foot of the mountains until they intersect the water table, so that groundwater will drain towards the village. Imaging the average drawdown caused by the khettaras is 2 m. A developer intends to grow crops in a new



4. a)

Figure 6.12: Picture of the GMMR project in Lybia

area and wants to install wells for its irrigation. The area is 50 ha and the required net consumption is 0.75 m/year over this area yielding a year-average extraction of $0.75 \times 50000/365 = 1030\text{m}^3/\text{d}$. What will be the impact of the extraction wells on the existing khettaras? Take into consideration that the aquifer at the foot of the mountains is closed and that its open to infinity away from these mountains. Assume the specific yield is 20% and the transmissivity is $500 \text{ m}^2/\text{d}$.

7. It may not seem immediately obvious to provide an answer with the simple tools of this course. But we can give it a try. We can compute the transient drawdown by the new well and include the effect of the closed side of the aquifer at the mountain foot. With this, we can compute the drawdown everywhere, and therefore, also at every point of the khettaras where they tap groundwater. We may assume that the yield of the khettaras is proportional to the drawdown they cause. When we subtract the drawdown of the new well at the khettaras from that of the khettaras themselves, we have at least an estimate of the impact. A difficulty arises only from the integration of the drawdown impact along each khettara. However, we can just take the drawdown at the center of their tapping length as an approximation.

Extraction by the new well will be $0.75 \times 50 \times 10^4/365 = 1030\text{m}^3/\text{d}$. The distance to the mountain foot is 2100 m. To take the closed aquifer into consideration, we put a mirror well of the same flow at 3000 m beyond the mountain foot. Then we can compute the impact of the development on the khettaras over time. Let's assume the nearest khettara is 500 m away, then the drawdown due to the well and the mirror well is

$$s = \frac{Q}{4\pi kD} W\left(\frac{r_1^2 S}{4kDt}\right) + \frac{Q}{4\pi kD} W\left(\frac{r_2^2 S}{4kDt}\right)$$

The distance between the well and the khettara tab section being $r_1 = \sqrt{(2100 - 325/2)^2 + 700^2} = 2060 \text{ m}$ and between the mirror well and the khettara tab section being $r_2 = \sqrt{(2100 + 325/2)^2 + 700^2} = 2370 \text{ m}$ and $Q = 1030\text{m}^3/\text{d}$. Using this formula we can now compute the drawdown at the khettara tab section over time and hence the impact on the khettara discharge.

A problem with the computation of the net effect for the khettara is that the situation at the khettara is one with a fixed head, i.e. the elevation of the drainage tunnel. This is cannot directly be superposed. But we can say that if the well reduces the water depth at the khettara this leaves less drawdown for the khettaras to be imposed on the groundwater to attract it to their drainage tunnel. We can also say that the remaining depth at the location of the khettara after the well has been extracting for some time reduces the khettara extraction in proportion.

1. In the Mid-West of the United States water rights to a creek have been fixed since the nineteenth century. A new development wants to circumvent those rights by using groundwater. Due to the distance from the creek, i.e. 800 m, no impact on the creeks discharge is expected. But will this be true? The aquifer is unconfined with a specific yield of 0.24, a depth of 60 m and a conductivity of about 25 m/d. Compute of there is an impact of the extraction by the new farmer, who intends to



Figure 6.13: Khettaras (qanats / drainage tunnels) to the west of Erfoud in Morocco draining groundwater from the foot of the Antiatlas mountains at the left to the fields and villagers at the right (coordinates lat 31.506, lon -4.484). The width of the figure is 5600 m.

extract a year-round average of 1000 m³/d. If so, how will this impact develop over time and when will it reach its maximum? What will be the maximum impact of this extraction?

6.3.10 Flow at distance r from the well

How much water is released from storage between r_1 and r_2 or how much is the flow toward the well at distance r . For such questions we need the flow in the aquifer at distance r . We can determine this flow from the drawdown, by taking the derivative with respect to distance.

$$s = \frac{Q_0}{4\pi kD} W(u)$$

$$\begin{aligned} Q_r &= -2\pi r k D \frac{\partial s}{\partial r} \\ Q_r &= -\frac{2\pi r k D Q_0}{4\pi k D} \frac{dW(u)}{du} \frac{\partial u}{\partial r} \end{aligned}$$

with $u = r^2 S / (4kDt)$ it follows that

$$\frac{\partial u}{\partial r} = \frac{2rS}{4kDt} = \frac{2}{r} \frac{r^2 S}{4kDt} = \frac{2u}{r}$$

hence

$$\begin{aligned} \frac{Q_r}{Q_0} &= -u \frac{dW(u)}{du} = -u \frac{d \int_u^\infty \frac{e^{-y}}{y} dy}{du} \\ &= +u \frac{e^{-u}}{u} \\ \frac{Q_r}{Q_0} &= e^{-u} \end{aligned} \tag{6.6}$$

This is a very simple relation between the flow Q_r at distance r and the constant extraction Q_0 from the well. Notice that u is proportional to r^2 , so that this ratio diminishes exponentially with distance from the well. The ratio Q_r/Q_0 in equation 6.6 is shown in figure 6.14 first as a function r and secondly as a function of t . Of course, all curves collapse to the same if plotted versus u or $1/u$ (not shown). From the practical point of view, one sees that at a distance of $r = 100$ m, even in a phreatic aquifer with a specific yield as high as 0.2, the Q_r is already 60% of Q_0 at 100 m from the well. This implies that the effect of partial penetration becomes indeed stationary very soon after the start of the well.

The total flow across a radius r may be computed as

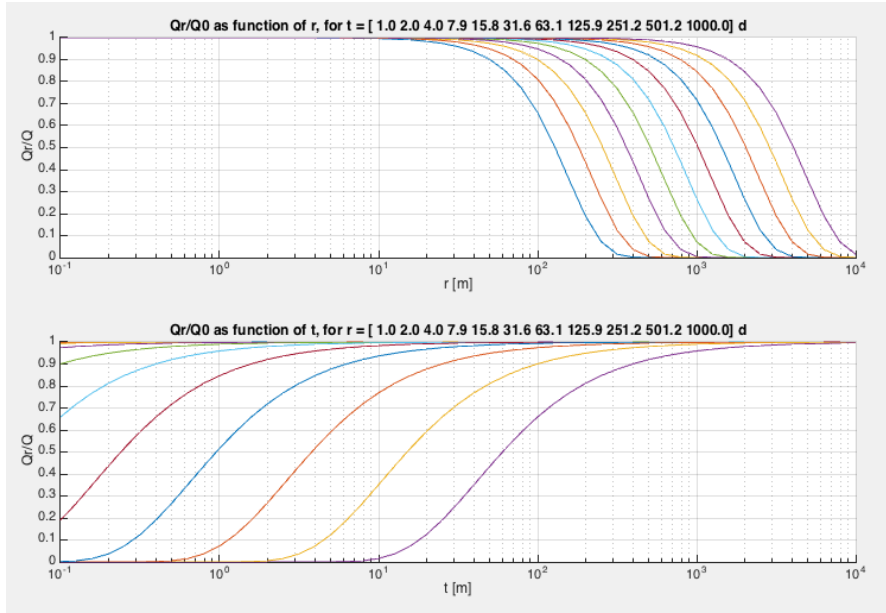


Figure 6.14: Q_r/Q_0 as a function of r for different times and as a function of time for different r . As before, $Q = 2400 \text{ m}^2/\text{d}$, $kD = 1200 \text{ m}^2/\text{d}$ and $S = 0.2$.

$$V_r = \int_0^t Q_r dt = Q_0 \int_0^t e^{-u} dt$$

However, I could not find the solution of that seemingly simple integral.

6.3.11 Pumping test Oude Korendijk

One of the most-used applications of the Theis solution is the analysis of transient pumping tests have been carried out all over the world since the solution was known in 1935. Before that only steady-state situations could be properly analyzed, but in many real-world cases this was insufficient as the drawdown would often not become stationary. In this section we show a classic Theis pumping test-analysis. We will workout the pumping test given by Kruseman and De Ridder (1972, 1994) carried out south of Rotterdam in 1963 called “Oude Korendijk”. As can be seen from the lithology, the aquifer is about 10 m thick and is confined above and below by layers with an extremely low permeability, that functioned as aquiclude during the test. Hence, an interpretation of the test by the Theis solution should be adequate.

The data provided by Kruseman and De Ridder (1994) are given in table 6.2. The student should interpret this pumping test using the classical graphical method by Theis, using double log graphs of both the Theis curve and the data. Given that we have implemented the solution of the Theis well function in Excel, we can just as well do

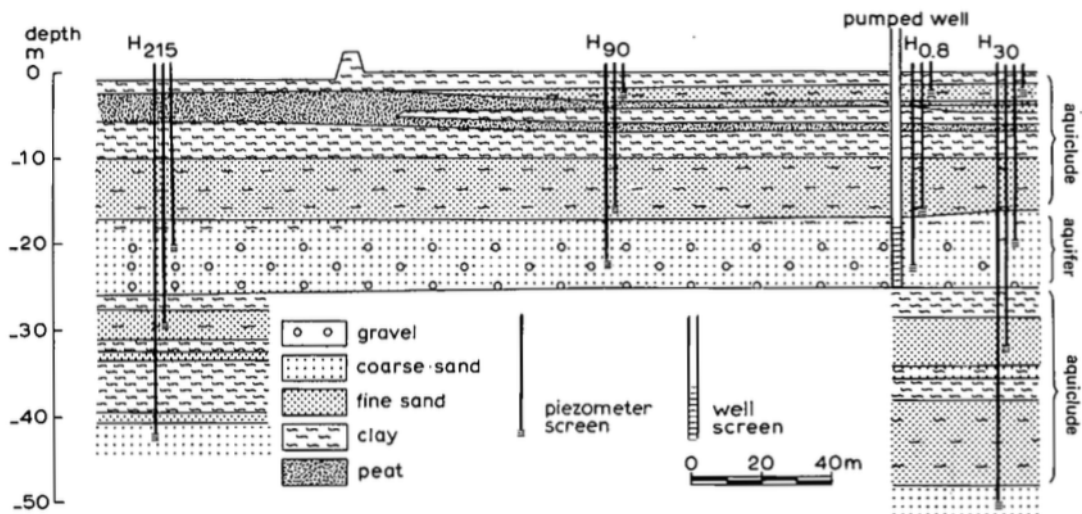


Figure 3.2 Lithological cross-section of the pumping-test site 'Oude Korendijk', The Netherlands (after Wit 1963)

Figure 6.15: Cross section pumping-test site 'Oude Korendijk' from Kruseman and De Ridder (1972, 1994)

the entire interpretation in Excel and use Excel's graphic capability for the purpose. The idea is to put the measurements on the same graph as the type-curve and then move them such that they match the curve as well as possible. Moving on double log scales is done by multiplying the values on the axes. i.e. the drawdown to move vertically and the time or rather t/r^2 to move the graph horizontally. With the data match the type curve interpret the transmissivity and the storage coefficient from the amount the measurements had to be moved to achieve the fit.

Figure 6.16 gives the drawdown data for the observation points with time on logarithmic scale and versus logarithm of t/r^2 . In the latter chart, the data of the different piezometers should fall on top of each other. As can be seen, that is more or less so for the two piezometers nearest to the well but not quite so for that at 215 m. There may be various reasons, but after all possible errors that could be made while measuring have been excluded, the reason should be that the spatial properties of the aquifer are not uniform. Without any further information it may only be guessed what the reason may be. One possibility to solve the problem may be to try if the Hantush method fits the data better.

Figure 6.17 shows the measurement on a double log chart, versus t/r^2 overlapping the Theis type curve after shifting until the best optical match between the measurements and the type curve was obtained.

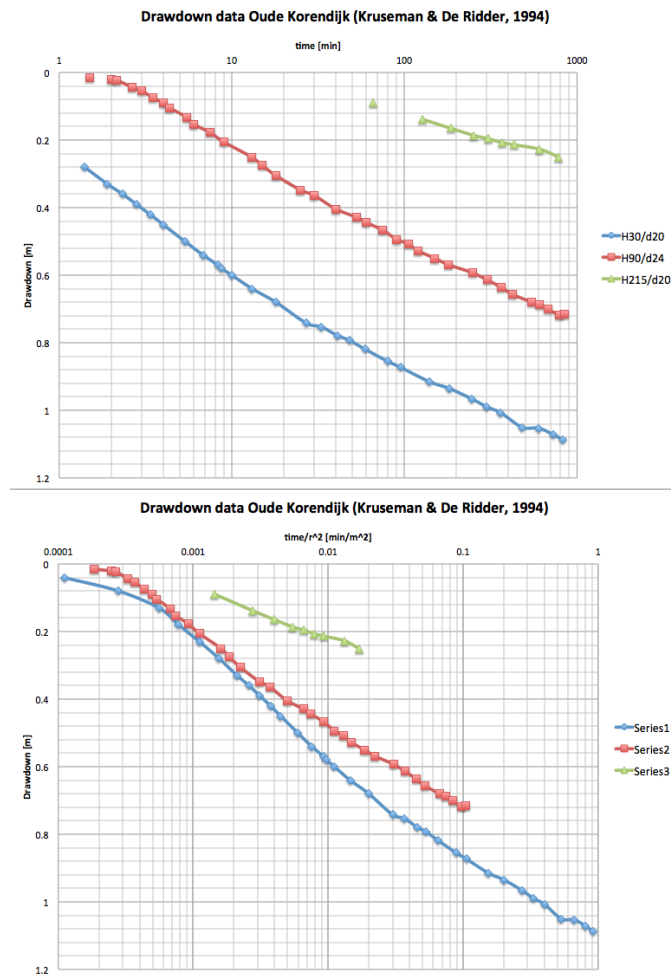


Figure 6.16: Drawdown for pumping test Oude Korendijk versus t/r^2 with time on logarithmic scale.

Data pumping test .Oude Korendijk' (Kruseman & De Ridder, 1970 / 1994)

The pumping test took place in July 1962 at a rate of 788 m³/d

H30 Obs well at r=30 m, screen depth 20 m

H90 Obs well at r=90 m, screen depth 24 m

				H215 Obs well at r=215 m, screen depth 20 m	
t [min]	s [m]	t [min]	s [m]	t [min]	s [m]
0	0	0	0	0	0
0.1	0.04	1.5	0.015	66	0.089
0.25	0.08	2	0.021	127	0.138
0.5	0.13	2.16	0.023	185	0.165
0.7	0.18	2.66	0.044	251	0.186
1	0.23	3	0.054	305	0.196
1.4	0.28	3.5	0.075	366	0.207
1.9	0.33	4	0.09	430	0.214
2.33	0.36	4.33	0.104	606	0.227
2.8	0.39	5.5	0.133	780	0.25
3.36	0.42	6	0.153		
4	0.45	7.5	0.178		
5.35	0.5	9	0.206		
6.8	0.54	13	0.25		
8.3	0.57	15	0.275		
8.7	0.58	18	0.305		
10	0.6	25	0.348		
13.1	0.64	30	0.364		
18	0.68	40	0.404		
27	0.742	53	0.429		
33	0.753	60	0.444		
41	0.779	75	0.467		
48	0.793	90	0.494		
59	0.819	105	0.507		
80	0.855	120	0.528		
95	0.873	150	0.55		
139	0.915	180	0.569		
181	0.935	248	0.593		
245	0.966	301	0.614		
300	0.99	363	0.636		
360	1.007	422	0.657		
480	1.05	542	0.679		
600	1.053	602	0.688		
728	1.072	680	0.701		
830	1.088	785	0.718		
		845	0.716		

Table 6.2: Data for pumping test Korendijk (Kruseman & De Ridder, 1994)

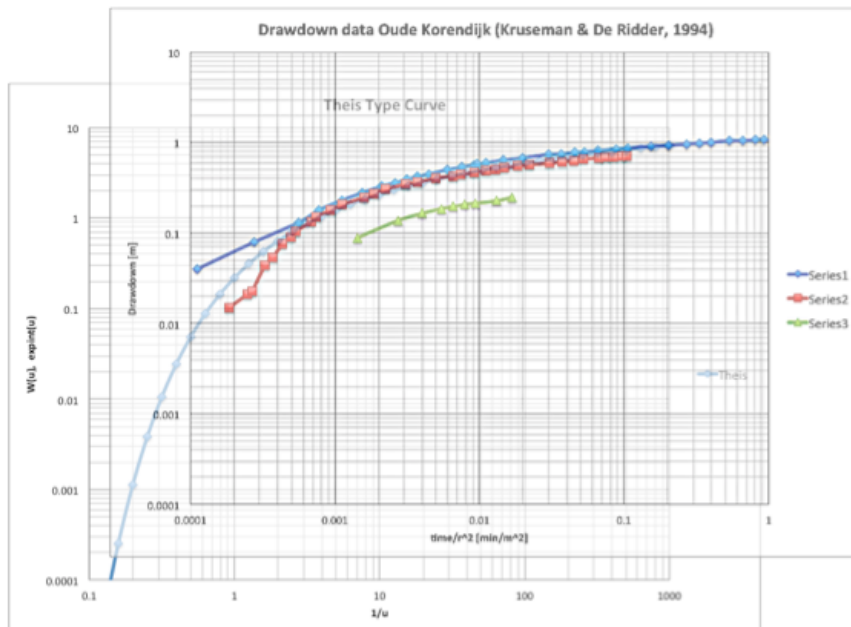


Figure 6.17: The drawdown on double logarithm scales versus t/r^2 overlying the Theis type curve shifted to obtain the best optical match between the data and the type-curve

Exercise: Interpret the given pumping test data. Also check how much different parameter values one obtains by interpreting the three piezometers separately.

6.3.12 Superposition in time

A well may be switched on and off at will. The effect of this switching can be taken into account by superposition. For instance a well that has been pumping for a time T since $t=0$, after which it's switched off, can be viewed as two wells that pump continuously. The first starts at $t_0 = 0$ with extraction Q_0 and the second at $t = t_0 + T$ with extraction $-Q_0$. This way the net extraction will be zero for $t > t_0 + T$. This way of superposition can be applied even with a large number of changes of the flow rate. The problem may only be that after many such changes one needs to carry on a large number of "wells" at the location of the real well to compute the current state. This is merely a computational burden, one that can be effectively dealt with through application of convolution, explained elsewhere in this syllabus.

Hence we have for this well that switches on at $t = t_0$ and off at $t = t_0 + T$

$$s_t = \frac{Q_0}{4\pi kD} W(u_t) - \frac{Q_0}{4\pi kD} W(u_{t-T})$$

where the second term is omitted al long as $t < t_0 + T$. In fact if we subdivide time in episodes during which the extraction from the well may be considered constant, then each "well" simply "extracts" the difference with that of the previous well. For example, let there be 5 episodes starting at times t_1, t_2, t_3, \dots in which the extraction of the well is respectively Q_1, Q_2, Q_3, \dots , then we can simulate the heads by starting a well at each of these times that extracts the difference of the Q in that episode with that of the previous episode. If, to generalize we imagine the first well to have a flow $Q_0 = 0$ that started at $t = -\infty$, the flow of these wells become respectively

$$Q_1 - Q_0, Q_2 - Q_1, Q_3 - \dots$$

and apply the superposition of the Theis drawdown to compute the drawdown at any moment:

$$s_t = \frac{Q_1 - Q_0}{4\pi kD} W(u_{t-t_1})_{t \geq t_1} + \frac{Q_2 - Q_1}{4\pi kD} W(u_{t-t_2})_{t \geq t_2} + \frac{Q_3 - Q_2}{4\pi kD} W(u_{t-t_3})_{t \geq t_3} + \dots$$

Example:

Consider an aquifer of infinite lateral extend with $kD = 1000 \text{ m}^2/\text{d}$ and $S_y = 0.02$. A well extracts at the the following flows during 5 consecutive months: $Q = 1200, 600, 1400, 200, 1200, 300, 0 \text{ m}^3/\text{d}$. Compute a the drawdown at 100 m from the well for a 180 day period since the first start of the pump. Make a graph based on the drawdown at the end of every day. Use Excel to make the computations.

The results are shown in figure 6.18. The top figure shows the extractions as specified, the second shows the drawdowns (notice that the vertical scale is reversed to show the

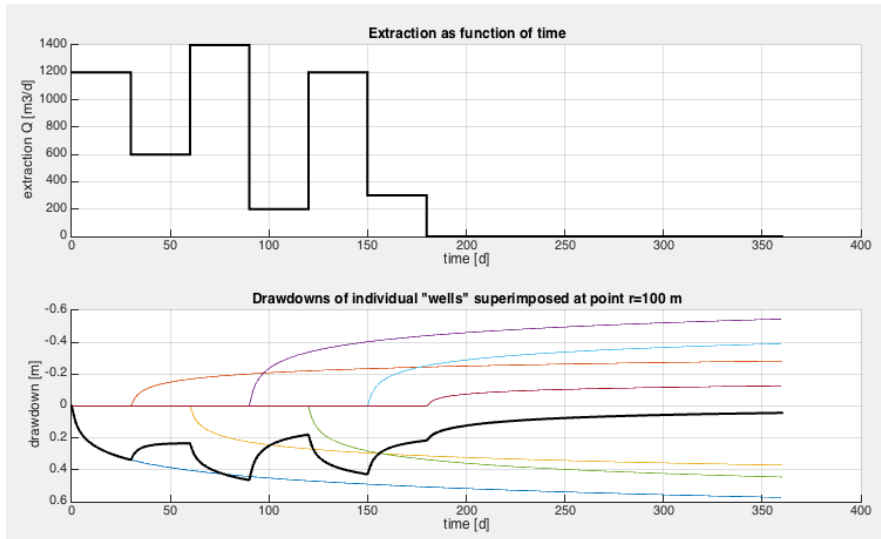


Figure 6.18: Superposition in time (for data given in the text example)

drawdown downward positive) of the individual “wells” and the sum, which is the net effect of the well with the varying extraction (thick black line).

6.3.13 Superposition in space

Superposition works in space as well as in time. In fact, one have have an arbitrary number of wells that pump arbitrary amounts of water, and compute the drawdown at an arbitrary point by superposition of the ensemble of wells, while per well the superposition in time is done as explained in the previous paragraph.

The drawdown can be superimposed on the actual groundwater head. For instance, the contributions of an arbitrary number of pumping wells can be added together, because the partial differential equation is linear. This applies to superposition both in time and space and will form the following example as an illustration how the Theis well function is mostly used superimposing the effects of more than one well to get the overall head change at the locations of interest.

Example: In an area there are four wells constructed 1 year after the other. The wells are placed on a square with sides of 1 km and the order in which they are constructed is NW, NW, SE, SW. The extraction is 1 m/y over the served area of 1 km^2 , which boils down to $Q = 2740 \text{ m}^3/\text{d}$, the same for all four wells, starting immediately after their construction. The transmissivity is $kD = 1200 \text{ m}^2/\text{d}$ and the specific yield is $S_y = 0.24$. Show the drawdown in the center between these wells as a function of time for a period of 50 years. Show snapshots of the drawdown at times $[1, 2, 2, 4, 5, 10, 25, 50]$ years after the start of the first extraction well.

For the graph showing drawdown versus time we can conveniently use a logarithmic time scale starting with $t = 0.01$ year and ending with $t = 100$ years. For the snapshot

we would compute the drawdowns in a dense-enough grid to allow contouring of the drawdown at specific point in time. The results for both time on logarithmic scale and linear scale are presented in figure 6.19. The snapshot for $t = 50$ years is shown in figure 6.20. As can be seen the drawdown in the center between the wells is almost flat. In case the wells are partially penetrating, a correction needs to be applied, especially for the drawdown in the wells and perhaps immediately around the wells, but this has no effect at distance larger than about the aquifer thickness.

Exercise: In Egypt an investments to grow fruits have been made in the desert along the motorway between Cairo and Alexandria. Imagine the enterprise to be 2 km wide having 500 ha of cropped area, that is 2 km along the road by 250 m perpendicular to the road. The crop requires 1 m of water per year to mature. Four wells are used arranged parallel to the road. They all have their screen from -50 to -100 m. What will be the drawdown in the middle two wells after 1 month, 1 year, 10 years and 50 years. Also compute what will be the drawdown at the neighbors, 2, 4, 6, 8 and 10 km away. Finally, what would be the drawdown in the center wells if these neighbors up to 10 km away on both sides would pump at the same rate? The transmissivity of the aquifer is 2000 m²/d, the specific yield is 24%, the depth of the aquifer is 240 m and the distance below ground surface 40 m initially.

Hint: Do the computations in Excel. Arrange your data well. Use the computation for one enterprise to compute the drawdown for the other enterprises as well by smartly arranging you computation setup in Excel.

Is the extraction possible? Does the real situation still meet the preconditions that underlay the Theis solution? What conditions are probably not valid? How can we take these into account?

See also the paragraph on partial penetration.

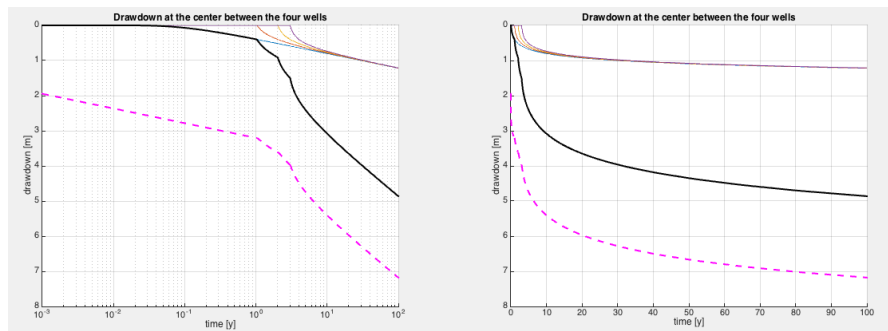


Figure 6.19: Computed drawdown for the example in the center between the four wells (thick black line) and at well #1 (thick dashed purple line)

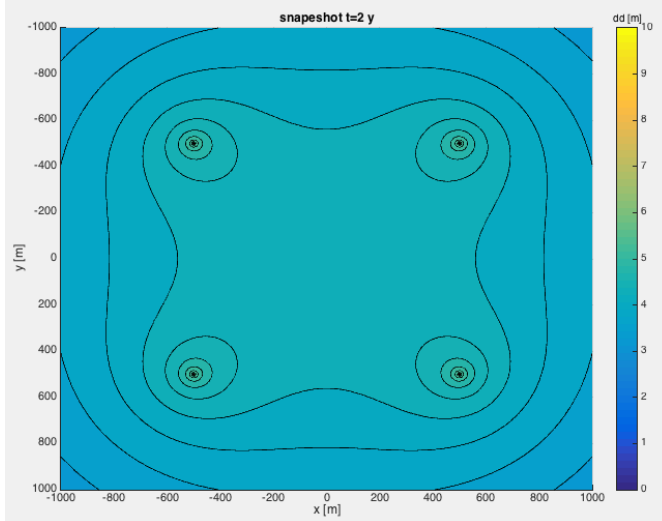


Figure 6.20: Snapshot of drawdown after 50 years of pumping; the colors match the drawdown shown in figure 6.19.

6.3.14 Questions

1. What groundwater situation was solved by Theis? What is the underlying groundwater system, and the initial and boundary conditions that apply?
2. Why do we prefer drawing the Theis well function on a double log graph using $1/u$ instead of u on the horizontal axis?
3. Explain how we can interpret a pumping test in a confined aquifer based on the Theis type curve on a double log graph?
4. What is the preferred variable to use on the horizontal axis when plotting our drawdown data coming from different observation wells?
5. What is the physical meaning of the partial differential equation on which the Theis solution was founded?
6. Is there a final steady situation that matches the Theis solution? Or does the Theis solution on the long run to a final equilibrium stage?
7. How is the outcome $h^2 - H^2 = \frac{Q}{2\pi k} W(u)$ related to that of a confined situation, $h - H = \frac{Q}{4\pi kH} W(u)$?
8. How can you determine u as a ratio of time t and a characteristic time T ?
9. Show how you can simplify the Theis well function for small values of u .
10. What is the general shape of the Theis drawdown on linear vertical and logarithmic horizontal scale?

11. What part of this general shape is covered by the simplification of the Theis drawdown?
12. Explain the shape of the drawdown versus distance using the simplified Theis well function.
13. Express this simplified function in terms of the ratio of distance and a characteristic distance for a chosen fixed time.
14. Explain the radius of influence mathematically using the simplified Theis well function.
15. What is the drawdown per log-cycle of time? Show this using the simplified formula?
16. What is the mathematical standard function that is equivalent to the Theis well function?
17. Given the Theis well function as a power series (equation 6.3), show the relation between two consecutive terms.
18. How would you use the Theis well function to compute the drawdown of a well in an aquifer of infinite extent to compute the transient drawdown due to a well at a given distance from a river that fully penetrates the aquifer without entry resistance?
19. Write down mathematically the superposition in time of well that changes the extraction in fixed steps from time to time.
20. How would you compute the drawdown due to a well in an aquifer bounded by two parallel fully penetrating canals in direct contact with the aquifer? The canals are a distance L apart and the well is at a distance l from one of them.
21. Does the situation posed in the previous question result in a steady-state situation on the long run? Explain your answer.
22. Assume that Libya's large pumping station in Kufra (E 24.149163°, N 23.392326°), with wells in the Nubian sandstone at 162 km from the Egypt's border extracted 1 million m^3/d starting in 2000. How long would it take for the drawdown to influence the head at the border of Egypt? Assume $kD = 600 \text{ m}^2/\text{d}$, $S = 0.005$. What would be the drawdown at Kufra after 10 and 50 years. What would be the drawdown at the Egyptian border after 10 and 50 years. For the Kufra well field use an effective well radius of 10 km. (have a look at the site on the given coordinates in Google Earth).
23. A groundwater level in a building pit of $50 \times 50\text{m}$ has to be lowered by 5 m, for which wells are placed at its corners. The transmissivity $kS = 1000 \text{ m}^2/\text{d}$ and the specific yield is $S_y = 0.2$. Compute the necessary extraction if the water level in

the center has to reach its objective (5 m drawdown) within two weeks of pumping. After reaching the necessary drawdown, the drawdown has to be maintained for 6 months. Compute the necessary extraction such that the objective is fulfilled. How much may the extraction be reduced after two weeks, to maintain the desired drawdown, such that the objective is met after 6 months?

24. A well is drilled in an unconfined aquifer to secure water for a refugee camp in Jordan. The transmissivity is small, only $250 \text{ m}^2/\text{d}$ and the storage coefficient also is modest with 0.005. The water table is at 50 m below ground surface. What is the necessary depth of the screen so that the well will yield the required demand of m^3/d for 10 years?

6.4 Partial penetration of well screens

More often than not, well screens only partially penetrate the exploited aquifers because very often aquifers are much thicker than the screen length that is needed to produce the required amount of water. Limiting well depth save money for the owner, although at the cost of some extra energy, because of the extra head loss due to the fact that the streamlines of the water flowing towards the well have to concentrate near the screen, which causes it to accelerate, and higher velocities entail greater losses of energy.

6.4.1 Huisman's method

The flow due to only the fact that the screen is partially penetrating can be superimposed on the ideal situation in which the streamlines are all horizontal and parallel towards a fully penetrating screens, for which the standard groundwater well formulas were derived. There are at least two ways to deal with it both leading to an extra drawdown that must be added to the drawdown obtained with the standard formula. The first method is to compute the effect of partial penetration based on the exact solution for the effect, which was derived for a confined aquifer by Hantush (see Kruseman and the Ridder, 1994). The other is a method developed by Huisman (1972), which summarizes the first method by a simple relation for the extra head loss. He writes (p130):

With a random position of the well screen as shown in figure ... (left), the additional drawdown at the well face is given by

$$\Delta s_0 = \frac{Q_0}{2\pi k D} \frac{1-p}{p} \ln \frac{\alpha h}{r_0}$$

with α a function of the amount of penetration $p = h/D$ and of the amount of eccentricity $e = \delta/D$. The value of α as a function of these parameters is given in the table.

The screen in the center of the figure shows the position that is most usual. This simplifies the formula, at least for penetrations larger than 20%, yielding:

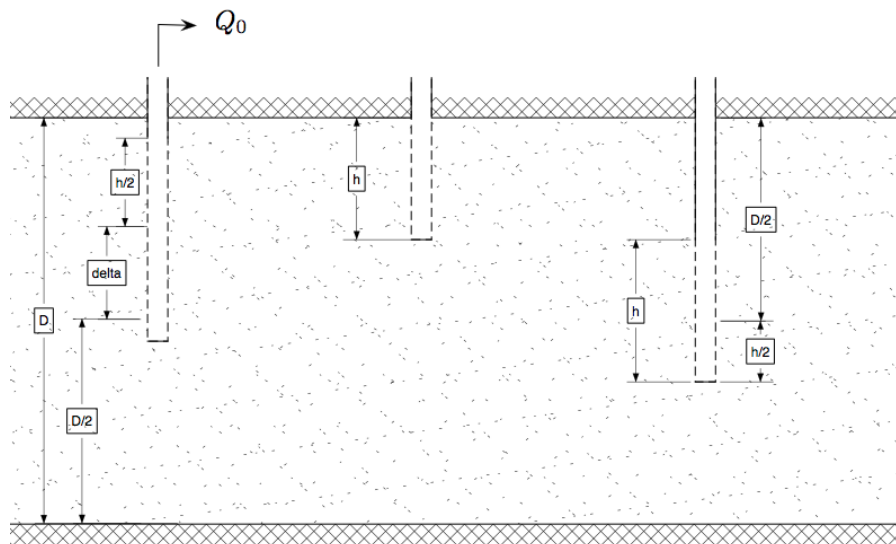


Figure 6.21: Partially penetrating wells

Table 6.3: Huisman's (1972) partially penetration table showing the values of α the formulas as a function of the relative screen length $p = h/D$ and the eccentricity $e = \delta/D$ with D the thickness of the aquifer, h the screen length and δ the distance of the center of the screen to the center of the aquifer.

α	0	0.05	0.1	0.15	0.2	0.25	0.3	0.35	0.4	0.45
$p \setminus e \rightarrow$	0.1	0.44	0.37	0.31	0.25	0.21	0.16	0.11	0.06	1.09
0.1	0.54	0.44	0.37	0.31	0.25	0.21	0.16	0.11	0.06	1.09
0.2	0.44	0.37	0.31	0.25	0.21	0.16	0.11	0.06	0.06	0.06
0.3	0.37	0.31	0.25	0.21	0.16	0.11	0.06	0.06	0.06	0.06
0.4	0.31	0.25	0.21	0.16	0.11	0.06	0.06	0.06	0.06	0.06
0.5	0.25	0.21	0.16	0.11	0.06	0.06	0.06	0.06	0.06	0.06
0.6	0.21	0.16	0.11	0.06	0.06	0.06	0.06	0.06	0.06	0.06
0.7	0.16	0.11	0.06	0.06	0.06	0.06	0.06	0.06	0.06	0.06
0.8	0.11	0.06	0.06	0.06	0.06	0.06	0.06	0.06	0.06	0.06
0.9	0.06	0.06	0.06	0.06	0.06	0.06	0.06	0.06	0.06	0.06

$$\Delta s_0 = \frac{Q_0}{2\pi k D} \frac{1-p}{p} \ln \frac{(1-p)h}{r_0}$$

The partial penetration for the right-most screen in the figure leads to a simplified formula:

$$\Delta s_0 = \frac{Q_0}{2\pi k D} \frac{1-p}{p} \ln \frac{(1-p)h}{2r_0}$$

For wells in a phreatic aquifer, where the thickness of the aquifer depends on the drawdown, the factor

$$\Delta s_0 2H = \frac{Q_0}{\pi k} \frac{1-p}{p} \ln \frac{\alpha h}{r_0}$$

has to be added to the value of $H^2 - h^2$, where H is the initial thickness of the water table aquifer and h is the final thickness of that aquifer at the well. In this case, the amount of penetration p and the eccentricity e should now be based on the depth of the water table h_0 that is valid for the fully penetrating well.

6.4.2 Hantush's solution for partial penetrating screens

An analytical computation of the extra drawdown due to partial penetration can be obtained from the analytical solution of the extra drawdown due to partial penetration, which reads

$$\Delta s = \frac{Q_0}{2\pi k D} \frac{2D}{nd} \sum_{n=1}^{\infty} \left\{ \frac{1}{n} \left[\sin \left(\frac{n\pi z_1}{D} \right) - \sin \left(\frac{n\pi z_2}{D} \right) \right] \cos \left(\frac{n\pi z}{D} \right) K_0 \left(\frac{n\pi r}{D} \right) \right\} \quad (6.7)$$

The variables are shown in figure 6.22. Notice that the distance can be either measured from the top or from the bottom of the aquifer.

This equation allows to compute the extra drawdown due to partial penetration at any point in the aquifer as specified by the coordinates r and z . Hence to estimate this extra drawdown for the well itself, one should choose some points at distance r_0 , the well radius and average over them, because, contrary to a real well screen that has a constant head inside, the derivation of the influence of partial penetration was under the assumption of a constant discharge per unit screen length. The latter causes some variation of head along the screen, while a uniform head causes some variation of inflow along the screen.

The extra drawdown presented here is a steady-state solution, which cannot account for dynamics. However, the effect of water release from storage close to the well where partial penetration matters becomes steady-state already after a short time. To determine the time after which the partial penetration effect can be considered constant, we can use the derived relation for the flow Q_r in equation 6.6. Considering that the any concentration of stream lines is gone beyond about $r > 1.5D$, we may state that the condition sought is (for instance)

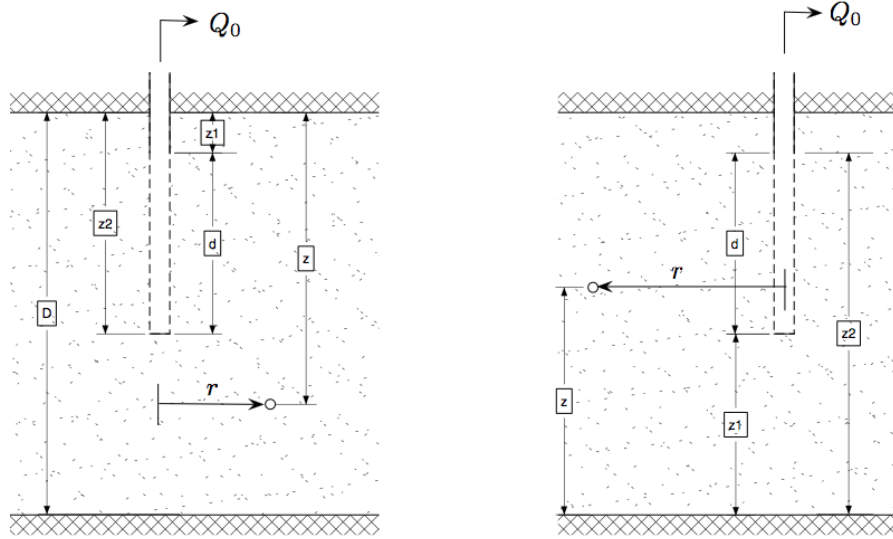


Figure 6.22: Partial penetrating screens with variables as used in equation 6.7

$$Q_R > 0.9Q_0$$

and so, with equation 6.6 we get

$$\begin{aligned} 0.9 &= e^{-u} \\ \ln 0.9 &= -u \\ -0.10536 &= -u \end{aligned}$$

so that

$$\begin{aligned} u &= \frac{r^2 S}{4kDt} \approx 0.1 \\ t &> 10 \frac{r^2 S}{4kD} \end{aligned}$$

While the range of r where effects of partial penetration can play is generally said to be $r \leq 1.5D$, we may need a larger distance when the aquifer is vertically anisotropic as given by different values of the horizontal and vertical conductivity, k_r and k_z respectively. In those cases

$$r \leq 1.5D \sqrt{\frac{k_r}{k_z}}$$

The code below shows how this partial penetration function can be implemented as a User Defined Function in Excel

```

1 Public Function PP(aD As Double, bD As Double, zD As Double, rD
As Double) As Double
2 'Hantush Partial Penetration, aD=a/D, bD=b/D, zD=z/D, rD=r/D
3 'a is distance from base of aquifer to bottom of screen /
thickness of aquifer D
4 'b is distance from base of aquifer to top of the screen divided
by D
5 'z is distance from base of aquifer /D
6 'r is distance from heart of well, horizontally / D
7 'see Kruseman & De Ridder, 1994,
8 Pi = 3.141592654
9 PP = 0
10 For i = 1 To 15
11     PP = PP + (Sin(i * Pi * bD) - Sin(i * Pi * aD)) * Cos(i * Pi
* zD) * BesK(i * Pi * rD, 0) / i
12 Next i
13 PP = 2 * PP / Pi / (bD - aD)
14 End Function

```

6.4.3 Example

Figure 6.23 shows the head contours due to a partially penetrating screen. The actual situation, figure c, is the superposition of the heads due to a fully penetrating well (a) and the effect of partial penetration (b). The streamlines (not plotted) are perpendicular to the head contours and show flow contraction. Figure 6.23, c was obtained by adding equation 6.7 to a simple Dupuit solution $s = Q/(2\pi kD) \ln(R/r)$. The contribution of the head due to partial penetration has a positive zone in front of the screen, where the drawdown is increased and negative zones above and below the screen, where the drawdown is reduced by partial penetration, but where the flow is much smaller than that opposite of the screen. As can be seen from the pictures, the effect of the partial penetration does not reach farther than about one aquifer thickness from the well. So the 1.5D mentioned above for the reach of the impact of partial penetration may even be called large.

6.4.4 Questions

1. What is partial (screen) penetration?
2. When is partial penetration important? To how far away from the well?
3. A screen penetrates the first third of the aquifer depth. Explain how the drawdown is affected by the partial penetration relative to the drawdown due to a fully penetrating well? Indicate where the drawdown is more and where it is less than the drawdown due to a fully penetrating screen.

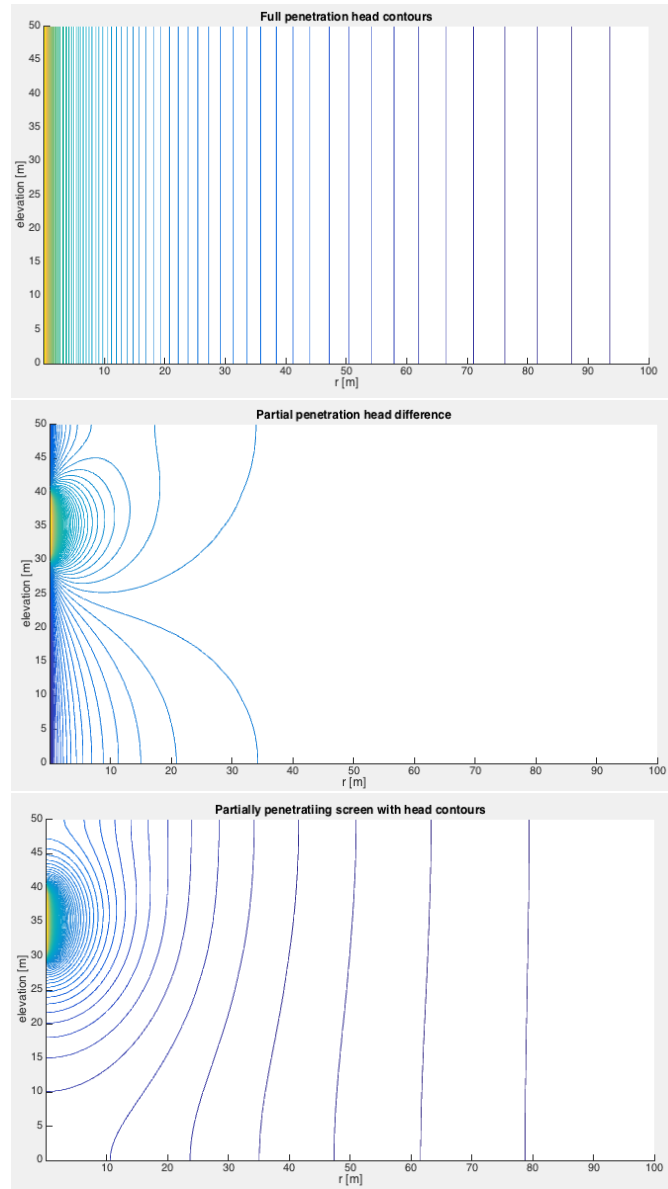


Figure 6.23: Effect of partial penetration: a) Head contours due to extraction by a fully penetrating well. b) The head change due to partial penetration, equation 6.7. c) Partial penetration impact superimposed on the heads of the fully penetrating well. (c = a + b). The flow is axially symmetric.

4. Why is the effect of partial penetration steady already after a short time after the extraction from the well started?
5. How could you handle partial penetration in a real case when you have to determine the drawdown from a screen that only penetrates part of the aquifer thickness.

6.5 Hantush: transient flow due to a well in a semi-confined (leaky) aquifer

Mahdi S. Hantush (1955) published a solution for the drawdown caused by a fully penetrating well pumping in a semi-confined aquifer, the situation of which is depicted in figure The situation differs from the one by Theis, in that now the aquifer is overlain by a semi-pervious layer, called an aquitard, on top of which a fixed head (water level) is maintained. So there is vertical leakage through the aquitard, which linearly depends on the head difference across it. Hantush (1955) formulated the problem as follows:

"The non-steady drawdown distributed near a well discharging from an infinite leaky aquifer is presented. Variation of drawdown with time and distance caused by a well of constant discharge in confined sand of uniform thickness and uniform permeability is obtained. The discharge is supplied by the reduction of storage through expansion of the water and concomitant compression of the sand, and also by leakage through the confining bed. The leakage is assumed to be at a rate proportional to the drawdown at any point. Storage of water in the confining bed is neglected."

We will implement the Hantush well function by numerical integration and by series expansion and then apply it. Both implementations are highly accurate across the entire range of values in tables given in the original paper and in various groundwater-hydrology books such as for instance the most well-known book on pumping-test analysis (Kruseman & De Ridder, 1994, free on the internet).

6.5.1 Hantush's partial differential equation and solution

The derivation is the same as for the Theis equation, with one addition, the vertical leakage through the overlying aquitard.

From continuity we obtain for a ring between r and $r + dr$ from the well center over a given time step $\partial t = t \rightarrow t + dt$ we have:

$$q_r(2\pi r) - q_{r+dr}(2\pi(r+dr)) + n_r 2\pi r dr = S(2\pi r dr) \frac{\partial \phi}{\partial t}$$

where not n_r is the leakage from (or to) the overlying layer with fixed head. Working out this continuity equation in the same way as we did before for the Theis solution, yields

$$-\frac{\partial q}{\partial r} - \frac{q_r}{r} + n_r = S \frac{\partial \phi}{\partial t}$$

The leakage can be set to

$$n_r = \frac{\phi_0 - \phi}{c}$$

with c the resistance of the top layer against vertical flow and ϕ_0 the maintained head in the top layer. With Darcy's law filled in we then obtain

$$\frac{\partial^2 \phi}{\partial r^2} + \frac{1}{r} \frac{\partial \phi}{\partial r} + \frac{\phi_0 - \phi}{kDc} = \frac{S}{kD} \frac{\partial \phi}{\partial t}$$

Whenever we deal with semi-confined flow systems we write

$$\lambda^2 = kDc$$

or

$$\lambda = \sqrt{kDc}$$

where we call λ [L] the spreading length or the characteristic length of this semi-confined aquifer system. Hence the PDE in terms of head is

$$\frac{\partial^2 \phi}{\partial r^2} + \frac{1}{r} \frac{\partial \phi}{\partial r} + \frac{\phi_0 - \phi}{\lambda^2} = \frac{S}{kD} \frac{\partial \phi}{\partial t}$$

Because the derivative of $\phi - \phi_0$ is the same as that of ϕ , because ϕ_0 is a constant, we may write as well

$$\frac{\partial^2 (\phi - \phi_0)}{\partial r^2} + \frac{1}{r} \frac{\partial (\phi - \phi_0)}{\partial r} - \frac{\phi - \phi_0}{\lambda^2} = \frac{S}{kD} \frac{\partial (\phi - \phi_0)}{\partial t}$$

Note that the sign of the third term has changed.

So that we see that the PDE does not depend on both ϕ and ϕ_0 but only on $\phi - \phi_0$, the difference from the initial head. Generally we call $s = \phi - \phi_0$ the drawdown. In fact, it is the head change relative to the initial head. (Notice the lowercase s for the head change, contrary to the storativity S , which we always write in uppercase).

So, the final PDE for semi-confined flow is

$$\frac{\partial^2 s}{\partial r^2} + \frac{1}{r} \frac{\partial s}{\partial r} - \frac{s}{\lambda^2} = \frac{S}{kD} \frac{\partial s}{\partial t}$$

which was solved by Hantush for specific initial and boundary conditions.

- Initial s zero everywhere.

$$s(r, 0) = 0$$

- Head change at infinity is always zero

$$s(\infty, t) = 0$$

- Head in upper aquifer always the same.

$$s_0 = 0$$

- Flow at the well face is constant for $t > 0$ and zero for $t \leq 0$.

$$Q_{r \rightarrow 0, t_0} = 2\pi r k D \frac{\partial s}{\partial r} \Big|_{r \rightarrow 0} = Q_0$$

Notice also, that, because the partial differential equation is linear, superposition may be applied to its solutions. That means that the value of the initial head ϕ_0 is immaterial; it may even vary in an arbitrary way in space; the differential equation only describes the change of the head due to the well alone without being affected by what happens elsewhere.

The solution obtained by Hantush is

$$s = \phi - \phi_0 = \frac{Q_0}{4\pi k D} W_h \left(u, \frac{r}{\lambda} \right)$$

where $W_h()$ is Hantush's well function. It is mathematically written as

$$W_h \left(u, \frac{r}{\lambda} \right) = \int_u^{\infty} \frac{\exp \left(-y - \frac{(\frac{r}{2\lambda})^2}{y} \right)}{y} dy$$

You may prove that the solution is correct by filling it into the partial differential equation and verifying that both sides of the PDE are then equivalent.

6.5.2 Implement Hantush's well function in Excel

To make use of this solution one needs the values of W_h for combinations of u and r/λ . One way is to look them up in the tables that you find in books on pumping test analyses for example (Kruseman & De Ridder, 1994). Another way is to implement the function as a function in for instance Visual Basic, Python or Matlab, so that you have them available for immediate use, just like any other function that you can use in those programs.

We will implement the Hantush function by numerical integration in the same way as we did with the Theis solution. The only thing that changes is the extra variable $\rho = r/\lambda$ that has to be passed to the function, and the addition of the term $-\rho^2/(4y)$ under the exponent.

In Visual Basic, the implementation can be as follows (in Python it would be similar)
Another way is through the expression of the well function as a power series.

$$W_h(u, \rho) = \sum_{n=0}^{\infty} \frac{(-1)^n}{n!} \left(\frac{\rho}{2} \right)^{2n} u^{-n} E_{n+1} \left(\frac{\rho^2}{4u} \right)$$

$$E_{n+1} = \frac{1}{n} \{ e^{-u} - u E_n(u) \}, (n = 1, 2, 3\dots)$$

```

Public Function Whan(u As Double, rho As Double) As Double
'�antush's well function (by integration, similar to Expint)
Dim dlny, y, w, lnINF, rho2 As Double

lnINF = 20           'end of integration
dlny = 0.01          'step size for integration, small part of log cycle
lny = Log(u) + 0.5 * dlny   'first location on log axis, use +0.5dlny to move to center of steps
rho2 = rho * rho / 4
w = 0               'Initialize and loop till lnINF wasreached
While lny < lnINF
    y = Exp(lny)
    w = w + Exp(-y - rho2 / y)
    lny = lny + dlny
Wend

'finally multiply by the step size, all at once is more efficient than while looping
Whan = w * dlny

End Function

```

Figure 6.24: Hantush' well function in Visual Basic for Excel

Exercise: It is left to the student to implement it and see if both implementations yield the same result.

6.5.3 Hantush type curves and comparison with Theis

Having implemented the Hantush well function in Excel or Python, we can compute the so-called Hantush type curves that are presented in nearly every book on pumping tests. The idea is to show the function in on double logarithmic axis so that it is directly comparable with a drawdown time curve. Thus we make graphs showing the Hantush function W_h on the vertical axis (because proportional to the drawdown) and the $1/u$ on the horizontal axis (because proportional to time). We do so for distinct values of r/λ and we also add the Theis function as it is equivalent to the Hantush function if leakage were absent, that is when $c \rightarrow \infty$.

We see from the type curves that the Hantush solution is equivalent to the Theis function for sufficiently small values of time, and that they all reach a constant value after a certain time that depends on the value of $r\lambda$. The larger the vertical resistance, the smaller the value of r/λ , the longer it takes before steady state equilibrium is reached.

It is also interesting to see the type curves on linear vertical and logarithmic horizontal scale. This yields the character of the absolute drawdown as a function of logarithmic time. This is done in the next figure.

These curves have an S-shape, except for the Theis curve which never reach an equilibrium and the drawdown will forever continue to grow. All Hantush curves represent a situation where the aquifer is recharged from above proportional to the drawdown. These Hantush cases will reach an equilibrium drawdown because of this recharge by induced leakage. For an arbitrary point at distance r , initially there is no drawdown. Then after some time the drawdown accelerates to finally decelerate towards steady-state.

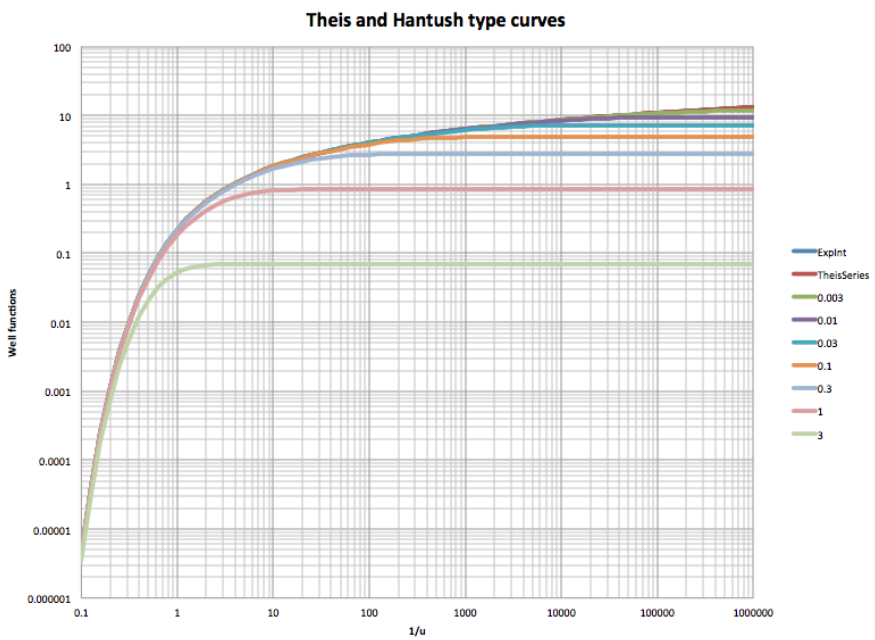


Figure 6.25: Theis and Hantush type curves plotted in Excel. The Hantush type curves are for different values of $\rho = r/\lambda$ as indicated by the numbers in the legend to the right.

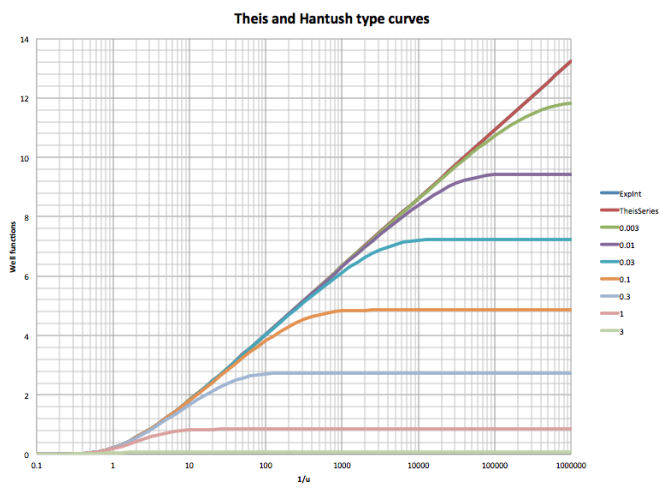


Figure 6.26: Theis and Hantush curves on a linear vertical scale while the horizontal scale is still logarithmic.

Because the steady-state solution of a well extracting in a semi-confined aquifer is

$$s = \frac{Q}{2\pi kD} K_0\left(\frac{r}{\lambda}\right)$$

it follows that $K_0\left(\frac{r}{\lambda}\right) = \frac{1}{2}W_h(u_{t=\infty}, \frac{r}{\lambda}) = \frac{1}{2}W_h(0, \frac{r}{\lambda})$ because $u = \frac{r^2 S}{4kDt}$ and so $t \rightarrow \infty$ implies $u \rightarrow 0$.

The curves have an reflection point, whit a drawdown that is exactly halfway zero and its final equilibrium. The drawdown at this point thus equals $s = \frac{Q}{4\pi kD} K_0\left(\frac{r}{\lambda}\right)$ (notice the 4 in the denominator).

It can be proven (see for instance Bruggeman (1999, p877) that the inflection point is obtained for $u = \frac{r}{2\lambda}$. With this knowledge, we can compute the time, which we call $t_{50\%}$, when this point drawdown reached by setting

$$\begin{aligned} u &= \frac{r^2 S}{4kDt_{50\%}} = \frac{r}{2\lambda} \\ \frac{r^2 Sc}{2\lambda^2 t_{50\%}} &= \frac{r}{2\lambda} \\ t_{50\%} &= Sc \frac{r}{2\lambda} \end{aligned} \quad (6.8)$$

This time bears two characteristics. First is the distance from the well relative to the characteristic length of the groundwater system, i.e. $r/(2\lambda)$. The 2 is not strange as we encounter it in both u and in the mathematical Theis well function. The other characteristic is Sc , a combination that is associated with the time an aquifer is filled by leakage. To show this consider an aquifer without horizontal flow with a top layer with constant head and at $t = 0$ a uniform different head in the aquifer, which will thereafter gradually disappear due to the induced leakage through the overlying aquitard. Using drawdown or head difference instead of heads, where $s = \phi - \phi_0$, without horizontal flow, the partial differential equation reduces to

$$-\frac{s}{c} = S \frac{ds}{dt}$$

which may be readily solved by integration

$$\begin{aligned} \frac{ds}{s} &= -\frac{dt}{cS} \\ \ln s + C &= \frac{t}{cS} \end{aligned}$$

with as initial condition the drawdown s_0 at $t = 0$, which yields the integration constant

$$t = 0, \quad s = s_0 \rightarrow C = -\ln s_0$$

so that

$$\frac{s}{s_0} = \exp\left(-\frac{t}{Sc}\right)$$

With $T = Sc$, this can be written as

$$\frac{s}{s_0} = \exp\left(-\frac{t}{T}\right)$$

Where we see that T functions as the characteristic time of that system: the drawdown s is reduced by a factor $1/e = 0.36788$ every time T further in the future. You may be more familiar with the word “halftime”, where each halftime further in the future implies that in this case s is reduced by a factor 2. This halftime can easily be derived by looking for the time $t_{50\%}$ where $s/s_0 = 0.5$

$$\begin{aligned} 0.5 &= \exp\left(-\frac{t_{50\%}}{T}\right) \\ \ln 0.5 &= -\frac{t_{50\%}}{T} \\ t_{50\%} &= T \ln 2 \\ &\approx 0.7 T \end{aligned}$$

This is always the case: the halftime of a system is just about 70% of its characteristic time.

We, therefore, notice that the quantity $T = Sc$ is the characteristic fill-up time of the leaky aquifer, which we also encountered in equation 6.8 that given the time that the drawdown at a point reaches half its final value.

Exercise: Show the flex-points in the Hantush type curves.

Exercise: Show that the Hantush function becomes the Theis function when $c \rightarrow \infty$.

6.5.4 Questions

1. What are the properties of the groundwater system leading to a Hantush-type of drawdown in a pumping test? Or: what groundwater system envisioned Hantush when he developed his well formula?
2. How does the finale drawdown expressed in terms of the Hantush well solution relate to the steady state solution for a well in a semi confined aquifer? Write down your answer mathematically?
3. At what time does the Hantush drawdown reach half its final steady state value? Give your answer in mathematical terms.
4. What is the characteristic time of a semi confined aquifer in following change of the barometer pressure?
5. Explain why the higher Hantush type-curves resemble more the Theis curve?

6. Explain why the Theis curve is an extreme case of the Hantush curve?
7. What is the characteristic length of a semi-confined aquifer (or, alternatively, the spreading length)? Give your answer mathematically?
8. How does the Hantush type curve change when the spreading length is increased?
9. Explain this change in terms of transmissivity of the aquifer and the resistance of the overlying aquitard.
10. What is the general shape of the Hanush well function no linear vertical and logarithmic horizontal scale?
11. Consider an aquifer with constant transmissivity, $kD = 900 \text{ m}^2/\text{d}$ and $S = 0.001$ with $c = 400 \text{ d}$. For an observation point at $r = 600 \text{ m}$ distance, determine when the drawdown has become steady state (to at least 95%). Use the Hantush-type curves to determine your answer.
12. For the same situation, when is the drawdown at this point equal to half the final drawdown?
13. For the same situation, when becomes the drawdown essentially larger than zero, say at least 5% of the final drawdown. Tip: use the Hantush type curves to determine your answer.
14. The head in a building pit of $50 \times 50 \text{ m}$ in a semi-confined aquifer with $kD = 1000 \text{ m}^2/\text{d}$, $c = 360 \text{ d}$ and $S = 0.002$ has to be lowered by 3.5 m. The wells are placed in the corners of the building pit. How long one needs to pump to reach steady state drawdown and what is the final drawdown in the center of the building pit?
15. What will be the head in the building pit one day after pumping started?
16. What will be the head in the building pit one day after pumping ended?

6.5.5 Assignment: pumping test Dalem (Kruseman & De Ridder, 1994) with new data

Kruseman and De Ridder (1972, 1994) describe a pumping test in a leaky aquifer near the village Dalem in The Netherlands, that was carried out in 1961. The pumping rate was $Q = 761 \text{ m}^3/\text{d}$. The cross section based on the drillings is given in figure 6.27. They also provide the data for that site and work out the test applying several methods. The student will work out this pumping test as an exercise/part of the assignment. Because the test concerns a semi-confined aquifer, the aim must be to determine the transmissivity, kD , the storage coefficient, S , and the resistance, c , of the overlying semi-pervious layer.

Instead of the data from the book, every student will be provided with his/her own set of measurements from a number of tube wells that are located a different locations and differs for each student.

The task is to work out the pumping test in the classical way by using the type curves. Clearly, by having implemented the well functions, one should be able to do the whole interpretation in Excel, including the graphics.

Hint: So plot your data on the same double log graph as the type curves and move your data such that they overlay a particular curve as well as possible. You move your data upward or downward by multiplying your drawdowns by a factor, and you move your data to the left or right by multiplying your time by a factor. The interpretation follows from the two factors after the measurements fit the graphs.

The exercise is part of the assignment for this course.

Figure 6.28 shows the data for all students and piezometers. The data for each students and 3 piezometers can be found in the accompanying Excel workbook Student-DataDalemPumpTest.xls.

6.6 Delayed yield (delayed water-table response)

6.6.1 Introduction

Pumping tests drawdowns do not always resemble the Theis or Hantush type curves, sometimes the drawdown shows a double dip, which is known as delayed yield. Because delayed yield is quite ubiquitous, it has been studied extensively by scholars in the past, most noticeably by Boulton (1954), Pricket (1971) and Neuman (1972). While Boulton introduced an extra delay parameter to explain the phenomenon. Pricket (1971) demonstrated for a large number of pumping test in his state that the Boulton solution well matched the curves that he obtained from real-world tests. However there was not direct physical mechanism behind Boulton's delay parameter and hence, it was unclear what its precise origin was. It was often assumed that it had to be the unsaturated zone, which is not accounted for in the known groundwater flow solutions. And indeed early groundwater flow models, that encountered for saturated and unsaturated flow simultaneously were able to match the curves that were measured by Pricket (Cooley, 1970). However, it was Neuman, who in 1972 solved the problem, showing that the delayed yield could be completely described by the combination of elastic storage that operates throughout the aquifer and the decline of the water table, which is generally accounted for by specific yield. Neuman (1972) solved the flow to a well in a water table aquifer while taking into account of vertical flow components. He showed that water initially stems from elastic storage, that is the expansion of the water and the compaction of the soil skeleton, which is a fast process due to the low value of this storage. Very soon after onset of the pump, the water table starts declining, which releases much more water and, therefore is a slow process. It means that after some time, the release of pore water at the water table becomes the dominant process. The result is a graph that resembles two Theis curves, an early one that declines according the the elastic storage and a late one, that declines according to the specific yield.

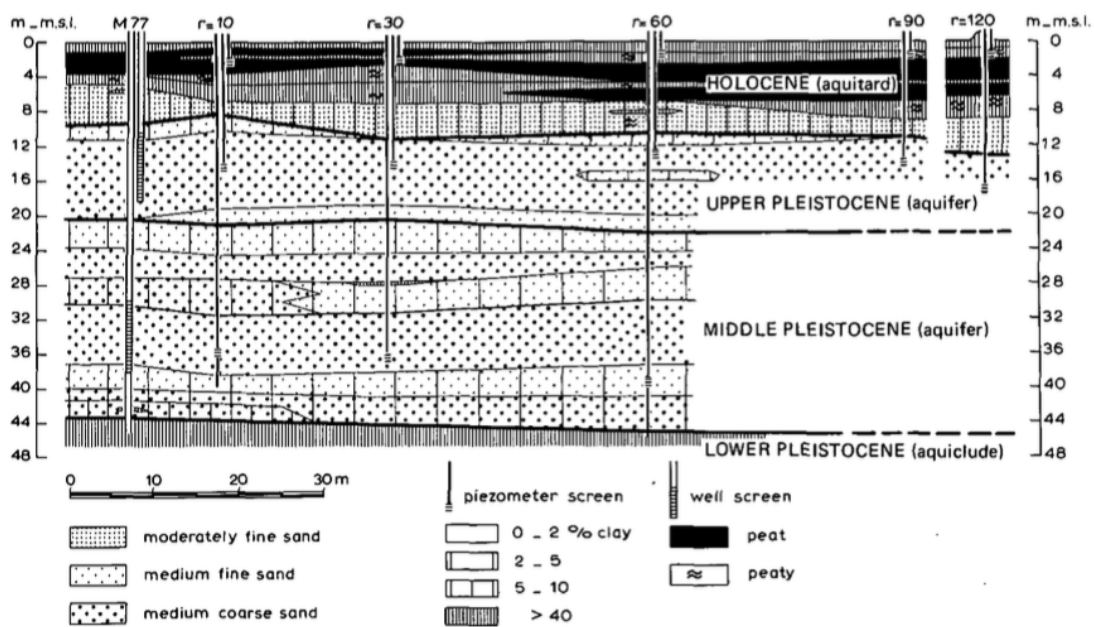


Figure 4.2 Lithostratigraphical cross-section of the pumping-test site 'Dalem', The Netherlands (after De Ridder 1961)

Figure 6.27: Dalem pumping-test site (Kruseman & De Ridder, 1994)

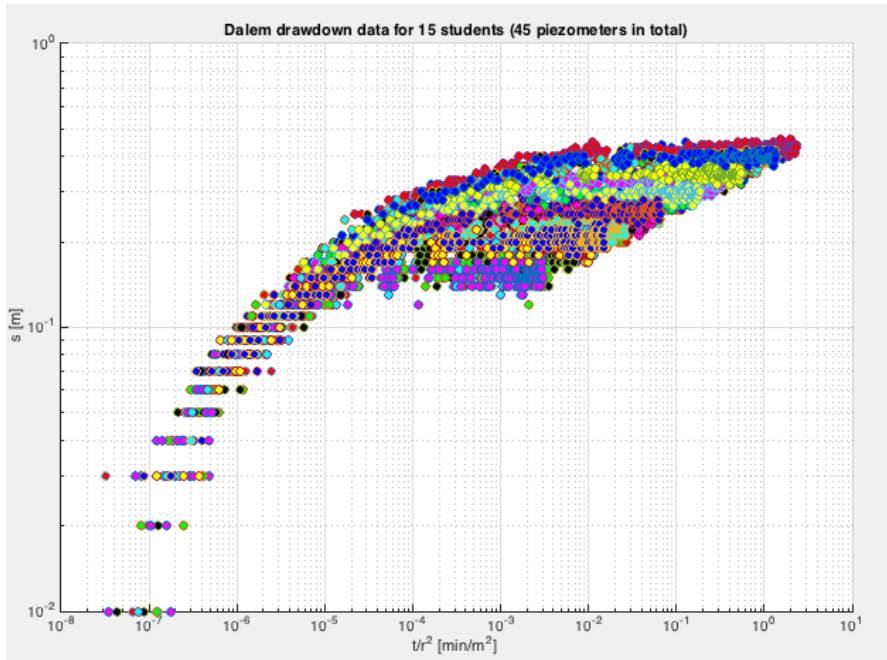


Figure 6.28: Piezometer data for students for Dalem pumping test (see accompanying Excel workbook StudentDataDalemPumpTest.xls)

6.6.2 Water-table aquifer

We may show the phenomena on the hand of some numerical simulations as shown in figure 6.29. The first picture shows the drawdown versus time for a number of points at different distances from the well and depths as expressed in % of the aquifer depth. The colors correspond to the three depths. The blue curves are near the top of the aquifer, the magenta curves in the center of the aquifer, and the green curves near the bottom. As the figure indicates the drawdownon differs with depth, but only for piezometers that are not far from the well; at later times this difference disappears. The second picture in the same figure shows the depth-averaged drawdown for a number of distances from the well. The later curves correspond to larger differences. One sees that the curves initially correspond to the Theis drawdown computed for the elastic storage coefficient, while later on they match the drawdown that corresponds to the Theis solution for the elastic yield as storage coefficient. The shorter the distance to the well, the more pronounced the transition between the two Theis curves is. Obviously, the curves that correspond to the larger distances are later. The effect of depth has been eliminated from the second chart by taking the average head over the full depth of the aquifer at each distance. The third picture in figure 6.29 demonstrates the difference of the drawdown at different depth at the same location, here chosen 28.4 m from the well. Here it becomes especially manifest that the closer to the water table, the later the drawdown graph.

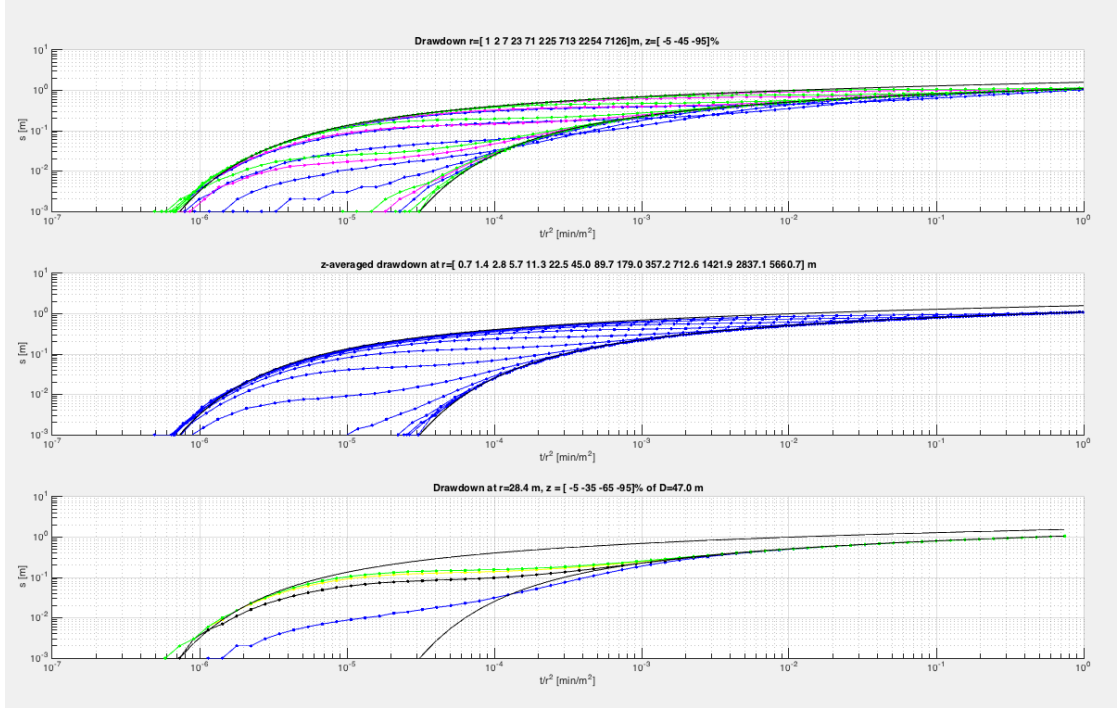


Figure 6.29: Delayed yield in a water table aquifer with a fully penetrating screen. The black lines in all three curves correspond with the Theis drawdown. The middle picture shows the elevation-averaged drawdown at different distances from the well. All lines are blue, but the closer to the water table, the later the drawdown is. The third pictures shows the drawdown at 28.4 m from the well at different depths. The colors indicate the depths, blue is shallow, then black then yellow and finally green for the deepest piezometer. The first figure shows the drawdown at a number of distances and at three different depths. Blue is shallow depth, magenta is the center of the aquifer and green near the bottom of the aquifer.

These graphs were computed using a numerical axially-symmetric model with elastic storage everywhere but only specific yield at the water table. There is no unsaturated zone involved. This is in accordance with Neuman (1972) explaining that the phenomenon of delayed yield can be fully explained by the simulations action of the elastic storage and the specific yield at the water table.

6.6.3 Generalization to semi-confined aquifers

We may now generalize delayed yield, by extending it to any groundwater system in which a water table will decline in a reaction to pumping. This especially hold true for semi-confined aquifers. The Hanush assumptions underlying his solution include a fixed head in the overlying layer. When in reality this head cannot be maintained, it will cause a delayed yield effect. This may be the case in many practical situations without it being determined in a pumping test, because the test pumping has stopped long before the delayed yield visually affects the drawdown curves. The reason is the delay caused by the resistance against vertical flow of the overlying layer. That this is so, is explained by the characteristic time for filling the semi-confined aquifer given an initial head difference with the overlying layer. This characteristic time, T , equals $T = Sc$ where S is the elastic storage coefficient of the aquifer and c the resistance of the overlying layer against vertical flow. With typical values of say $S = 0.001$ and $c = 500$ d, we have $T = 0.5$ d. This means that a sudden lowering of the head in the semi-confined aquifer would be compensated by increased leakage in about $5T \approx 2.5$ d. This characteristic time affects only the level of the transition zone between the two Theis curves. We can show this by computing the drawdown in a semi-confined aquifer. For this we use the an aquifer system consisting of a resistance cover layer that is $D_{cover} = 12$ m thick on top of a $D_{aquif} = 35$ m thick aquifer. The well is fully penetrating. Four models are compared that differ only in the vertical resistance of the cover layer, which is $c = [10, 100, 1000, 10000]$ days respectively. Specific yield is $S_y = 0.2$, the elastic storage coefficient of the aquifer is $S = 0.002$, i.e. $S_s = S/D_{aquif}$; the hydraulic conductivity of the aquifer is $k_h = 10m/d$, hence the transmissivity $kD = 350\text{ m}^2/\text{d}$. The results are presented next.

Figure 6.30 shows the drawdown averaged over the thickness of the aquifer for different distances from the well. We expect the first branch of the graphs to resemble Hanush's semi-confined drawdown, for which the spreading length r/λ determines the elevation of their horizontal equilibrium branch. The $\lambda = [59, 187, , 591, 1870]$ m for the four models respectively. The lower r/λ

the more the later deviates the Hantush curve from the Theis curve. This effect is clearly visible when the first picture is compared to the fourth. When the vertical resistance is high, the transfer to the late theis curve is much delayed. One sees this in the fourth picture when the graphs don't even reach the second Theis branch at the end of the simulation time, which was 600 days! Then the resistance is low, as in the first figure, the graphs do show a clear transfer from the elastic Theis curve to the water-table Theis curve (first picture). The picture also shows that the drawdown for points near the well resemble the elastic Theis curve, while the points at large distance do not feel elastic behavior, they immediately follow the specific-yield Theis curve. The reason is that the

first branch should follow Hantush which has an equilibrium $Q/(2\pi kD) K_0(r/\lambda)$ which approaches zero for large r . Hence, points at larger r , say at $r > 3\lambda$ will never see the elastic drawdown due to the leakage. The second branch, however, is a pure Theis curve, which has no equilibrium, because it has not recharge. Therefore, points far away from the well will eventually all feel the phreatic drawdown predicted by Theis.

To determine the resistance of the overlying layer, one should use the piezometers that reach a Hantush-equilibrium and use the Hantush solution for the interpretation. This also yields the elastic storage coefficients. If the test is sufficiently long so that one or more piezometers reach the phreatich Theis branch, then also the specific yield of the overlying layer can be determined by applying the Theis solution to the second branch. As was said earlier, the resistance of the overlying layer does not determine the position of the two bounding Theis curves, it only determines the height of the horizontal branch of the curves where they transfer from the elastic to the specify yield Theis curve.

the more

Figure 6.31 shows the drawdown at one distance, i.e. $r = 28.4$ m, in the top of the overlying layer and in all 35 model layers of the aquifer. First of all one sees that the head difference between the top and the bottom of the aquifer can be neglected; only the model with the low resistance shows a small difference, because their the vertical velocities in the aquifer are large enough to cause a small head loss between the top and the bottom of the aquifer (notice that $k_z = k_r = 10$ m/d was used). Again one observes that the horizontal branch climbs with reduced r/λ between the four models. The blue line is the drawdown in the top of the overlying layer, i.e. that of the water table itself. It is caused by the emptying of the top layer due to the downward leakage invoked by the drawdown in the pumped aquifer below.

6.6.4 The two Theis bounding curves

It was explained before, that position of the two boundary Theis curves only depend on their respective storage coefficients and not on the resistance of the cover layer. Noticing that we have for the two Theis curves

$$\frac{1}{u_1} = \frac{4kD}{S} \frac{t}{r^2}, \quad \frac{1}{u_2} = \frac{4kD}{S_y} \frac{t}{r^2}$$

Hence, the horizontal axis of both Theis curves only differ in their storage coefficient. And so

$$\frac{u_2}{u_1} = \frac{S_y}{S}$$

Hence the horizontal axis of the specific yield Theis curve is the one of the elastic storage Theis curve multiplied by S_y/S . On the logarithmic scale this is a horizontal shift. Because we have chosen values $S_y/S=100$, the second Theis curve is shifted over exactly two log-cycles to the right of the first, elastic storage Theis curve, which can be verified immediately in the graphs.

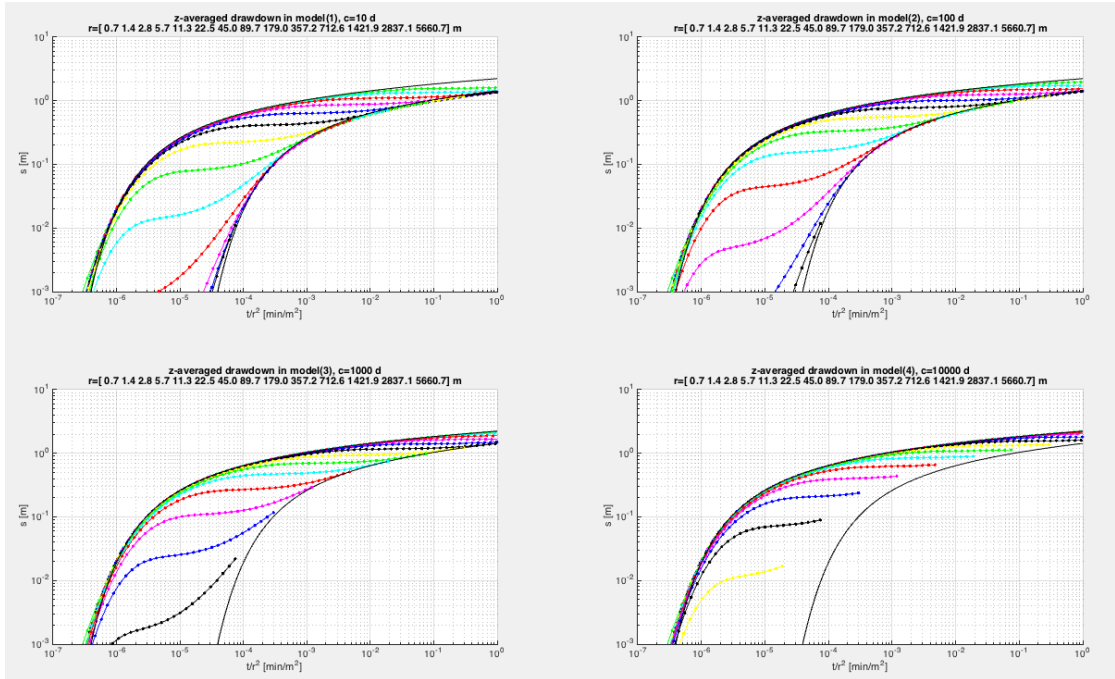


Figure 6.30: z-averaged drawdown in the aquifer at different distances. Four models differing only in the vertical resistance of the top layer. The Theis elastic storage Theis curve and the specific yield Theis curve are also shown (black lines)

This also implies the following for the determination of the specific yield from a pumping test that shows a clear delayed yield behavior. Simply determine the horizontal shift of the second with respect to the first, which is factor τ , and then apply $S_y = \tau S$.

Figure 6.32 shows the drawdown of the water table (blue lines), at the top of the aquifer (cyan) and at the bottom of the aquifer (magenta) for different distances from the well as noted in the title of the pictures. It is essentially equal to the previous picture but now for several distances. Once again, the time-drawdown curves for points inside the aquifer stay between the two bounding Theis curves. The curve for the water level lags behind and only joins the specific yield Theis curve late, later the higher the vertical resistance of the overlying layer and the distance from the well. The lower the resistance of the overlying layer, the more will this semi-confined aquifer system resemble the purely phreatic aquifer system that we discussed in the beginning of this chapter.

6.6.5 Influence of partial penetration of the well screen

It should be clear that partial penetration causes the drawdown near the well opposite the screen to become larger than the Theis drawdown. Hence one should first correct piezometers closer than about 1D from the well for partial penetration (see section on partial penetration) before analyzing any pumping test. This is illustrated in figure 6.33 that shows the drawdown in the top (cyan) and bottom (magenta) of the aquifer for a nearby point ($r = 9$ m, thick lines) and a distant point ($r = 90$ m, thin lines). The figures show that at a point at a large distance from the well is not influenced by partial penetration, as the drawdown in the top and bottom of the aquifer are practically the same and the curves stay between the Theis envelopes and are the same as in the cases with fully penetrating screens. However a point close to the well, i.e. less than about 1 to 1.5 aquifer thicknesses away, does experience a serious deviation caused by partial penetration. The point opposite the screen at the top of the aquifer (thick cyan line) has a drawdown that is larger than that for a fully penetrating screen; the point at the same distance but at the bottom of the aquifer (far below the screen, thick magenta line) has a much lower drawdown than in case the well had a fully penetrating screen. Moreover these differences do not disappear with time. On the other hand if one corrects for partial penetration by subtracting the effect from all measurements, we regain the fully penetrating drawdowns, which are directly amenable to interpretation using the standard solutions of Theis and Hantush.

6.6.6 Questions

1. Explain the cause of delayed yield.
2. Is delayed yield limited to water table aquifers?
3. What are the bounding curves of the delayed yield curves.

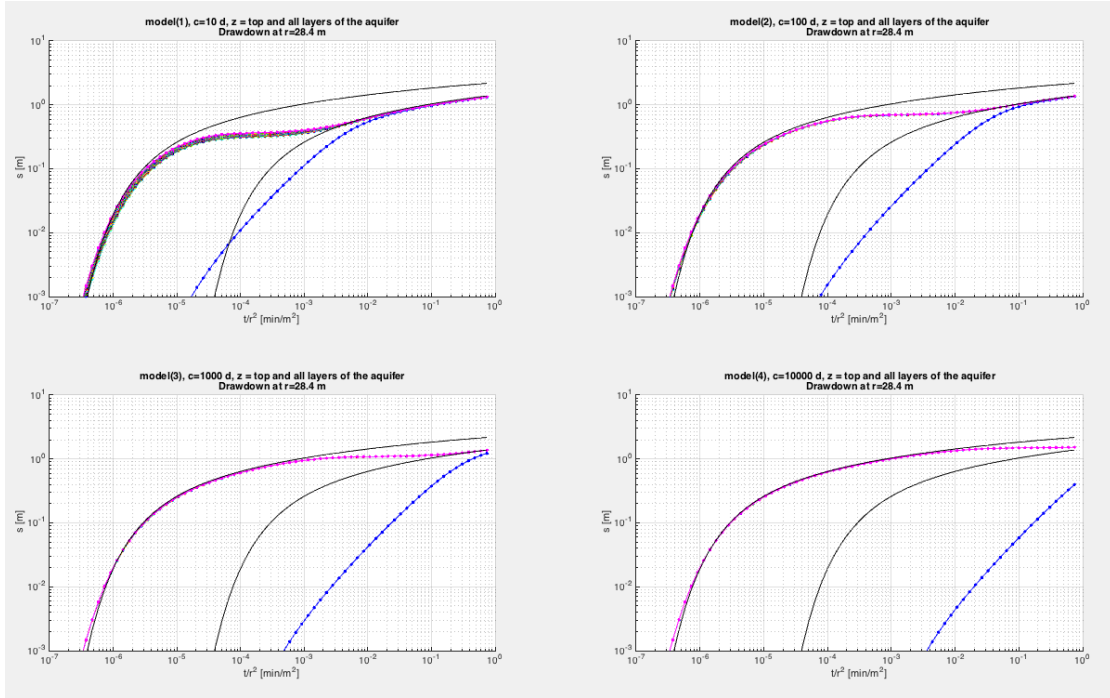


Figure 6.31: The drawdown at $r = 28.4$ m from the well in the top of the overlying layer and in all 35 model layers of the aquifer for models differing only in the resistance of the overlying layer. The blue line is the drawdown of the water table, all 35 other lines are at different elevation in the aquifer at the same distance from the well, they essentially fall on top of each other.

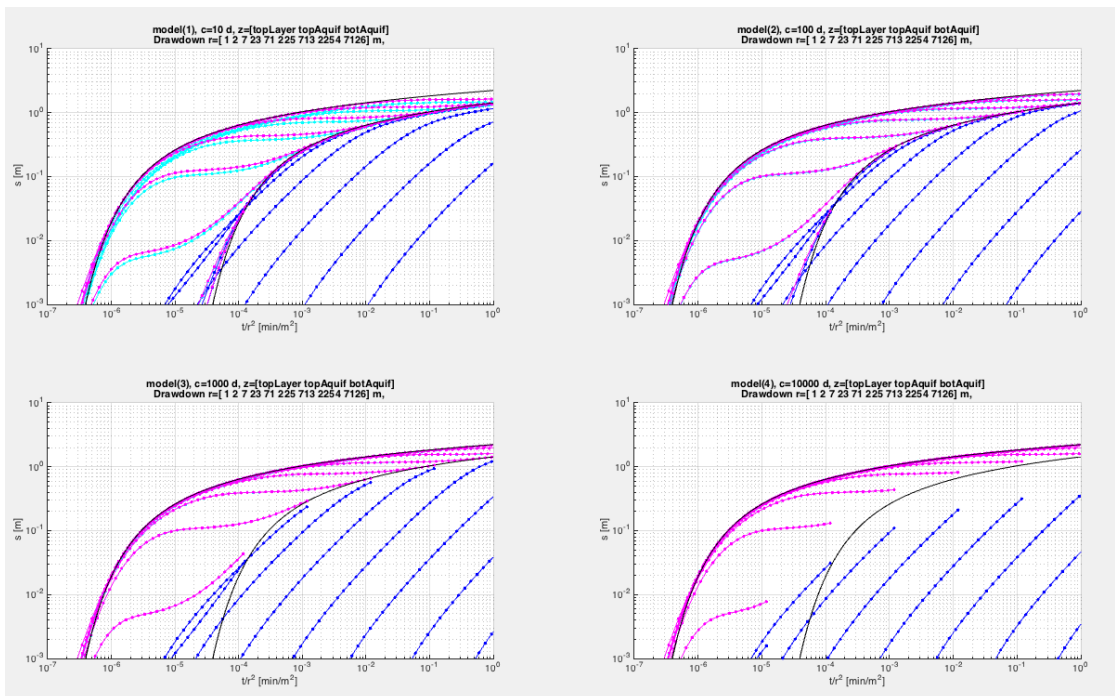


Figure 6.32: Drawdown in overlying layer (water table, blue), top of the aquifer (cyan) and bottom of the aquifer (magenta) for different distances to the well.

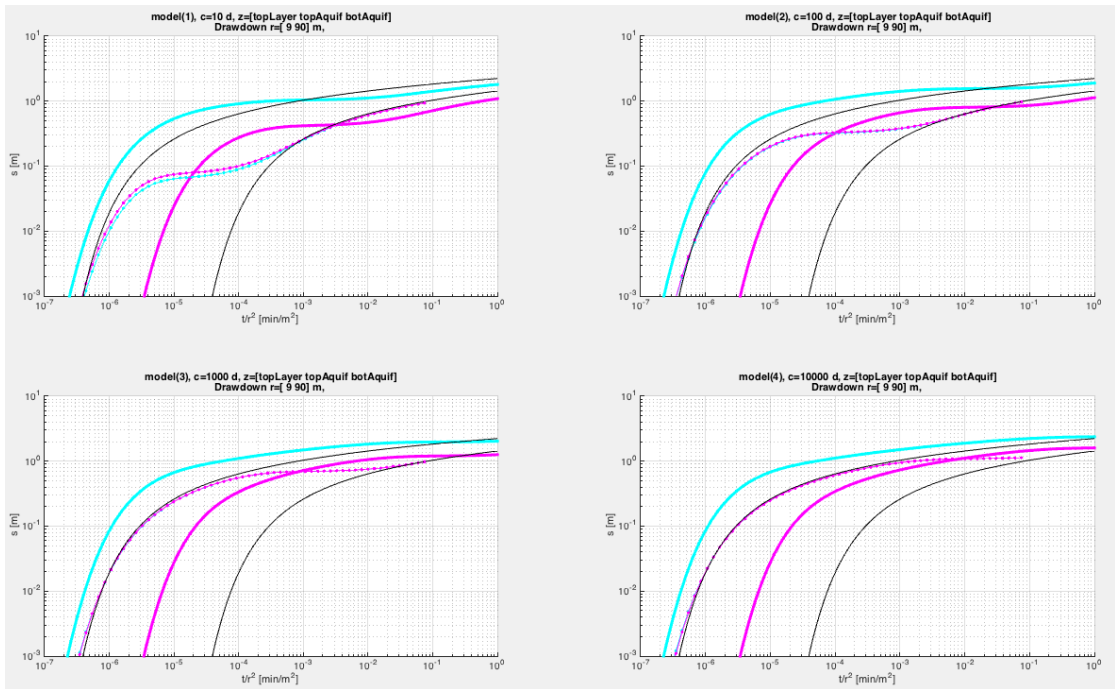


Figure 6.33: Effect of partial penetration. The screen of only 7 only perforating the top of the 35 m thick aquifer. Drawdown in top and bottom of the aquifer at 9 and 90 m from the well.

4. How do the two bounding curves of the delayed yield relate? (What is the relation between the two?)
5. What determines the elevation of the transition curve (the more or less horizontal branch of the delayed yield curve between the two bounding curves?)

6.7 Large-diameter wells (not for the exam)

The solution of Theis for transient flow in an unbounded confined or unconfined aquifer is based on the assumption that the storage inside the well casing can be neglected. While this is generally a valid assumption for tube wells, and, therefore, for wells in semi-confined and confined aquifers, it may not hold in unconfined aquifers when large-diameter dug wells are used, such as the one shown in Figure 44, which is a picture of a large open well in India. Especially when the transmissivity of the aquifer is low, the storage in a large diameter well represents a large portion of the water extracted, at least on the short run, and will thus have a substantial influence on the drawdown. This influence must be taken into account when interpreting drawdown tests on such wells. It should be clear that the formula for a large-diameter well will also hold true when pumping water from a pond.

Papadopoulos and Cooper (1967) derived an analytical solution for the drawdown in a fully penetrating large-diameter well, taking into account the storage in the casing of the well. The partial differential equation upon which it is based is the same as the one used by Theis. However, the boundary condition at the well face differs; the extraction must now match both the inflow from the aquifer and the drawdown inside the well casing. It thus becomes

$$Q = \pi r^2 \frac{\partial h}{\partial t} - 2\pi rkh \frac{\partial h}{\partial r}, \quad \text{for } r = r_w$$

where Q is the constant extraction from the well for $t > 0$. Notice the difference between the well radius r_w and the radius of the well casing r_c .

The solution derived by means of the Laplace Transform, while linearizing by taking $kh \approx k\bar{h}$ is

$$s = \frac{Q}{4\pi k\bar{h}} \int_0^\infty \left(1 - e^{-\frac{\beta^2}{4u_w}}\right) \frac{J_0\left(\frac{\beta}{r_w}\right) \Psi(\beta) - Y_0\left(\frac{\beta}{r_w}\right) \nu(\beta)}{\beta^2 \left\{ \Psi(\beta)^2 + \nu(\beta)^2 \right\}} d\beta$$

where

Figure 6.34: A large-diameter well having a well casing radius r_c different from the well-bore radius r_w

$$\begin{aligned}\nu(\beta) &= \beta J_0(\beta) - 2\alpha J_1 \\ \Psi(\beta) &= \beta Y_0(\beta) - 2\alpha Y_1(\beta)\end{aligned}$$

$J(-)$ and $Y(-)$ are Bessel functions and $\alpha = r_w^2 S / r_c^2$ with S the storage coefficient (specific yield) and $u_w = \frac{r_w^2 S}{4kht}$.

These expressions may be computed, for instance in Visual Basic as a User Defined Function in Excel. The Visual Basic code is given below. Type curves for different values of α but constant ratio $r_w/r_c = 1$ are given in figure ..

Because often large-diameter wells are shallow, there will be an extra drawdown due to partial penetration. The extra drawdown due to partial penetration will be constant for large times already vary soon after the drawdown starts (see section on partial penetration). In practice the impact of partial penetration will be virtually immediate. Therefore the extra drawdown due to partial penetration obtained from that section can immediately be added to the computed drawdown for the fully penetrating large-diameter well.

An implementation of the function $F(u, \alpha, r/r_w)$ in Visual Basic is given below. It exploits the Bessel functions that come standard with Excel. The method to use them in Visual Basic is somewhat complicated and not intuitive. Therefore I wrapped the Excel Visual Basic method in separate functions *BesJ* and *BesY* as shown below. The advantage is that these Bessel functions don't have to be implemented by ourselves using the methods that are given in Abramowitz and Stegun (1964) for example. With this function implemented in Excel, one can reproduce the type curves and compute the drawdown in large diameter wells such as the one shown in figure 6.1

```

1 Public Function F(Uw As Double, alfa As Double, rrw As Double)
2     As Double
3     ' Large diameter well function of Papadopoulos and Cooper 1967
4     ' alfa=S(rw/rc)^2, uw=rw^2S/(4kht), rrw=r/rw,
5     Dim J As Double, Y As Double, Arg1 As Double, Arg2 As Double,
6     Beta As Double, dBeta As Double
7     Const Pi = 3.141592654, p = 0.05
8     F = 0#
9     Beta = 0.0000001
10    Arg2 = 0
11    For i = 1 To 150
12        dBeta = Beta * (10 ^ p - 1)
13        Beta = Beta * 10 ^ p ' 10 steps per log cycle
14        Arg1 = Arg2
15        J = Beta * BesJ(Beta, 0) - 2 * alfa * BesJ(Beta, 1)
16        Y = Beta * BesY(Beta, 0) - 2 * alfa * BesY(Beta, 1)
17        Arg2 = (1 - Exp(-(Beta ^ 2) / 4 / Uw)) * (BesJ(Beta * rrw,
18            0) * Y - BesY(Beta * rrw, 0) * J) /_

```

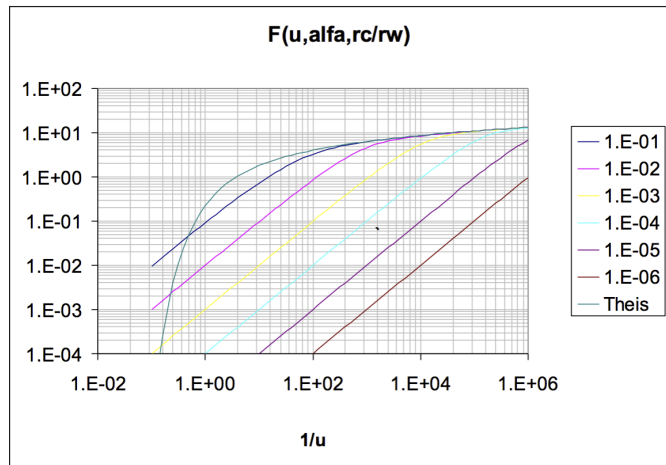


Figure 6.35: Large-diameter well drawdown type curves of Papadoulos-Cooper function $F(u_w, \alpha)$ for different values of α versus $1/u$, for $r = r_w$ and $r_c = r_w$ and different values of $\alpha = Sr_w^2/r_s^2$.

```

16      (Beta ^ 2 * (Y ^ 2 + J ^ 2))
17      F = F + 0.5 * (Arg1 + Arg2) * dBeta
18  Next i
19  F = F * 8 * alfa / Pi
20 End Function
21
22 Public Function BesJ(z As Double, n As Integer) As Double
23 Const BES As String = "ATPVBAEN.XLA!BESSELJ"
24     BesJ = Run(BES, z, n)
25 End Function
26
27 Public Function BesY(z As Double, n As Integer) As Double
28 Const BES As String = "ATPVBAEN.XLA!BESSELY"
29     BesY = Run(BES, z, n)
30 End Function

```

7 Convolution

7.1 What convolution is and how it works

Convolution is applied in many branches of science. Because it is so widely and flexibly applicable, it is important to have a thorough understanding of it.

Convolution is a general principle that can be seen as smart superposition and allowing efficient simulation of linear systems with arbitrary time (or space) varying inputs. In dealing with groundwater it allows interpreting pumping tests with arbitrarily varying extractions. It further allows simulation of the groundwater head due to arbitrarily varying river stages as well has groundwater head fluctuations as a function of varying recharge and interpretation. It is also heavily used in time-series analysis. In mathematical course books, convolution is mostly explained in connection with the Laplace transform, which has some advantages in dealing with it mathematically. However, it is not necessary to understand or apply it. So we do not need this here.

The essential condition for convolution to work is that the response of the system in question due to some physical pulse is unique and proportional to the magnitude of that pulse. A short rain shower is an example of such a pulse due to which the groundwater level will respond by first rising and subsequently declining until the effect of the shower has completely disappeared. The reaction of the system in question to a pulse of unit magnitude is called the impulse response $IR(\tau)$, $\tau = t - t_0$ (figure 7.1). Notice that the dimension of the pulse (in this case 1 mm of rain for instance) may be completely different from the dimension of the reaction of the system (change of head or change of flow for instance).

If one imagines an infinite series of unit pulse glued together, say after $t = t_0$, then we have a continuous unit input for $t > t_0$. This is what is called the step response, $SR(\tau)$, $\tau = t - t_0$. In our example this would mean that at $t = t_0$ it starts raining with intensity 1 mm/d and it keeps raining with this constant intensity forever thereafter.

Notice that most analytic solutions of groundwater flow are, in fact, step responses. For instance the solution for a sudden change of the water level at the river, $s(x, t) = a \operatorname{erfc}(u)$, $u = \sqrt{x^2 S / (4kDt)}$ is an example. The same is true for the Theis and the Hantush solutions, they assume a sudden change from zero to Q_0 for the extraction at $t = 0$, which remains constant thereafter, and do so forever.

Because the step response can be regarded as the response due to an infinite number of unit pulses for $t > t_0$, it immediately follows that

$$SR(\tau) = \int_{t=0}^{\tau} IR(\nu) d\nu$$

$$IR = \frac{\partial SR(\tau)}{\partial \tau}$$

In practice we deal with pulses that have a given duration, such as the rainfall during one day. Even if rain varies during the day, then still we may not possess data on a shorter time scale, and the daily figures are the best we have. We will then probably deal with them as average rainfall for each day that we have data for as the best approximation of the time-varying precipitation. Of course, if one has hourly data, one may use that data as average values for each hour as the best approximation.

So in general we will have a series of figures for daily (or hourly, weekly or monthly) precipitation, evapotranspiration, river stage etc. We then need the so-called block response $BR(\tau, \Delta\tau)$. The block response is the result of a sudden change of an input variable, for instance rain, with a unit magnitude, constant during a given time $\Delta\tau$ and zero thereafter. It's the result of a unit pulse of fixed duration. The easiest way to compute the block response is by superposition

$$BR(\tau, \Delta\tau) = SR(\tau) - SR(\tau - \Delta\tau)$$

Which is what we have been doing by our superposition. For instance, with a well in an groundwater system of infinite extent, that fulfills the presumptions underlying the Theis solution, we may write

$$BR(\tau, \Delta\tau) = 0, \quad \tau \leq 0 \quad (7.1)$$

$$BR(\tau, \Delta\tau) = \frac{1}{4\pi k D} W\left(\frac{r^2 S}{4k D \tau}\right), \quad 0 < \tau \leq \Delta\tau \quad (7.2)$$

$$BR(\tau, \Delta\tau) = \frac{1}{4\pi k D} \left[W\left(\frac{r^2 S}{4k D \tau}\right) - W\left(\frac{r^2 S}{4k D (\tau - \Delta\tau)}\right) \right], \quad \tau > \Delta\tau \quad (7.3)$$

Based on the previous superposition we can readily compute the required response of the system using the standard groundwater solutions.

Figure 7.2 shows how standard superposition would work once we have the block response as explained above. For every subsequent actual input pulse of, per let's say a day, we would have to compute the block response and multiply it with the actual magnitude of the input to obtain its true response. Each such system reaction would have to be shifted down time in accordance with the moment that the pulse occurred, and finally all these reaction have to be superimposed to obtain the combined reaction of the system. This procedure is what we actually do with superposition and is illustrated in figure 7.2.

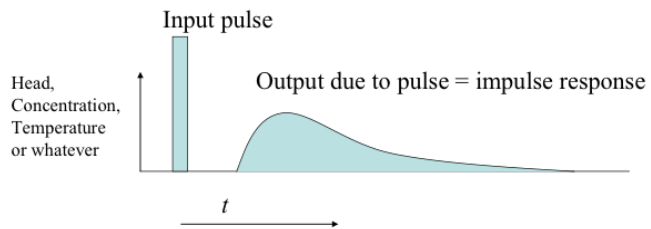


Figure 7.1: Impulse response

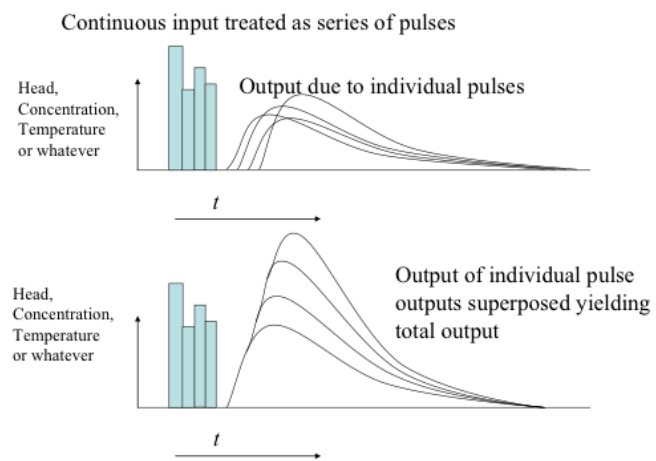


Figure 7.2: The effect of a series of pulses: the output is obtained by superposition

Convolution as a smart way of doing this superposition takes a different perspective, one that is illustrated in figure 7.3; to do so it turns the system response around. Let's see how that works.

Consider a fixed point in time t , a time τ after the pulse occurred. The top image shows this pulse, its reaction, the $IR(\tau)$ or the $BR(\tau, \Delta\tau)$ and the considered time t (indicated by the vertical line connecting the two graphs). The impact of the pulse happening at time $t - \tau$ on the system at time t time equals the pulse or block response for τ multiplied by the actual height of the pulse, p . Hence the result s of the pulse is

$$s = p(t - \tau) IR(\tau) \quad (7.4)$$

as indicated in the top figure.

But this is identical in the bottom figure in which the impulse response is taken relative to t itself and reversed in time. Taking this perspective, we would say: the effect of a pulse at time $t - \tau$ (or “a time τ ago”) equals the reversed impulse response at τ , i.e. $IR(\tau)$ times the height of the pulse at $t - \tau$. This is exactly the same as equation 7.4. This perspective is illustrated in the bottom picture of figure 7.3.

But this holds for the effect now of any pulse in the past. So with this perspective, the only thing we have to do to compute the result of the past, that is the pulses from $-\infty < t$ is to multiply each pulse happening a time τ ago, that is at $t - \tau$ by the value of the impulse response at τ . This is illustrated in figure 7.4. If we compare this procedure with the basic superposition shown in figure 7.2, we see that, to compute the state of the system at any given point of time due to what happened in the past, requires only one reversed impulse response, that has to be multiplied by the corresponding intensity of the past input (such as rain of river stage).

Mathematically this can be generalized as follows

$$h = \int_{\tau=0}^{\infty} IR(\tau) p(t - \tau) d\tau \quad (7.5)$$

where the input p is continuous. In the case we split up the past in discrete steps $\Delta\tau$ for which we only have the average intensity with each step, we use the block response for the corresponding step length $\Delta\tau$. Then we have

$$h = \sum_{i=1}^{\infty} BR(\tau, \Delta\tau) p_{t-\tau_i - \Delta\tau \rightarrow t-\tau_i} \quad (7.6)$$

where $p_{t-\tau_i - \Delta\tau \rightarrow t-\tau_i}$ means the intensity of the input between $t - \tau_i - \Delta\tau$ and $t - \tau_i$ and $BR(\tau, \Delta\tau)$ as defined in equation 7.3. This procedure is called convolution, continuous in case we work with the impulse response or discrete in case we work with the block response.

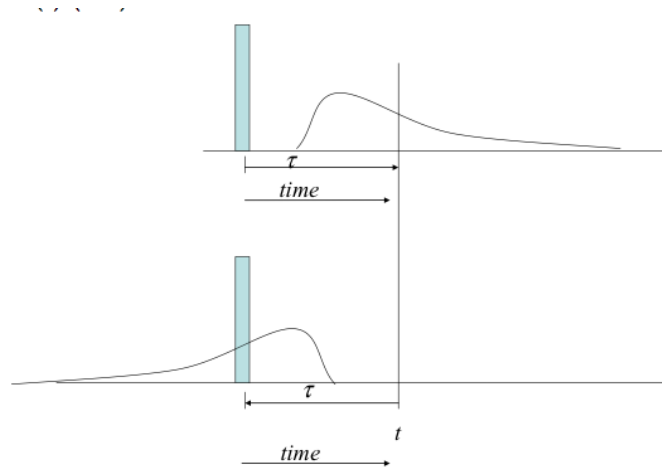


Figure 7.3: Turning the impulse response around

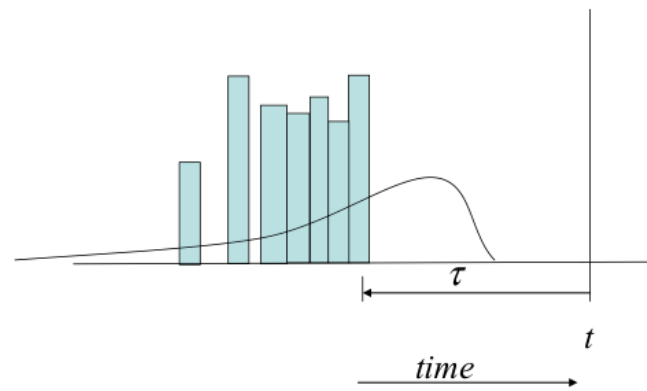


Figure 7.4: Convolution is the multiplication of the value of the impulse response (reversed in time) at τ with that of the actual impulse at time $t - \tau$ and summing the result to get the total response of the system (=the head) at time t

Final note: Mathematicians mostly take the integral in equation 7.5 over $-\infty < \tau < \infty$, which is equivalent to $\infty < \tau < 0$, because the $IR(\tau)$ is zero for $t < 0$ for physical reasons (a response can only exist after its cause happened).

7.2 Examples in Excel

7.2.1 Arbitrarily fluctuating river stage

We can readily carry out a convolution in a spreadsheet and, therefore, compute the groundwater head resulting from an arbitrary fluctuation of the surface-water level over time of due to an arbitrary varying extraction from a well.

Let's assume we have daily values of the river stage. The the block response for the head change at any x at τ equals

$$BR(\tau, \Delta\tau) = \operatorname{erfc} \left(\sqrt{\frac{x^2 S}{4kD\tau}} \right) - \operatorname{erfc} \left(\sqrt{\frac{x^2 S}{4kD(\tau - \Delta\tau)}} \right) \quad (7.7)$$

where $\Delta\tau = 1$ d. In Excel we make a column with values of $BR(\tau, \Delta\tau)$ of a length that equals the length of the past that we wish to take into account. The implementation in Excel is shown in figure 7.5, where the block responses for different values of x are in columns H, I, J, and K with τ in column G.

The formula in cell I10 is

`=ERFC(SQRT(I$6^2*S/(4*kD*tau)))`

Which has only one erfc function because the corresponding $\tau \leq \Delta\tau$.
and that in cell I11

`=ERFC(SQRT(I$6^2*S/(4*kD*tau)))-ERFC(SQRT(I$6^2*S/(4*kD*(tau-Dt))))`

with, of course, the two erfc functions.

As can be deduced from these formulas, the cells with the kD and S values have been given proper names so that the formula can reference their names rather than their location. This was also done for the time step Dt . Then the whole column under the cell with "tau" was given the name "tau", so that it can be directly referenced by its name.

Then we need another column with the daily values of the river stage next to the date at which the river stage appeared from the desired or relevant starting point in the past. See columns A and B in figure 7.5 It is wise to have a longer period, as we need also the past river stage of the first time that we are interested in, else zero will be used automatically in Excel.

The values below the cell with the label "Stage" contain the river levels on the corresponding dates. In this case these levels were generated to allow playing with them. The stage is the sum of three cosines as follows (in cell B10):

`=a_1*COS(2*PI()*A10/T_1)+a_2*COS(2*PI()*A10/T_2)+a_3*COS(2*PI() * A10/T_3)`

It uses the amplitudes a_{-1} , a_{-2} and a_{-3} and the cycle times T_{-1} , T_{-2} and T_{-3} as shown in figure 7.5. This generates the curve with label “Stage” (which lies under the curve with label “ $h(0)$ ”, the computed stage at $x = 0$).

Then we need to flip around (up down) the block response. In a spreadsheet it, however, far more intuitive to flip around the time series of the river stage instead of the block response, because the head of the block response for small τ will be in the top of the spreadsheet, while for the actual time series where each value of river stages stands next to an actual date, this reversal of the column is o.k.. It just means that the most recent time is on top instead the oldest time. It is even necessary to flip the stage time series instead of the block response, because we will copy a formula that references the entire stage series and will be copied to include the past. When not flipped, the past of the first time would extend way above the top of our spreadsheet, which cannot be dealt with by Excel. When flipped, that past will extend to higher column numbers in Excel with possibly empty cells. This does not matter as empty cells are treated as zeros. If that is not acceptable, then the past of the first cell should be included, is necessary with some average value. Hence column “tau” increases downward, while the stage time (column A) decreases downward (youngest date on top).

In the final step we have to carry out the multiplication and summation and do so for each time. The output will be in a column C, right next to the river-stage time series, so we already have the dates. Then for each such time we will multiply and sum in a single standard Excel formula, called “sumproduct(A,B)”. What this does is the following. A and B are two ranges in the spreadsheet of equal size and shape. sumproduct will take the product of the corresponding elements of A and B and sum everything together. This is exactly what we need.

To implement the formula, select an arbitrary cell in column B where the output comes (not the top one for convenience, so use B12 for instance). Then type “sumproduct(“ and select the column with the river stage from the top to the cell adjacent to the selected cell. Hence “sumproduct(B9:B12)”. Then type a comma (or semi-colon depending on the settings of your Excel) to start defining range B. Then select range B. This is the column with the block response from the top to the cell next to the selected one, hence H9:H12. Finally type “)” to finish the formula. Inspect the formula to make sure that you selected the correct ranges. It should be “=sumproduct(B9:B12,H9:H12)”. If not, correct the input. Once they are correct, we want to copy the formula to the other cells of the column with the outcomes. But this fails because we did not fix the block response. To fix the block response use \$ for the row in the formula. So change the formula in cell B12 to

¹ =SUMPRODUCT(B12 : B203 , H\$10 : H\$201)

Finally then we copy this formula over the entire column where we want the outcomes, that is from C9:C100. The result is the change of head at the given x for an arbitrary fluctuation of the river in the past.

In the example spreadsheet we also prepared block response columns I, J and K for different distances to the river. We did that by copying the formulas in column H to

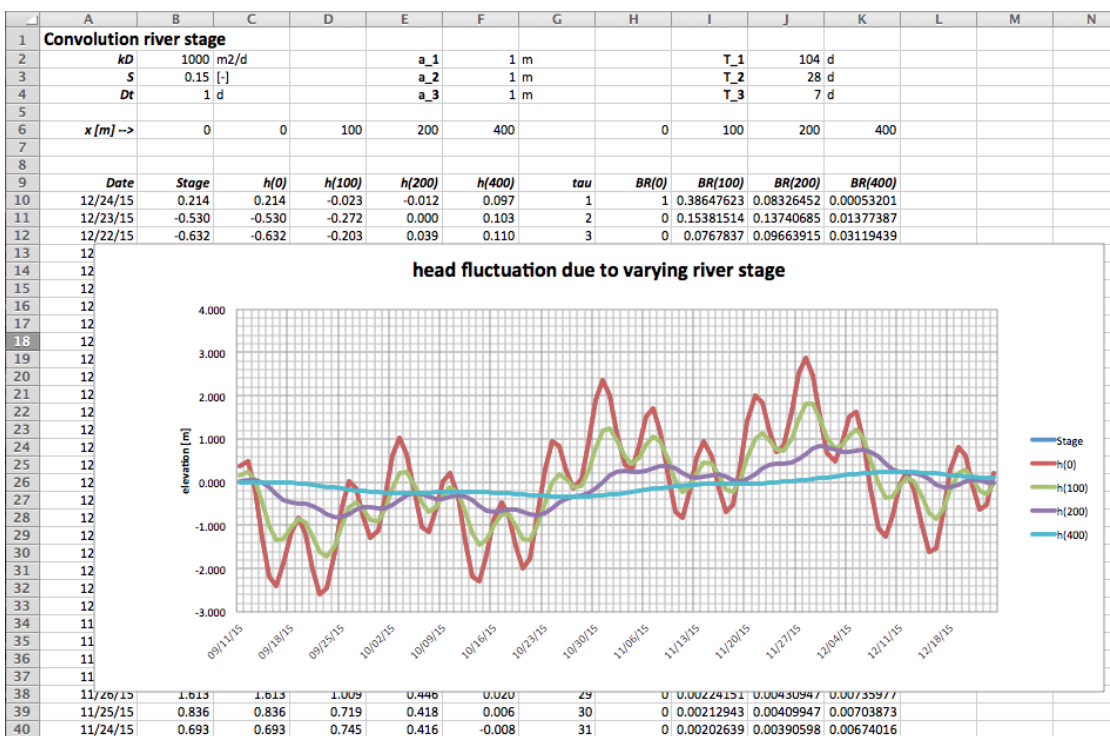


Figure 7.5: Convolution of river stage in Excel

columns I, J, and K.

To also compute the head change at these distances copy the formula in column C to columns D, E, and F.

Notice that the head under label “ $h(0)$ ” is the same as the “stage” because we used $x = 0$. Fill in any other number for x in cell C6 and the values will change, including the label itself. Make sure that the x-value in cell H6 remains the same as in C6. There is a formula in cells H6:K6 that references the corresponding cells in C6:F6.

One can now experiment with the values of a_1 , a_2 , a_3 , T_1 , T_2 and T_3 , as well as with the x-values. The result will be shown immediately. In fact we have not computed the result of several waves at $x = 0$ not using the solution with the sines but that for a sudden change of head. We did so efficiently with convolution.

7.2.2 Impulse response, block response, and step response comparison

Than make a graph to show the result, which should be as in figure 7.5.

Let us now illustrate the difference between impulse response and block response, also for the river stage.

The block response of the river stage is given in equation 7.7, while the step response is the known solution itself:

$$SR(\tau) = \operatorname{erfc} \left(\sqrt{\frac{x^2 S}{4kD\tau}} \right)$$

Then the impulse response is obtained by differentiation of the step response with respect to time.

No

$$IR(\tau) = \frac{\partial}{\partial \tau} \left\{ \operatorname{erfc} \left(\sqrt{\frac{x^2 S}{4kD\tau}} \right) \right\} \quad (7.8)$$

$$= \frac{\partial}{\partial \tau} \left(\int_u^\infty \frac{2}{\sqrt{\pi}} e^{-\nu^2} d\nu \right), \quad u = \sqrt{\frac{x^2 S}{4kD\tau}} \quad (7.9)$$

$$= -\frac{2}{\sqrt{\pi}} e^{-u^2} \frac{\partial u}{\partial \tau} \quad (7.10)$$

$$= -\frac{2}{\sqrt{\pi}} e^{-u^2} \left(-\frac{1}{2\tau\sqrt{\tau}} \sqrt{\frac{x^2 S}{4kD}} \right) \quad (7.11)$$

$$= \frac{\sqrt{\frac{x^2 S}{4kD\tau}}}{\tau\sqrt{\pi}} e^{-u^2} \quad (7.12)$$

$$= \frac{u}{\tau\sqrt{\pi}} e^{-u^2}$$

Note that time is embedded in u . For small step widths $\Delta\tau$ the values of the block response almost equal those of the impulse response multiplied by $\Delta\tau$,

$$B(\tau, \Delta\tau) \approx IR(\tau) \Delta\tau$$

for $\tau > \Delta\tau$ or more generally $\tau \gg \tau$. This is illustrated in figure 7.6 below. The two responses are virtually identical except for smaller τ and especially for $\tau < \Delta\tau$, but this does not affect practical usage of either. In practice I prefer to use the block response as it is exact and always obtainable from the given step response by a simple subtraction.

7.2.3 Arbitrarily fluctuating extraction of multiple Theis wells

Convolution is also suitable to compute the results of a varying extraction of wells. The same procedure as before can be applied using the Theis (or Hantush) well function. We'll show here that we can handle an arbitrary number of wells each with an extraction that varies in an arbitrary way to compute the head as a function of time at a concrete location.

As an example we consider 5 wells at given coordinates and a point xp, yp where the drawdown is to be computed using the Theis solution. First the distance r between each well and the observation point is computed. Then we set up the $BR(\tau, \Delta\tau)$ that is different for each well because the distance to the observation point is different. The block response is

$$BR(\tau, \Delta\tau) = \frac{1}{4\pi kD} \left[W\left(\frac{r^2 S}{4kD\tau}\right) - W\left(\frac{r^2 S}{4kD(\tau - \Delta\tau)}\right) \right]$$

with $W(-)$ the Theis well function and the notion that the second well function only comes in when $\tau > \Delta\tau$. This gives 5 columns, one for each well. Next we need the discharge of each well on a per day (per week, per month or whatever time step basis). Then let the time run such that the youngest date is on top. Then we compute the drawdown for each well as a “sumproduct(A,B)” as explained before. This gives another

<i>tau</i>	<i>BR(200)</i>	<i>IR(200)*dt</i>	<i>SR(200,t) - SR(200,t-dt)</i>
1	0.0833	0.0973	0.0833
2	0.1374	0.1384	0.2207
3	0.0966	0.0959	0.3173
4	0.0692	0.0687	0.3865
5	0.0521	0.0519	0.4386
6	0.0409	0.0408	0.4795
7	0.0332	0.0331	0.5127
8	0.0276	0.0275	0.5403
9	0.0234	0.0234	0.5637
10	0.0202	0.0202	0.5839
11	0.0176	0.0176	0.6015

Figure 7.6: Block response, $BR(\tau, \Delta\tau)$, Impulse Response $IR(\tau - 0.5\Delta\tau)$ and Step Response $SR(\tau)$ and $-SR(\tau - \Delta\tau)$ for the same situation as in figure 7.5. One sees that $BR(\tau, \Delta\tau) \approx IR(\tau - 0.5\Delta\tau) \Delta\tau$ already for small τ

5 columns. Finally add the contribution of the five wells together by summing them. This is it.

Finally a graph is made to show the discharges and the drawdowns, both for each well individually and the total drawdown in the observation point. Figure 7.7 gives the results of this example, the discharge of each well, the drawdown contribution of each well to the drawdown at the observation point and the total drawdown (black line in right-hand picture).

7.3 Questions

1. Explain what convolution is and how it compares with superposition.
2. Explain impulse response, block response and step response.
3. Why did we reverse the direction of the time series in the implementation of convolution in the spreadsheet.
4. What is the consequence of lack of past data on the results of convolution, especially on those of the oldest times, without any past?
5. In terms of convolution, what, in fact, are the solutions of groundwater flow like those for a sudden change of river stage and the Theis and Hantush well functions?
6. Explain in your own words the meaning of equation 7.5?
7. How does the impulse response relate to the step response mathematically?
8. How can you compute the block response $BR(\tau, \Delta\tau)$ of a system?

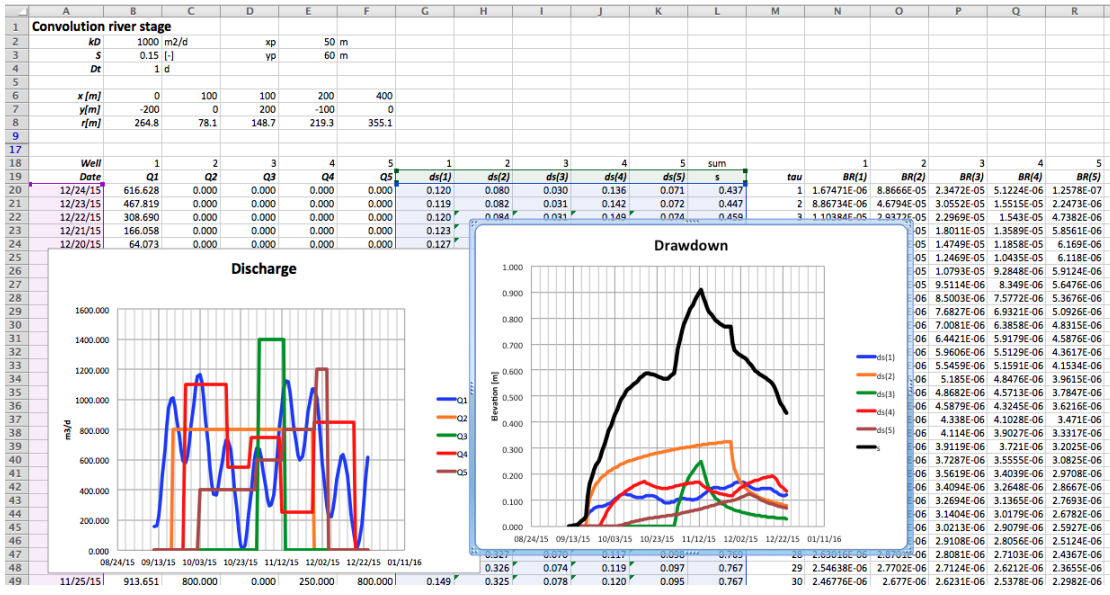


Figure 7.7: Results of the explained example. Five wells, their discharge (left picture) their darwdown (right picture) and the total drawdown (black line in right-hand picture).

8 Laplace solutions (illustration, not for exam)

8.1 Sudden head rise at the boundary of a one-dimensional semi-infinite aquifer

The Laplace transform is used to solve the one-dimensional partial differential equation, known as the diffusion equation. The Laplace transform removes time from the partial differential equation after which we only have to solve a steady state situation, whose solution we already know. Once we have this solution in Laplace space we convert it back to time by looking up the result in a Laplace transform table ([[Abramowitz and Stegun \(1964\)](#)]).

We consider a one-dimensional aquifer with constant transmissivity kD with initial head zero at a boundary a river at $x = 0$ whose water level is suddenly increased at $t = 0$.

The differential equation is

$$\frac{kD}{S} \frac{\partial^2 \phi}{\partial x^2} = \frac{\partial \phi}{\partial t}$$

with as boundary conditions:

$$\begin{aligned}\phi(0, r) &= 0 \\ \phi(t, 0) &= h\end{aligned}$$

Taking the Laplace transform of the differential equation and its boundary conditions yields:

$$\begin{aligned}\frac{kD}{S} \frac{\partial^2 \bar{\phi}}{\partial x^2} - s\bar{\phi} &= 0 \\ \bar{\phi}(s, 0) &= \frac{h}{s}\end{aligned}$$

The solution in Laplace space is easily found as it is the same as the stationary solution for a 1-D leaky aquifer with fixed head at $x = 0$:

$$\bar{\phi} = \frac{h}{s} e^{-x/\lambda}$$

The steady state solution was for the differential equation

$$\begin{aligned}\frac{\partial^2 \phi}{\partial x^2} - \frac{\phi}{\lambda^2} &= 0 \\ \phi(0) &= h\end{aligned}$$

$$\phi = h e^{-\frac{x}{\lambda}}$$

From which it follows that

$$\lambda = \sqrt{\frac{kD}{sS}}$$

So that

$$\bar{\phi} = \frac{h}{s} e^{-x\sqrt{\frac{s}{kD}}\sqrt{s}}$$

The inverse transform is given by Abramowitz and Stegun (1964, p1026, item 29.3.83):

$$F(s) = \frac{1}{s} e^{-\kappa\sqrt{s}} \rightarrow f(t) = \operatorname{erfc}\left(\frac{\kappa}{2\sqrt{t}}\right)$$

Hence, with κ replaced by $\frac{x^2 S}{kD}$ we find

$$\phi = h \operatorname{erfc}\left(\sqrt{\frac{x^2 S}{4kDt}}\right)$$

Which is the sought solution.

8.2 Laplace solution for the Theis well function

The Laplace transform is one method, perhaps the most practical and universal to solve partial differential equation that depend on time. The Laplace transform removes the time derivative from the partial differential equation ([Bruggeman (1999)]), after which is can be solved as a steady-state problem. Once we have the steady-state solution in Laplace space, we have to transfer it back to time, which is done with conversion tables ([Abramowitz and Stegun (1964)]). [Bruggeman (1999)] gives a full derivation for the leaky aquifer case of Hantush. Here we apply the Laplace transform on the transient well extraction studied by Theis.

The partial differential equation for transient flow in an aquifer with constant transmissivity is

$$\frac{\partial^2 \phi}{\partial r^2} + \frac{1}{r} \frac{\partial \phi}{\partial r} = \frac{S}{kD} \frac{\partial \phi}{\partial t} \quad (8.1)$$

$$\frac{Q_0}{2\pi kD} = \lim_{r \rightarrow 0} r \frac{\partial \phi}{\partial r} \quad (8.2)$$

$$\phi(0, r) = 0 \quad (8.3)$$

$$\phi(t, \infty) = 0 \quad (8.4)$$

Denoting the Laplace transform of $\bar{\phi} = L\{\phi\}$ and the inverse transformation by $\phi = L^{-1}\{\bar{\phi}\}$, the Laplace transform of 8.1 through 8.4, becomes, with p as the Laplace constant:

$$\frac{\partial^2 \bar{\phi}}{\partial r^2} + \frac{1}{r} \frac{\partial \bar{\phi}}{\partial r} - \frac{S}{kD} p \bar{\phi} = 0 \quad (8.5)$$

Its general solution we already know from steady state groundwater flow:

$$\bar{\phi} = AK_0\left(r\sqrt{\frac{Sp}{kD}}\right) + BI_0\left(r\sqrt{\frac{Sp}{kD}}\right) \quad (8.6)$$

It is clear that B must be zero to meet the condition for $r \rightarrow \infty$, because $I_0(\infty) = \infty$.

The flow at Q_r distance r becomes in Laplace, where $Q_r/(2\pi kD)$ is a time-invariant, becomes

$$\frac{Q_r}{p} = 2\pi kD r \frac{\partial \bar{\phi}}{\partial r} \quad (8.7)$$

$$Q_r = 2\pi kD p r A \sqrt{\frac{Sp}{kD}} K_1\left(r\sqrt{\frac{Sp}{kD}}\right) \quad (8.8)$$

so that, after substituting $B = 0$ and A from the previous expression (8.8) into equation 8.6 yields

$$\bar{\phi} = \frac{Q_r}{2\pi kD p} \frac{K_0\left(r\sqrt{\frac{Sp}{kD}}\right)}{r\sqrt{\frac{Sp}{kD}} K_1\left(r\sqrt{\frac{Sp}{kD}}\right)} \quad (8.9)$$

Because $raK_1(ra) = 1$ for $r > 0$ and a a positive constant, we have, writing $Q_r \rightarrow Q_0$

$$\bar{\phi} = \frac{Q_0}{2\pi k D p} K_0 \left(r \sqrt{\frac{pS}{kD}} \right) \quad (8.10)$$

$$\bar{\phi} = \frac{Q_0}{2\pi k D} \int_0^{\tau} f(p) d\tau \quad (8.11)$$

because

$$L^{-1} \left\{ \frac{1}{p} f(p) \right\} = \int_0^t F(\tau) d\tau \quad (8.12)$$

with, in our case,

$$f(p) = K_0 \left(r \sqrt{\frac{pS}{kD}} \right) \quad (8.13)$$

and from the tables of the Laplace transforms (Abramowitz and Stegun, 1964, p1028)

$$L^{-1} \{ K_0(\kappa\sqrt{p}) \} = \frac{1}{2t} \exp \left(-\frac{k^2}{4t} \right) \quad (8.14)$$

we find

$$\phi = \frac{Q_0}{4\pi k D} \int_0^t \frac{1}{\tau} \exp \left(-\frac{r^2 S}{4k D \tau} \right) d\tau \quad (8.15)$$

$$= \frac{Q_0}{4\pi k D} \int_{\tau=0}^{\tau=t} \frac{r^2 S}{4k D \tau} \exp \left(-\frac{r^2 S}{4k D \tau} \right) d \left(\frac{4k D \tau}{r^2 S} \right) \quad (8.16)$$

Replace

$$\frac{1}{y} = \frac{4k D \tau}{r^2 s}$$

$$\begin{aligned}
\phi &= \frac{Q_0}{4\pi kD} \int_{\tau=0}^{\tau=t} ye^{-y} d\left(\frac{1}{y}\right) \\
&= \frac{Q_0}{4\pi kD} \int_{\tau=0}^{\tau=t} -ye^{-y} \frac{1}{y^2} dy \\
&= \frac{Q_0}{4\pi kD} \int_{\tau=t}^{\tau=0} \frac{e^{-y}}{y} dy \\
&= \frac{Q_0}{4\pi kD} \int_{y=\frac{r^2 S}{4kDt}}^{y=\infty} \frac{e^{-y}}{y} dy \\
&= \frac{Q_0}{4\pi kD} \int_{y=u}^{y=\infty} \frac{e^{-y}}{y} dy \\
&= \frac{Q_0}{4\pi kD} E_1(u) \tag{8.17}
\end{aligned}$$

$$\phi = \frac{Q_0}{4\pi kD} W(u), \quad u = \frac{r^2 S}{4kDt} \tag{8.18}$$

Where $E_1(-)$ is the exponential integral, a standard function in Matlab and tabled in many groundwater hydrology books as the Theis well function $W(u)$. It can be developed in a series expansion as well (Abramowitz and Stegun (1964, p228-229)):

$$\begin{aligned}
E_1(z) &= \int_u^{\infty} \frac{e^{-y}}{y} dy \\
&= -\gamma - \ln u - \sum_{n=1}^{\infty} \frac{(-1)^n u^n}{nn!} \\
&= -\gamma - \ln u + u - \frac{u^2}{2 \times 2!} + \frac{u^3}{3 \times 3!} - \frac{u^4}{4 \times 4!} + \dots
\end{aligned}$$

$$\gamma = 0.5772156649$$

Bibliography

- [Abramowitz and Stegun (1964)] Abramowitz M. and I.A. Stegun (Eds) (1964) Handbook of mathematical functions with formulas, graphs and mathematical tables. Dover Publications Inc. New York. ISBN 0-486-61272-4
- [Bloemen et al. (1989)] Bloemen, P.J.T.M., Lekkerkerker, C. and Molen, W.H.v.d., 1989. Aardgetijden in grondwater: een voorbeeld uit Burkina Faso (earth tides in groundwater, an example from Burkina Faso). H2O, 22(17): 536-538.
- [Boulton (1963, 1964)] Boulton, N.S. (1963, 1964) Analysis of data from non-equilibrium pumping tests allowing for delayed yield form storage. Proc. Inst. Civ. Eng. 26 (November 1963): 469-482. Discussion, 28 (August 1964): 603-610
- [Bredehoeft (1967)] Bredehoeft, J.D., 1967. Response of Well-Aquifer systems to Earth Tides. Journal of Geophysical Research, 72(12): 3075-3087.
- [Bruggeman (1999)] Bruggeman, G.A. (1999) Analytical solutions of geohydrological problems. Elsevier, Amsterdam etc. 959p ISBN 0-444-81829-4.
- [DuFour (2000)] Dufour, F.C. (2000) Groundwater in the Netherlands, Facts and Figures. Netherlands' Institute of Applied Geoscience, TNO, National Groundwater Survey, Delft Utrecht, The Netherlands. ISBN 90-6743-654-2, 96pp
- [Van der Gun (1980)] Gun, J.A.M., 1980. Schatting van de elastische bergingscoëfficiënt van zandige watervoerende pakketten (Estimation of the elastic storage coefficient of sandy aquifers, in Dutch); Dienst Grondwaterverkenning TNO, Jaarverslag 1979. Dienst Grondwaterverkenning TNO, Delft, pp. 51-61.

- [Hantush (1955)] Hantush, M.S. (1955) Non-steady radial flow in an infinite leaky aquifer. *Transm. Amer. Geophys. Union*, 36: 95-101
- [Hemker and Maas (1984)] Hemker, C.J. and Maas, C. (1987) Unsteady flow to wells in layered and fissured aquifer systems. *Journal of Hydrology*, 90: 231-249.
- [Shieh et al. (1987)] Hsieh, P.A., Bredehoeft, J.D. and Farr, J.M., 1987. Determination of aquifer transmissivity from earth tide analysis. *Water Resources Research*, 23(10): 1824-1832.
- [Kamp and Gale (1983)] Kamp, G.v.d. and Gale, J.E., 1983. Theory of Earth Tide and Barometric Effects in Porous Formations With Compressible Grains. *Water Resources Research*, 19(2): 538-544.
- [Kruseman and De Ridder (1970)] Kruseman, G.P. and De Ridder, N.A., 1970. Analysis of pumping test data. *Bulletin 11. ILRI*, Wageningen, 200 pp.
- [Lee (1999)] Lee, T-C (1999) Applied mathematics in hydrogeology. Lewis Publ. Boca Raton etc. 382pp. ISBN 1-56670-375-1.
- [Maas (1986)] Maas, C. (1986) The use of matrix differential calculus in problems of multiple aquifer flow. *Journal of Hydrology*, 88: 43-67,
- [Olsthoorn (2008)] Olsthoorn, T.N. (2008) Transient Groundwater Flow, Analytical Solutions. Syllabus LN0080/0811. UNESCO-IHE, Delft, Netherlands, 100pp.
- [Rasmussen and Crawford (1997)] Rasmussen, T.C. and Crawford, L.A., 1997. Identifying and removing barometric pressure effects in confined and unconfined aquifers. *Ground Water*, 35(3): 502-511.
- [Todd (1959)] Todd, D.K., 1959. *Groundwater Hydrology*. John Wiley & Sons Inc., 336 pp.
- [Todd and Mays (2005)] Todd, D.K. and Mays, L.W., 2005. *Groundwater Hydrology*. John Wiley & Sons Inc.
- [Verruijt (1999)] Verruijt, A. (1999) *Grondmechanica (Soil Mechanics)*. Delft University Press, Delft, 295pp.

- [De Vries (1984)] Vries, J.J. de (1984) Holocene depletion and active recharge of the Kalahari Groundwater - A review and an indicative model. *Journal of Hydrology*.
- [De Vries (2000)] Vries, J.J. de (2000) Groundwater level fluctuations - the pulse of the aquifer. In: *Elevation and protection of groundwater resources*, Conference Wageningen, Netherlands National Committee for IAH, Wageningen, pp 27-43.
- [Wösten et al. (1994)] Wösten, J.H.M., Veerman, G.H. and Stolte, J. (1994) Water retention and hydraulic conductivity functions of top- and subsoils in the Netherlands. *The Staring Series*. Wageningen University, Wageningen.